

NEW ENGLAND TRANSPORTATION CONSORTIUM

CURVED INTEGRAL ABUTMENT BRIDGE RESEARCH – DRAFT FINAL REPORT



WSP USA

Revision History:

Initial Submission	Rev. 0	01/28/2022
Amendment	Rev. 1	11/21/2022
Final	Rev. 2	12/28/2022

Contents

1	INTRODUCTION.....	9
1.1	PURPOSE AND INTENT OF THIS RESEARCH EFFORT.....	9
1.2	STRAIGHT INTEGRAL ABUTMENT BRIDGE DESIGN IN NEW ENGLAND	9
1.3	NATIONAL SURVEY	10
1.4	LITERATURE REVIEW	11
2	FINITE ELEMENT STUDY PARAMETERS	12
2.1	DETERMINATION OF STUDY PARAMETERS	12
2.1.1	<i>Parameters Related to the Superstructure</i>	<i>12</i>
2.1.2	<i>Parameters Related to Substructures</i>	<i>13</i>
2.2	LOADING.....	16
2.3	MODELING PROCEDURE.....	17
2.3.1	<i>Geometry and General Layout.....</i>	<i>18</i>
2.3.2	<i>Construction Staging.....</i>	<i>18</i>
2.3.3	<i>Live Load Placement.....</i>	<i>21</i>
2.3.4	<i>Backfill Soil Springs.....</i>	<i>23</i>
2.4	ANALYSIS	26
3	FINITE ELEMENT STUDY RESULTS.....	27
3.1	GENERAL STRUCTURE PERFORMANCE.....	28
3.2	THERMAL MOVEMENT	30
3.3	PILE HEAD DISPLACEMENTS	33
3.3.1	<i>By Radius</i>	<i>33</i>
	<i>34</i>	
3.3.2	<i>By Pile Orientation and Wingwall Orientation.....</i>	<i>34</i>
3.3.3	<i>By Skew</i>	<i>36</i>
3.3.4	<i>By Pile Length.....</i>	<i>40</i>
3.3.5	<i>By Span.....</i>	<i>41</i>
3.4	PILE HEAD ROTATIONS	42
3.4.1	<i>By Radius</i>	<i>43</i>
3.4.2	<i>By Pile Length.....</i>	<i>43</i>
3.4.3	<i>By Skew</i>	<i>44</i>
3.4.4	<i>By Pile Orientation and Wingwall Orientation.....</i>	<i>45</i>
3.4.5	<i>By Span.....</i>	<i>45</i>
3.5	PILE FORCES / REACTIONS	46
3.5.1	<i>By Radius</i>	<i>46</i>
3.5.2	<i>By Skew</i>	<i>49</i>
3.5.3	<i>By Pile Length.....</i>	<i>49</i>
3.5.4	<i>By Pile Orientation and Wingwall Orientation.....</i>	<i>51</i>
3.5.5	<i>By Span.....</i>	<i>52</i>
3.6	BEAM END FORCES	52
3.6.1	<i>By Construction Staging</i>	<i>52</i>
3.6.2	<i>By Radius</i>	<i>53</i>
3.6.3	<i>By Skew</i>	<i>55</i>
3.6.4	<i>By Pile Length.....</i>	<i>57</i>
3.6.5	<i>By Pile Orientation and Wingwall Orientation.....</i>	<i>57</i>
3.7	DECK STRESSES.....	58
3.7.1	<i>By Radius</i>	<i>58</i>
3.7.2	<i>By Skew</i>	<i>58</i>
3.7.3	<i>Other Parameters.....</i>	<i>59</i>

3.8	SUMMARY OF FINDINGS.....	59
4	APPLICATION OF RESULTS TO DESIGN GUIDELINES	61
4.1	WINGWALL AND PILE ORIENTATION	61
4.2	PILE LENGTHS	63
4.3	MULTI-SPAN BRIDGES.....	68
4.4	DESIGN OF SUPERSTRUCTURE	70
4.5	REQUIREMENTS FOR THE APPLICATION OF THE SIMPLIFIED DESIGN METHOD	71
4.6	IMPLEMENTATION PLAN	72
5	CONCLUSIONS.....	73

Appendices

A	National Survey Questions and Results
B	Literature Review
C	Technology Toolbox
D	Example Model Input

Tables

TABLE 1-1: SUMMARY OF STATE REQUIREMENTS FOR STRAIGHT INTEGRAL ABUTMENT BRIDGES.....	9
TABLE 2-1: SPAN AND RADIUS COMBINATIONS FOR FE STUDY	13
TABLE 2-2: MASSDOT STRAIGHT IAB PILE LENGTH TO FIXITY AND EQUIVALENT PILE LENGTH.....	14
TABLE 2-3: PILE SIZES BASED ON SPAN LENGTH	14
TABLE 2-4: ABUTMENT HEIGHTS UTILIZED FOR FINITE ELEMENT STUDIES	15
TABLE 2-5: DEFINITION OF STUDY PARAMETERS.....	15
TABLE 2-6: SUMMARY OF CASES.....	15
TABLE 2-7: ADDITIONAL 15 FT. CASES (P15)	15
TABLE 2-8: APPLICATION OF LOADS FOR ALL ITERATIONS	16
TABLE 2-9: SUPERELEVATION.....	18
TABLE 2-10: CONSTRUCTION STAGING.....	19
TABLE 3-1: CHART KEY DESCRIPTIONS	27
TABLE 3-2: CHART SYMBOLOGY DESCRIPTIONS	27
TABLE 4-1: RECOMMENDED LATERAL DISPLACEMENT FOR SIMPLIFIED DESIGN METHOD.....	61
TABLE 4-2: TRANSVERSE DISPLACEMENTS FOR 5 FT. AND 10 FT. U-WINGWALL LENGTHS.....	63
TABLE 4-3: ALLOWABLE TRANSVERSE DISPLACEMENTS FOR ACCEPTABLE RESPONSE.....	65
TABLE 4-4: TARGET TRANSVERSE STIFFNESS VALUES FOR BRIDGES WITH 0-DEGREE SKEW ANGLES.....	66
TABLE 4-5: TARGET TRANSVERSE STIFFNESS VALUES FOR BRIDGES WITH 10-DEGREE SKEW ANGLES.....	ERROR! BOOKMARK NOT DEFINED.
TABLE 4-6: TARGET TRANSVERSE STIFFNESS VALUES FOR BRIDGES WITH 20-DEGREE SKEW ANGLES.....	ERROR! BOOKMARK NOT DEFINED.
TABLE 4-7: STICK AND REFINED MODEL COMPARISON	67
TABLE 4-8: COMPARISON OF RESULTANT SHEAR FROM PASSIVE EARTH PRESSURE TO MODELED SHEAR ON PIER	69
TABLE 5-1: OUTCOMES OF PROPOSAL INTENTIONS	73

Figures

FIGURE 2-1: TYPICAL CROSS SECTION	12
FIGURE 2-2: GLOBAL COORDINATE SYSTEM.....	18
FIGURE 2-3: LIVE LOAD APPLICATION TO MAXIMIZE BENDING IN GIRDER 2	22
FIGURE 2-4: LIVE LOAD APPLICATION TO MAXIMIZE CENTER PILE REACTION	22
FIGURE 2-5: NUMERICAL COMPARISON OF MIDAS AND MASSDOT SPRING CALCULATIONS.....	23
FIGURE 2-6: COMPARISON OF FULL ABUTMENT STIFFNESS.....	24
FIGURE 2-7: COMPARISON OF MOBILIZED SOIL FORCE ON ABUTMENT	25
FIGURE 2-8: TYPICAL DISPLACEMENT CONTOUR FOR 50 FT. SPANS.....	26
FIGURE 3-1: DEFORMATION CONTOURS FOR THERMAL RESPONSES	28
FIGURE 3-2: STAGE 1 MY RESULTS - BENDING ABOUT TRANSVERSE BRIDGE AXIS W.R.T. LOCAL GIRDER AXIS.....	28
FIGURE 3-3: STAGE 4 MY RESULTS - BENDING ABOUT TRANSVERSE BRIDGE AXIS W.R.T. LOCAL GIRDER AXIS.....	29
FIGURE 3-4: STAGE 1 MZ RESULTS - BENDING ABOUT TRANSVERSE BRIDGE AXIS W.R.T. LOCAL PILE AXIS	29
FIGURE 3-5: STAGE 4 MZ RESULTS - BENDING ABOUT TRANSVERSE BRIDGE AXIS W.R.T. LOCAL PILE AXIS	29
FIGURE 3-6: 2-SPAN CONTINUOUS BEAM FLEXURE ENVELOPE.....	29
FIGURE 3-7: RESULTANT DISPLACEMENTS ON 100 FT. SPAN, 0-DEGREE SKEW.....	30
FIGURE 3-8: RESULTANT DISPLACEMENTS ON 100 FT. SPAN, 20-DEGREE SKEW.....	31
FIGURE 3-9: RESULTANT DISPLACEMENTS FOR 200 FT. SERIES, NO SKEW	32
FIGURE 3-10: RESULTANT DISPLACEMENTS FOR 200 FT. SERIES, 20-DEGREE SKEW	32
FIGURE 3-11: SPAN VS. RADIUS DISPLACEMENTS – EXPANSION.....	33
FIGURE 3-12: SPAN VS. RADIUS DISPLACEMENTS – CONTRACTION.....	34
FIGURE 3-13: SPAN VS. RADIUS DISPLACEMENT COMPARISON OF WINGWALL AND PILE ORIENTATION	34
FIGURE 3-14: LONGITUDINAL AND TRANSVERSE DISPLACEMENT COMPARISON OF WINGWALL AND PILE ORIENTATIONS.....	35
FIGURE 3-15: LONGITUDINAL AND TRANSVERSE DISPLACEMENT COMPARISON BY SKEW	36
FIGURE 3-16: DISPLACEMENT COMPARISON OF WINGWALL AND PILE ORIENTATION BY SKEW	38
FIGURE 3-17: DISPLACEMENT COMPARISON OF ABUTMENT 1 & 2 BY SKEW AND WINGWALL ORIENTATION	39
FIGURE 3-18: DISPLACEMENT COMPARISON W.R.T PILE LENGTH.....	40
FIGURE 3-19: TRANSVERSE DISPLACEMENT COMPARISON W.R.T. PILE LENGTH AND WINGWALL AND PILE ORIENTATION	41
FIGURE 3-20: LONGITUDINAL DISPLACEMENT DUE TO CONTRACTION W.R.T. PILE LENGTH	41
FIGURE 3-21: TRANSVERSE DISPLACEMENT COMPARISON W.R.T. SPAN CONFIGURATION – EXPANSION	42
FIGURE 3-22: TRANSVERSE DISPLACEMENT COMPARISON W.R.T. SPAN CONFIGURATION – CONTRACTION	42
FIGURE 3-23: PILE HEAD ROTATIONS FOR 150 FT. CASE	43
FIGURE 3-24: X AND Y ROTATIONS BASED ON PILE LENGTH	44
FIGURE 3-25: X AND Y ROTATIONS BY SKEW ANGLE	44
FIGURE 3-26: X AND Y ROTATION COMPARISON W.R.T. WINGWALL AND PILE ORIENTATION.....	45
FIGURE 3-27: X AND Y ROTATIONS W.R.T. BRIDGE LENGTH AND CURVE RADIUS	46
FIGURE 3-28: AXIAL UTILIZATION OF PILES FOR 150 FT. CASES.....	47
FIGURE 3-29: RADIUS COMPARISON OF SHEAR AND MOMENT IN LONGITUDINAL AND TRANSVERSE DIRECTIONS - EXPANSION	47
FIGURE 3-30: RADIUS COMPARISON OF SHEAR AND MOMENT IN LONGITUDINAL AND TRANSVERSE DIRECTIONS - CONTRACTION	48
FIGURE 3-31: MOMENT RESPONSES IN PILES AT ABUTMENT 1 (75 FT. SPANS)	49
FIGURE 3-32: PILE UTILIZATION RATIOS FOR THE 50/750 SERIES AND 100/425 SERIES	50
FIGURE 3-33: PILE MOMENTS ABOUT THE TRANSVERSE BRIDGE AXIS DUE TO CONTRACTION W.R.T PILE LENGTH.....	51
FIGURE 3-34: COMPARISON OF PILE SHEAR W.R.T. PILE AND WINGWALL ORIENTATION	51
FIGURE 3-35: MOMENT REACTION RATIO FOR 340 FT. RADIUS.....	52
FIGURE 3-36: TORSION IN BEAM ENDS SORTED BY CONSTRUCTION STAGES FOR 100 FT SPAN - 340 FT RADIUS – 0 DEGREES SKEW	53
FIGURE 3-37: END OF BEAM FORCE EFFECTS – 100 FT. SPANS.....	53
FIGURE 3-38: TORSION IN BEAM ENDS – 100 FT. SPANS.....	53
FIGURE 3-39: TORSION IN BEAM ENDS – 150 FT. SPANS.....	54
FIGURE 3-40: GIRDER END HORIZONTAL SHEAR IN EXPANSION AND CONTRACTION LOAD CASES	54

FIGURE 3-41: GIRDER END VERTICAL SHEAR AND STRONG AXIS MOMENT.....	55
FIGURE 3-42: TORSION AND AXIAL FORCE AT GIRDER ENDS VS SKEW FOR 100 FT. SPANS WITH 10 FT. PILES.....	55
FIGURE 3-43: STRONG AXIS MOMENTS FOR 20-DEGREE SKEW CASES.....	55
FIGURE 3-44: MAXIMUM POSITIVE END MOMENT BEAM DIAGRAM FOR 100-500 S2 CASE	56
FIGURE 3-45: LIVE LOAD PLACEMENT FOR MAXIMUM POSITIVE END MOMENTS IN 100-500 S2 CASE.....	56
FIGURE 3-46: 150 FT. SPAN GIRDER END TORSION	57
FIGURE 3-47: 150 FT. SPAN GIRDER END AXIAL LOAD	57
FIGURE 3-48: 150 FT. SPAN GIRDER END STRONG AXIS MOMENT	57
FIGURE 3-49: GIRDER END WEAK AXIS MOMENT AND AXIAL LOAD W.R.T. PILE AND WINGWALL ORIENTATION	58
FIGURE 3-50: 75 FT. SPAN DECK STRESSES.....	58
FIGURE 3-51: 300 FT. SERIES DECK STRESSES.....	59
FIGURE 3-52: DECK STRESSES IN 150 FT. SPANS BY PILE LENGTH.....	59
FIGURE 4-1: U-WINGWALL PILE DISPLACEMENTS (TOP LEFT) AND TRANSVERSE DISPLACEMENTS AS A PERCENTAGE OF FREE LONGITUDINAL EXPANSION BASED ON SKEW.....	ERROR! BOOKMARK NOT DEFINED.
FIGURE 4-2: PILE MODEL DIAGRAM.....	64
FIGURE 4-3: SUBSET OF TRANSVERSE DISPLACEMENT TRENDLINES FOR PILE STIFFNESS ANALYSIS	ERROR! BOOKMARK NOT DEFINED.
FIGURE 4-4: STICK MODEL FOR VERIFICATION	67
FIGURE 4-5: PIER CONFIGURATION IN MIDAS MODELS	68
FIGURE 4-6: RESULTANT FORCES ON THE PIER FOR NO SKEW (LEFT) AND SKEWED (RIGHT) SUBSTRUCTURE COMPONENTS.	69

1 INTRODUCTION

1.1 PURPOSE AND INTENT OF THIS RESEARCH EFFORT

The New England Transportation Consortium (NETC) has facilitated over three decades of practice as a research cooperative between the New England state agencies (Connecticut, Maine, Massachusetts, New Hampshire, Rhode Island and Vermont). The purpose of this research initiative is to investigate the effects of the degree of curvature on the behavior of curved integral abutment structures, with consideration for various skews, span lengths and layouts, and pile cantilever lengths. The results of this research will provide recommendations to implement findings through a design guideline, to enhance the bridge design practice throughout the region.

Integral abutment bridge structures are single- or multi-span continuous deck structures with each abutment monolithically connected to the bridge superstructure. The primary purpose of this bridge type is to eliminate the need for deck joints and bearings at abutments, shifting the accommodation of movement in the system below grade to a single row of flexible piles. Use of this type of bridge structure has a demonstrated history of lowering life cycle costs through reduced need for routine maintenance and improved durability. The removal of the joint from the abutments not only eliminates the need for joint maintenance, but also removes a point of access for water intrusion at girder ends and bridge seats. This is a substantial benefit in northern states where heavy salt usage necessary for winter maintenance increases the rate of deterioration. Use of integral abutment structures has increased in popularity for straight structures, with many states providing simplified design methods or standard guidelines for use including pile size and span limitations.

Given the availability of funding compared to the necessary repair and replacement demand for the bridge inventory in the New England states, an urgent need exists to reduce bridge maintenance costs and extend the service life of structures. Extending integral abutment bridges to curved alignment applications offers an immediate opportunity to address this concern. The construction of curved structures, however, has been limited due to uncertainty of performance and limited research. Beyond the operating savings inherent with a jointless bridge, constructing bridges on horizontal curves is often advantageous from an alignment perspective, and can reduce costs associated with lengths of approaches and right-of-way acquisitions that would otherwise be required to achieve a tangent alignment. More data is needed to develop standard guidelines for curved integral abutment bridge structures design and construction. This research effort strives to collect available guidelines that exist and complete a parametric study to aid in the advancement of guidelines and use of curved integral abutment bridges.

1.2 STRAIGHT INTEGRAL ABUTMENT BRIDGE DESIGN IN NEW ENGLAND

The simplified methods for straight integral abutment bridges (IAB's), such as those discussed in Section 1.2.1 of Appendix B, provide a straightforward design process for integral abutments by using general assumptions on the way the bridge will perform. This research project intends to develop a similar simplified approach for curved integral abutment bridges (CIAB's). Given that the goal is to develop a simplified method for a set of common bridge systems, the decision on project boundaries and load application should be limited to parameters that may be applicable to a simplified procedure. Additionally, the intention of this study is not to provide designs of structures at each case, but rather to consider several major design parameters to determine whether a standard procedure is applicable for a structure of a given size/span/arrangement. Girder sizes are estimated for each span length under consideration based on positive moment capacity of the girders in order to provide an applicable stiffness of the horizontal leg of the frame. All projects utilizing the simplified procedure for pile design will require a full superstructure design by the Engineer of Record.

Table 1-1 outlines the current parameters required or recommended for straight integral abutment bridges in each of the New England states. For each state it is noted whether these requirements are applicable to IAB's in general, or if they are explicitly noted to be required for use of the Simplified Design Methods.

Table 1-1: Summary of State Requirements for Straight Integral Abutment Bridges

Parameter	MaineDOT	NHDOT	VTrans	MassDOT	ConnDOT	RIDOT
-----------	----------	-------	--------	---------	---------	-------



APPENDIX D – TECHNOLOGY TOOLBOX

	<i>General</i>	<i>Simplified Method</i>	<i>Simplified Method</i>	<i>Simplified Method</i>	<i>General</i>	<i>General</i>
Pile Type	Steel HP	Steel HP	Steel HP	Steel HP	-	Steel HP
Pile Head	Fixed	Fixed	Fixed	Fixed	Pinned	Fixed
Pile End	Fixed	Fixed	-	Fixed	-	
Pile Orientation	Weak Axis Preferred	Either	-	Weak Axis Required	Weak Axis	Weak Axis Required
Minimum Pile Length	10 ft.	-	16 ft.	Must extend 5 ft. past point of fixity**	-	10 ft.
Concrete Abutment Height Limit	12 ft.	13 ft.	13 ft.	15 ft.	8 ft.	-
Skew Limit	20 deg	20 deg	20 deg	30 deg	-	30 deg
Max. Total Length Steel	300 ft. *	300 ft.	395 ft.	140 ft.	-	350 ft.
Max. Total Length Concrete	500 ft. *	600 ft.	695 ft.	200 ft.	-	600 ft.
Max. Single Span	-	150 ft.	145 ft.	-	-	-
Curvature Limit	Straight Beams	Straight Beams	Straight Beams	Straight Beams	-	Straight
Approach Slabs	Required for steel spans > 80 ft. and concrete spans > 140 ft.	Required with Sleeper Slabs	-	Required	Required	Required
Wing Orientation	In Line Preferred	In Line Preferred	U-Wing preferred	U-Wing Required	U-Wing Required	U-Wing - separate from abutment
Wingwall Length	10 ft.	10 ft.	10 ft.	10 ft.	-	N/A - Joint
Design Thermal Range	150°	125°	150° Range 88° Rise 130° Fall	70° Rise 100° Fall	Ignores thermal movements – Pinned Head	115°

All fields left blank for criteria not explicitly addressed in state guidelines

* Steel bridge lengths between 200 ft. and 300 ft. and concrete bridges between 330 ft. and 500 ft. are considered long span IAB's, and require multiple additional requirements. Currently long span IAB's in Maine are required to be straight.

** Regions of high bedrock explicitly disallowed

These requirements reveal a consensus for use of steel H piles for simplified methods, with most states assuming a fixed head condition in the piles. Abutment height limitations to limit passive pressure effects are generally included in state guidance with a typical maximum height of approximately 13 ft. Most states also require approach slabs, which serve to bridge the settlement gap that is likely to develop over time behind the abutment stem. Though wingwall lengths are typically limited to 10 ft., the orientation of the wings indicates different preferences between the states. These straight IAB parameters were used as a basis for the discussion of applicable study parameters for curved structures.

1.3 NATIONAL SURVEY

A survey was sent to state agencies to assess the use, design, and maintenance of straight and curved integral abutment structures throughout the country. Responses were received from representatives of 26 states. A full listing of survey questions



and results is provided in Appendix A. In general, it was evident that though many states are using straight integral abutment bridges, the use and available design recommendations for curved structures is highly variable and lacking in guidance.

Survey responses led to correspondence with Stephanie Wagner of Indiana DOT and Dr. Frosch of Purdue University. The following summarizes the result of these conversations and the Indiana DOT guidance.

- Simplified design method where piles are designed for axial load only is allowed for curves with the subtended angle less than 30 degrees over the full bridge length. The research leading to this allowance was based on a straight, skewed, concrete test bridge at Purdue University. Data was extrapolated to apply to curved structures.
- Approach slabs must be used for all integral abutment bridges in Indiana with a sleeper slab at the far end, and a pre-compressed foam joint between the approach slab and the sleeper. 2"x1" joint sealant is placed between the back end of the sleeper and the full depth pavement. This detail was developed after transverse pavement cracking was noticed at the end of the approach slabs on several structures.
- U-Wingwalls are required (wingwalls parallel to roadway centerline), which shall not exceed 10 ft. in length.
- Piles must be oriented about the weak axis. Spiral reinforcement is utilized around the embedded portion of the piles.

Given that the research supporting these recommendations did not consider curvature, the applicability of those research results to this study is not favorable and has not been addressed herein.

1.4 LITERATURE REVIEW

A targeted literature review of curved integral abutment research applications was completed to synthesize the present body of knowledge, including data on in-place structures in Vermont and Iowa. This review focused on documentation of curved integral abutment bridges with instrumentation and structural model verification. In addition, a review of the design and construction processes for straight integral abutment bridges, documentation, and condition assessment programs used by all NETC states was completed. A portion of this information is included in Section 1.2. The full literature review is provided in Appendix B. The results of the literature review did not impact the selection of parameters for this study.

The complex interaction between possible characteristics and components of a curved integral abutment bridge means there are many parameters and bridge responses that could be included in the finite element study. In order to maintain a manageable dataset, the parameters and bridge responses that were considered for this study were expected to be critical to determine the applicability of a simplified design guidance. These parameters and responses were targeted based on design experience, NETC discussions, review of state and federal guidance, and the literature review of research. Though not addressed in the literature review, torsion in girder ends is also anticipated to be a potential measure that may determine whether a given combination of design parameters will result in unfavorable conditions. Tension in the deck ends is also included as it poses a serviceability challenge that should be included in any simplified design guidance, particularly for skewed bridges. The application and further discussion of these design and response parameters is presented in following sections on the finite element study portion of this project report.

2 FINITE ELEMENT STUDY PARAMETERS

2.1 DETERMINATION OF STUDY PARAMETERS

The determination of boundaries is essential to the successful completion and implementation of this research effort. Boundaries should be representative of general state procedures and encompass the typical ranges expected to be applicable to the bridge inventory. The limitations for straight integral abutment bridge simplified design methods were used to lay the groundwork for a companion set of parameters for curved structures. Several of the requirements for straight IAB's vary substantially between states. Directly including all criteria from all states on straight IAB's into the CIAB research would result in a broad range of parameters and findings. An envelope approach has been utilized to encompass the likely parameters that are expected to be encountered to focus the research results.

2.1.1 PARAMETERS RELATED TO THE SUPERSTRUCTURE

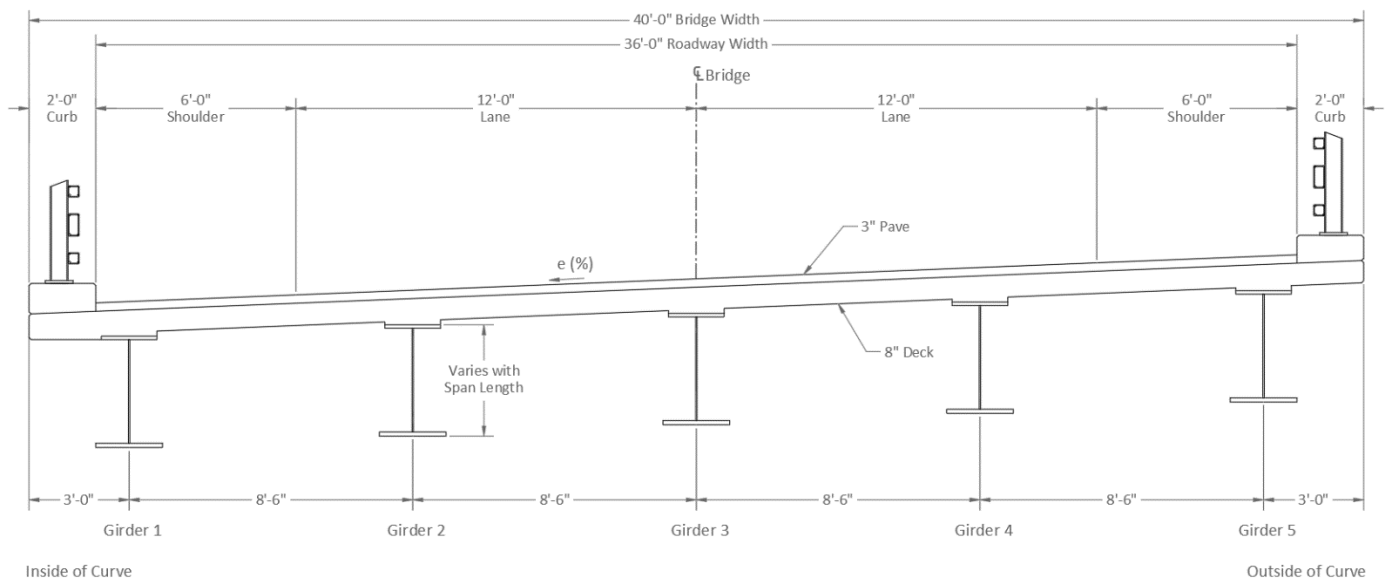


Figure 2-1: Typical Cross Section

The construction of curved highway structures is generally completed using curved steel I girders, curved steel tub girders, segmental concrete, or chorded prestressed straight I girders. Given the inherent complexity of tub and segmental concrete structures, refined analysis will almost always be required. As such these superstructure types were omitted from the study. Given the radius limitations to accommodate chorded girders, this superstructure type was also omitted and only curved steel I girder shapes are considered. An 8-inch normal weight composite concrete deck was assumed. Steel girder sizes were approximately sized to provide the expected stiffness and weight of the superstructure for the various span ranges encountered, as well as to determine a typical expected abutment height for the various spans. The weight of bridge barrier on both sides of the bridge was included as a pressure load at the edges of the deck. The magnitude of the pressure reflects the assumption of a concrete barrier weight of 425 plf, though a steel barrier is shown below. A typical cross section used in all models is shown in Figure 2-1, detailing the assumptions regarding the superstructure layout.

The range of bridge lengths considered encompass the typical range of spans that would be expected on structures that would fall under the simplified analysis umbrella. As such, bridge lengths exceeding the limits for straight IAB's were not included, which creates an upper bound of 300 ft. for steel structures. The individual span length is limited to 150 ft. All multi-span structures are assumed to be continuous at the pier with equal span lengths. Pier alignment was oriented to correspond with the alignment of the abutments, be it radial, or skewed from the radial configuration. A minimum span length of 50 ft. was determined with the NETC Technical Committee as the lower bound for an adequate crossing over a local roadway with ditches and side slopes not requiring slope protection.

APPENDIX D – TECHNOLOGY TOOLBOX

AASHTO LRFD Design Specifications allows the effects of curvature to be ignored when the arc-span divided by the girder radius is less than 0.06 radians. This serves as the upper bound for the radius, which varies with the span length. Table 2-1 provides the range of applicable span and radius combinations included in this study.

Most state-owned bridges are located on state routes and interstates. The applicable maximum super elevation rate for most of these structures is likely to be 6% - 8%. The 6% limit will result in tighter radii than an 8% limit. For an expected design speed range of 35 to 70 mph, the tightest allowable radius by the AASHTO Policy on Geometric Design of Highways and Streets for this range of speeds and superelevation is 340 ft. (6% at 35mph – AASHTO Table 3-9). Therefore, a 340 ft. radius was set as the lower bound for this project.

Bridge span length to width ratios can significantly impact the influence of skew. These effects tend to be maximized in skewed bridges with smaller span length to width ratios (wider structures). For the purposes of this study, a typical two-lane roadway with shoulders and bridge rail (40 ft. structure width) is assumed for all cases. Larger width structures may be addressed in future studies with a more limited radius window, as these structures tend to be located on higher speed facilities. Skews of 0, 10, and 20 degrees from radial were included in the study. All substructure components have the same skew from the radial orientation of that particular substructure component. For the no skew case, all substructure components are radially oriented, and for the 10- and 20-degree skew cases, all substructure components are oriented either 10 or 20 degrees from radial, as appropriate.

Table 2-1: Span and Radius Combinations for FE Study

Bridge Length (ft)	# of	Span Length	Radius (ft)									
			340	425	500	750	1000	1500	2000	2500	3000	
50	1	50	✓	✓	✓	✓						
75	1	75	✓	✓	✓	✓	✓			L _{as} / R < 0.06 Radians		
100	1	100	✓	✓	✓	✓	✓	✓				
150	1	150	✓	✓	✓	✓	✓	✓	✓	✓	✓	
200	2	100	✓	✓	✓	✓	✓	✓		L _{as} / R < 0.06 Radians		
300	2	150	✓	✓	✓	✓	✓	✓	✓			
Totals:			6	6	6	6	5	4	2	1	= 36 total	

2.1.2 PARAMETERS RELATED TO SUBSTRUCTURES

Research conducted in the 1980's (Griemann, et.al.) resulted in a rational design method for integral abutment piles that is based on the ability of the steel piles to develop plastic hinges and experience inelastic rotation without a local buckling failure. Many states require that steel piles be used for simplified design methods, given the lower ductility of concrete piles. This research effort is also limited to steel piles to keep the focus of the effort on the behavior of the bridge as the span and radius cases progress, and to provide an implementation plan that is familiar to both the governing agencies and consulting designers. Project-specific situations that require the use of alternate pile types, such as micropiles, may still be able to implement curvature, but a refined analysis will be required in those cases.

The variability of soil conditions and bedrock elevations at every bridge site can be problematic for comparative studies. Soil-structure interaction in this study is limited to the nonlinear backfill soil springs on the abutment stem walls, which is relatively consistent for standard backfill materials. Pile lengths of 10, 15, 20, and 30 ft. used in this study represent a range of pile stiffness resulting from soil parameters at any given site utilizing an equivalent cantilever method, similar to the approach used by the Massachusetts Department of Transportation.



Piles modeled using the equivalent cantilever method allow the designer to omit the soil interaction springs along the full depth to fixity in the model by providing the same pile head stiffness, resulting in the same resistance to deflection and therefore also the same maximum force effects. Equivalent cantilevers will be significantly shorter than their analogous depth to fixity pile since they remove the soil spring support. See Table 2-2 for a summary of suggested equivalent cantilever pile lengths for straight integral abutment bridges from the MassDOT LRFD Bridge Manual Tables 3.10.11-2 through 3.10.11-4.

Table 2-2: MassDOT Straight IAB Pile Length to Fixity and Equivalent Pile Length

	Soil Type	HP 10 x 57 Piles		HP 12 x 84 Piles	
		Estimated Length to Fixity (Lf, ft.)	Corresponding Equivalent Pile Length (Le, ft.)	Estimated Length to Fixity (Lf, ft.)	Corresponding Equivalent Pile Length (Le, ft.)
1	Dry Loose Sand	26	8.3	31	9.5
2	Wet Loose Sand	28	8.5	32	9.8
3	Dry Dense Sand	19	7.3	22	8.3
4	Wet Dense Sand	20	7.5	23	8.5
5	Wet Stiff Clay	16	7.5	18	8.5
6	Wet Soft Clay	26	10	30	11.5

Maximum unbraced lengths are included as a limiting parameter for the simplified design method recommendations, resulting in the need for refined analysis at bridge sites with very poor geotechnical conditions. Regions with very high bedrock conditions will also be omitted from the simplified method as a site-specific consideration, with a minimum pile depth to fixity of 10 ft. as a lower bound of applicability. The pile sections used for this study are shown in Table 2-3 and were used for each pile length.

Table 2-3: Pile Sizes Based on Span Length

Span Length (ft):	50	75	100	150	2x100	2x150
Pile Size:	HP 10x42	HP 12x84	HP 12x84	HP 14x89	HP12x84	HP 14x89

Each state has individual preferences on the method of analysis for substructure components, which directly impact results of the analyses. For example, Connecticut DOT assumes a pinned cap to pile connection with piles designed for vertical forces only, while MaineDOT utilizes a fixed head for fully integral abutments with piles designed for both axial and moment demands. For this research effort it is assumed that the piles are fixed at the base with a full moment connection at the cap. Equal leg heights at each abutment were assumed. Instances where piles do not develop fixity are not common and should be considered on a project-specific basis. Bridges with substantially unequal leg heights to the point of fixity should be analyzed with a project-specific finite element model regardless of whether the bridge is located on a curved alignment. Pile cantilever lengths varying from 10 ft. to 30 ft. were considered to test the sensitivity of the frame behavior to the leg height.

Maximum abutment heights are generally dictated for integral abutment structures to limit passive pressure forces and the stiffness of the upper portion of the frame. These limits range from 8 ft. (Connecticut) to 15 ft. (Massachusetts) in New England. Embedment of integral abutment stems in soil is generally 4 ft. regardless of the site-specific frost depth, with an inspection shelf to access the underside of girders. Girders were preliminarily sized for the expected loads in the span for positive moment. The abutment height has been adjusted to be representative of the expected heights for the various span lengths to account for this difference in girder height, as shown in Table 2-4. The stem heights will vary in the analyses for this study in a stepwise fashion to provide expected heights as the girder depths increase with span, ranging from 10 ft. for shallow girders on short spans to 14 ft. maximum for deep girders on long spans. The intention of this study is to allow the states to maintain their specific standards and requirements if desired. The simplified guidelines developed will default to state standards where appropriate and provide a limiting abutment height for states that do not have a requirement in their straight integral abutment guidance.

APPENDIX D – TECHNOLOGY TOOLBOX

Table 2-4: Abutment Heights Utilized for Finite Element Studies

Span Length	Girder Height	Stem Height	Diaphragm Height	Total Abutment Height
<i>Ft.</i>	<i>Inches</i>	<i>Ft.</i>	<i>Ft.</i>	<i>Ft.</i>
50	28	6	4	10
75	40	6	5	11
100	53	6	6	12
150	79	5.5	8.5	14
2 x 100 = 200	53	6	6	12
2 x 150 = 300	79	5.5	8.5	14

For continuous span cases, the type, location, stiffness, and boundary conditions of the pier can impact study results. In order to provide comparable data, the pier properties were kept constant for all of the 200- and 300 ft. span cases. Traditional three column piers with a pier cap and pinned bearings were utilized. Piers were assumed fixed at their base. Irregular or extreme pier conditions should be evaluated on a case by case level to determine whether a refined analysis should be utilized.

U-Wingwalls provide significant lateral stiffness to the structure compared to in-line wings. After discussions with the NETC committee it was agreed to look at in-line wings for all span and radius combinations, and both U-wingwalls and in-line wings for the 50 ft. and 100 ft. spans. Similarly, weak axis pile orientation is assumed for all span and radius combinations, with both strong and weak axis pile orientations considered for the 50 ft. and 100 ft. span cases.

Table 2-5 summarizes the initial study parameters and Table 2-6 provides the initial number of cases analyzed in this study. A series of 15 ft. pile length models were added to the study following the first submission of the project. The intent of these cases was to refine the results of the study. Table 2-7 outlines these additional cases along with the final number of models included in the finite element study.

Table 2-5: Definition of Study Parameters

Item	Range of Applicability to Research Study
Piles	Grade 50 Steel H Piles Aligned radially to girder lines
Pile Length	Iterate for 10, 20, & 30 ft. depth to fixity (ECM). Equal leg heights
Pile Orientation	Weak or Strong Axis for 50 ft. and 100 ft. spans. Weak axis only for all others
Abutment Height	See Table 2-4
Bridge Length	50 to 300 ft. (See Table 2-1)
Curve Radius	340 to 2,500 ft. (See Table 2-1)
Skew	0, 10, 20 degrees
Wingwalls	10 ft. long cantilevered monolithic wing
Wingwall Orientation	In-line or U back for 50 ft. and 100 ft. spans. In-line only for all others
Superstructure	Steel I girder Beam Slab Bridge
Superstructure Width	Two 12 ft. lanes, two 6 ft. shoulders, two 2 ft. barriers - 40 ft.

Table 2-6: Summary of Cases

	# Iterations	Naming
A) Span and Radius Combinations:	36	Base
<i>B) Additional for U back wings, 50' & 100' spans:</i>	<i>10</i>	<i>U</i>
<i>C) Additional for strong axis bending, 50&100' spans, Inline Only</i>	<i>10</i>	<i>W, S</i>
D) Iterate for Pile Lengths (10, 20, 30ft):	3	P1,P2,P3
E) Iterate for Skew (0, 10, 20):	3	S0,S1,S2
Total Iterations (A+B+C)*D*E	504	

Table 2-7: Additional 15 ft. Cases (P15)

Span (ft.)	Radii (425 ft. -1500 ft.)	Skews (0, 10, & 20-deg)	# Iterations
------------	---------------------------	-------------------------	--------------

APPENDIX D – TECHNOLOGY TOOLBOX

50	3	3	9
75	4	3	12
100	5	3	15
150	5	3	15
200	5	3	15
300	5	3	15
Additional Iterations:			81
Total Study Iterations (Original from Table 2.4 + Additional):			586

The recommended boundaries were determined to allow for successful accomplishment of project objectives. Considering a range of variables that is too narrow may result in missing the sensitivity window and result in recommendations that are too conservative. Considering a range of variables that is too broad can sacrifice the schedule and budget available for this effort. The cases included in this study aim to strike a balance to allow for a workable and meaningful sample size of results.

2.2 LOADING

Each analysis iteration considers the staged effects of non-composite and long-term/short-term composite loadings. For all cases, non-composite dead loads are transferred as vertical loads on the lower cap and pile system. All composite loadings assume a rigid closure pour connection that distributes loads through frame action to the piles. The following provides more detail for each type of loading, and the suggestion for inclusion for analysis in this study. Load combinations are limited to service loads for consideration of deck stresses and strength 1 for all other data. Loads were combined in accordance with AASHTO LRFD Article 3. The strength 1 combination was evaluated for four separate conditions:

- HL-93 with Thermal Expansion
- HL-93 with Thermal Contraction
- HL-93 Modified with Thermal Expansion
- HL-93 Modified with Thermal Contraction

The MaineDOT HL-93 Modified Loading was included to encompass the loading of the NETC member states. Findings indicated that impacts of using this higher live load were minor and could be limited to the increased axial demand on the piles.

The service limit state was also evaluated for the same four conditions listed above for calculations of deck stresses. Load factors for dead, live, braking, and centrifugal forces were specified as designated in AASHTO LRFD Table 3.4.1-1 and Table 3.4.1-2. The thermal load factor was set to 1.0 in accordance with AASHTO Article 3.4.1 for steel substructures and is consistent with guidance for straight IAB’s in New Hampshire, Rhode Island and Massachusetts.

Table 2-8 provides more detail for each type of loading and whether it is included in the analyses for this study:

Table 2-8: Application of Loads for All Iterations

Load Type		Inclusion	Application
DC ¹	Dead load of components	Included	Self-weight of all components and pressure load on deck from barrier on each side of the bridge
DW	Dead load of wearing surface	Included	3” Asphalt
DW	And Utilities	Omitted	No provisions were made for utilities, as the structural response is likely to be limited to small additional axial loads in the piles and design of the girders
LL ¹	Live Load	Included	HL-93 and HL-93 modified with Impact and Multiple Presence
CE	Centrifugal	Included	Included (varies by radius)

APPENDIX D – TECHNOLOGY TOOLBOX

BR²	Braking	Included	Included as longitudinal force along the girder tangent line at abutment 1 with vertical force couple
EH	Horizontal Earth	Indirect	The effect of horizontal earth on the frame system is included as a boundary condition rather than an applied load via nonlinear soil springs on the abutment stem walls.
LS	Live Load Surcharge	Omitted	Approach slabs are typically used for integral abutment bridges in New England states to minimize the impact of LS on the design of the frame system, therefore this effect is omitted from the models. LS loads may be applied to the abutment explicitly for the design of reinforcement in the abutment in accordance with state standards.
TU	Thermal	Included	Thermal contraction and expansion for steel structures in cold climates (Procedure A)
WS/L	Wind Loads	Omitted	Integral abutment bridges are very stiff in the transverse directions. The integral closure pour provides a rigid end diaphragm connection and generally piles are oriented with their strong axis to resist transverse loads. Most bridge structures in inventory are also generally below the 30 ft. above ground level threshold. For bridge sites where wind is a considerable factor, a refined analysis is recommended.
WA	Water / Scour	Omitted	Structures in flood zones where the superstructure may be subjected to water pressure are outside of the realm of simplified analysis criteria and were not investigated. Structures with severe scour potential where the scoured depth to fixity is beyond the pile depth to fixity limits require a case specific analysis and would not fall into simplified design method parameters.
EE1	Seismic	Omitted	Structures requiring seismic analysis beyond the requirements of Seismic Zone 1 / Seismic Design Category A require refined analysis methods and are not applicable for simplified methods of analysis.
EE2	Ice, collision, etc.	Omitted	Structures requiring extreme event analysis for demands on bridge components from ice, vessels, and vehicular collisions where such impacts could control system response fall outside the realm of simplified design methods and are not included.

¹ No provisions were made for sidewalks for either dead or live loads, as sidewalk loading was not anticipated to impact bridge behavior in a measurable way.

² Braking forces are explicitly included for NHDOT and VTrans, explicitly omitted for MassDOT, and not addressed for MEDOT, CTDOT and RIDOT. In order to provide simplified criteria that could be incorporated throughout New England, braking was included as a longitudinal force with a vertical force couple from the force being applied 6 ft. above the deck surface, as described in the VTrans Integral Abutment Manual Appendix A. All design lanes were considered loaded in the same direction with multiple presence.

2.3 MODELING PROCEDURE

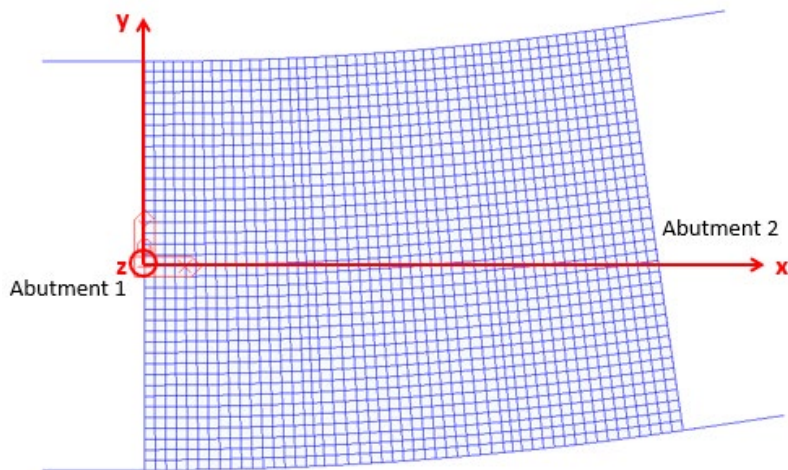


Figure 2-2: Global Coordinate System

2.3.1 GEOMETRY AND GENERAL LAYOUT

All model cases were created in Midas Civil® version 2021 (hereinafter “Midas”). All models were generated with the center girder of abutment one located at the origin of the x-y plane. The global coordinate system of all models was created as shown in Figure 2-2, which looks down at the top of the bridge deck. The positive z axis extends out of the page. Displacements and rotations provided in charts throughout this report are given with respect to this global axis system.

At abutment 1, global y displacements correspond with lateral bridge movements. Similarly, global x displacements would indicate longitudinal bridge movements at abutment 1. Movements are impacted by the curve geometry and layout of abutment 2 with respect to the global axis system. As such, any results taken at abutment 2 should consider its variable position in the x-y plane, depending on the case in question. Superelevation was included in the model geometry and adjusted as indicated in Table 2-9 to provide an expected rate for the given radius.

Table 2-9: Superelevation

Radius (ft.)	340	425	500	750	1000	1500	2000	2500
Superelevation (%)	6	6	6	5	5	4	4	3

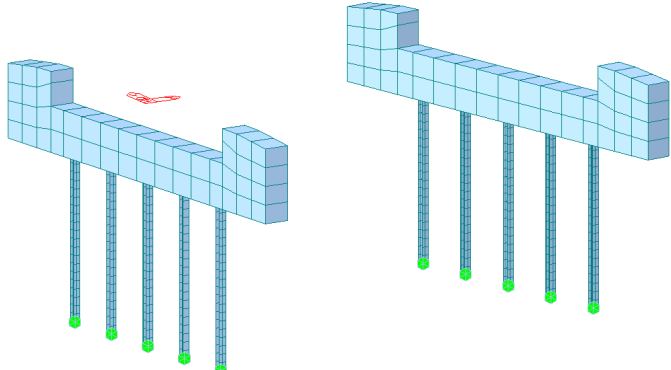
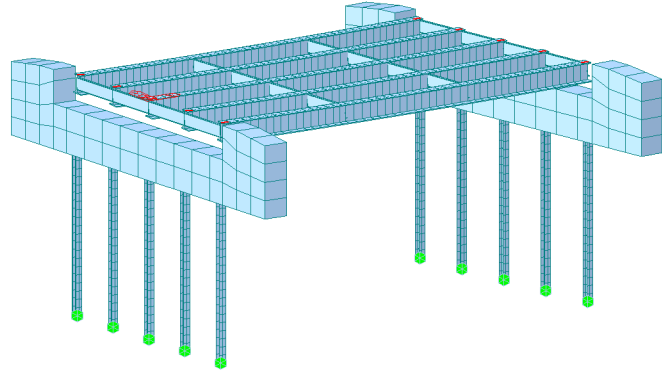
All piles are fixed at the base and comprised of beam elements capable of 6 degrees of freedom (DOF’s) at each node. No releases are specified at the pile connection to the cap, allowing full moment transfer from the cap to pile. All girders are comprised of a special beam element with 7 DOF’s, the 7th being the inclusion of warping stress potential. If warping had not been an option for the beam elements, an all-plate approach would have been utilized.

All surface elements (abutments, wings, and deck) are comprised of plate bending elements with 6 DOF’s at each of the four corner nodes.

2.3.2 CONSTRUCTION STAGING

The construction stage manager in Midas was utilized to activate or deactivate structure groups, boundary groups, and loading groups as appropriate for the various stages of construction. Simply supported behavior for loads applied prior to the deck and closure pours was accomplished by the activation of moment releases at the beam ends, with frame action for loads applied after deck cure is achieved by removal of the release group. The construction sequence utilized for all models is shown in Table 2-10. Note that loads are additive across all stages, and deactivation of loads and/or boundary conditions was necessary to correctly model their application.

Table 2-10: Construction Staging

Stage 0	Screenshots: 50 ft. span, 500 ft. radius, 0 Skew, In-line Wings, Weak Axis 20 ft. Piles
<p>Geometry: Abutments, Wingwalls, Piles</p> <p>Boundaries: Piles fixed at base</p> <p>Loads: Self weight of components (group 1)</p> <p>Group 1 self-weight includes piles, pile cap, wingwalls, and steel</p> 	
Stage 1	
<p>Geometry: Activate Steel Superstructure</p> <p>Boundaries: Add pin connections/moment releases at beam ends</p> <p>Loads: Self weight of components (group 1)</p> 	
Stage 2a	

Geometry: Activate Closure Pour Elements (Maintain Beam End Releases to not allow any moment transfer through the closure pour region)

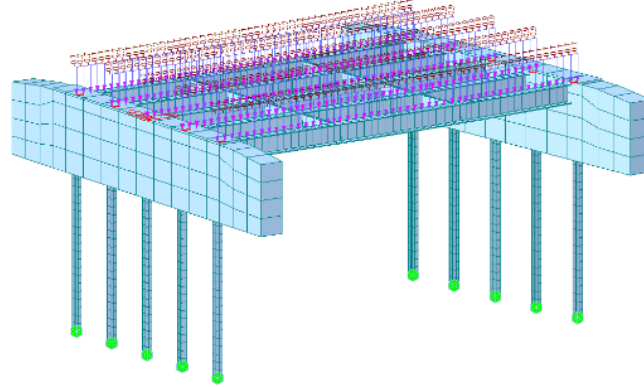
Boundaries: Deactivate self-weight

Loads: Deactivate self-weight (group 1)

Activate self-weight (group 2)

Group 2 includes the abutment stem and closure pour

Apply deck weight as line load on girders



Stage 2b

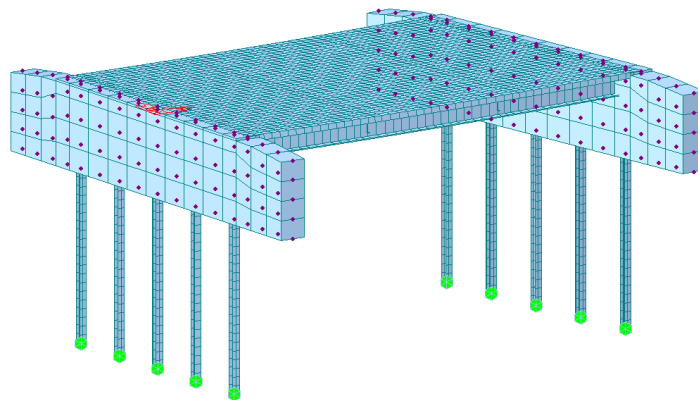
Geometry: Activate composite properties

Boundaries: Activate soil springs

Activate end of deck rigid links to closure pour elements

Remove beam releases

Loads: None

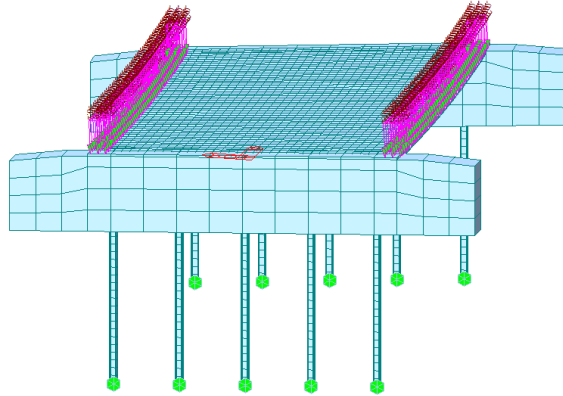


Stage 3

Geometry: Long term composite properties

Boundaries: No change

Loads: Barriers and wearing surface

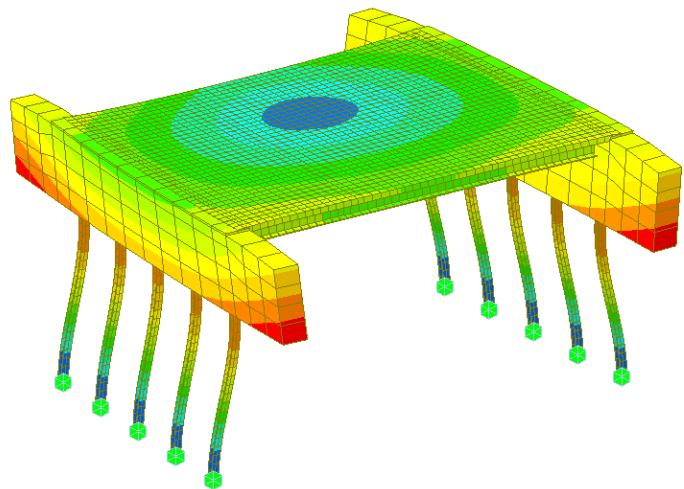


Stage 4

Geometry: Short term composite properties

Boundaries: No change

Loads: LL, CE, BR, TU



Contour for X-Y Displacement for Contraction Load applied in Stage 4

2.3.3 LIVE LOAD PLACEMENT

Live loads were generated as a combination of lane and truck loads for 0, 1, 2, or 3 lanes loaded. MIDAS generates influence surfaces during analysis to capture the maximum and minimum responses for every reaction, beam, and plate element under consideration. Multiple presence is applied as appropriate for the number of lanes loaded along with a dynamic load allowance of 33% applied to the axle weights. Centrifugal effects are included in truck wheel loads, amplifying the wheel load on the outside of the curve.

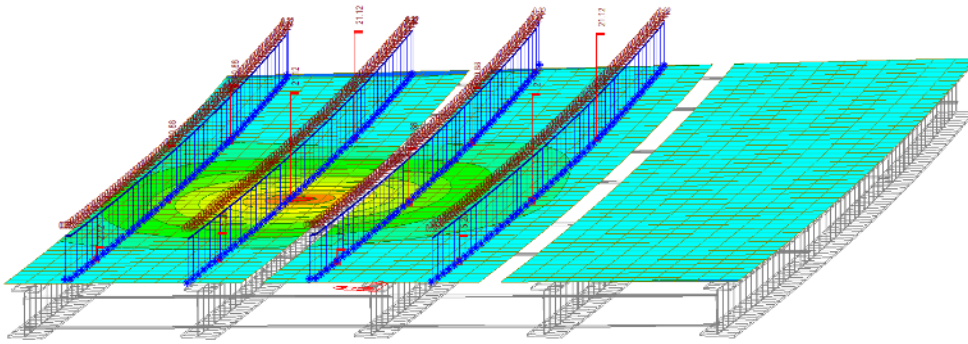


Figure 2-3: Live Load Application to Maximize Bending in Girder 2

For two span structures, when the program envelopes maximum and minimum results, the two-design truck scenario is only considered for negative moment response and reaction. All other force effects are computed for single truck placements.

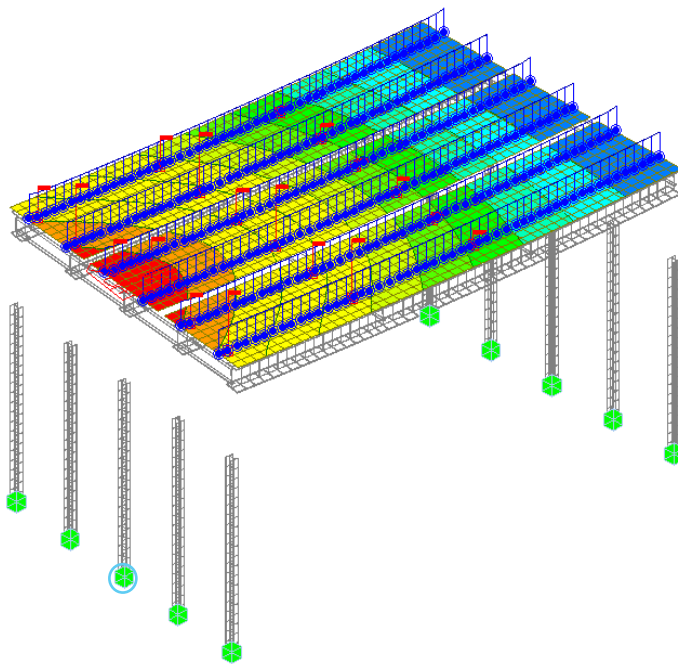


Figure 2-4: Live Load Application to Maximize Center Pile Reaction

Design lane designations (12 ft.) were defined for each model case, with loaded lane placement (10 ft.) varied within the design lane width in accordance with AASHTO LRFD Guidelines. Live Load Truck paths were located within each lane and a live load generator was utilized to determine the truck placement producing the largest force effect for the element or response in question. Similarly, any combination of 0-3 lanes were loaded to produce the maximum (or minimum) response as appropriate.

Figure 2-3 shows the influence surface, lane loading, and truck placement to maximize the strong axis bending response at a specific member near midspan within Girder 2 (member 12020) (see Figure 2-1 for girder numbering in the cross Section). For this girder, the 2 lanes loaded with a multiple presence factor of 1 controlled the response.

Figure 2-4 shows the influence surface, lane loading and truck placement to maximize the reaction at the base of the center pile at abutment 1. Note that plate members are not represented graphically in this image, as the reaction response at the pile base is the response at the base of a beam member, and only beam members are shown. For this case, all three lanes loaded with a multiple presence factor of 0.85 controlled the design.

2.3.4 BACKFILL SOIL SPRINGS

Compression only soil springs were utilized behind the abutments and wingwalls. Midas uses the Lehane Approach to spring stiffnesses. In order to ascertain how this approach corresponds to other guidance, a study was completed that considered the Caltrans soil spring stiffness and MassDOT soil spring stiffness approaches. The user input values for the Midas spring stiffnesses were then calibrated to provide agreement with traditional approaches.

The Caltrans application of soil springs was developed based on the maximum passive pressure response that the structure would experience during an earthquake. In version 1.7 of their Seismic Design Criteria (SDC) (April 2013), the spring stiffness was based off an initial stiffness of 50 kips/inch/foot of wall if Caltrans Standard Specifications were met for backfill. This value was halved to 25 kips/inch/foot for all other backfills. Both of these levels of stiffness were included for the SDC 1.7 calculations, which assumes the springs are oriented in the bridge longitudinal direction, independent of skew. Within this calculation an effective displacement at the idealized yield point is calculated as the maximum passive pressure force divided by an effective spring stiffness. The ratio of the thermal displacement to this effective displacement is then calculated to obtain an abutment displacement coefficient. If this coefficient is less than 2, the elastic response of the structure is assumed to be dominated by the stiffness of the abutments themselves. For coefficients greater than 4, the elastic model is insensitive to the abutment stiffness. For the thermal displacements effective for this study, all coefficients were less than 1, indicating the stiffness of the abutment controls the response. Therefore, this result is not directly comparable to a flexible abutment response condition but is included for information.

Version 2.0 of the Caltrans SDC (April 2019) revamped the approach and included a skew reduction factor for skews < 66 degrees. The equations utilized to develop the abutment springs are empirically based but are still intended to provide passive pressure responses. These calculations were run for the three skew iterations that have been included in this research effort (0, 10, and 20 degrees from radial).

The MassDOT LRFD Bridge Manual approach to soil spring stiffness for integral abutments is based on the actual mobilized earth pressure due to thermal expansion, which is between at-rest and passive levels of force (as opposed to Caltrans, which assumes the maximum passive pressure is present). The MassDOT spring values are expected to be generally lower than the Caltrans values, but more representative of the soil response to non-seismic loading and integral abutment behavior.

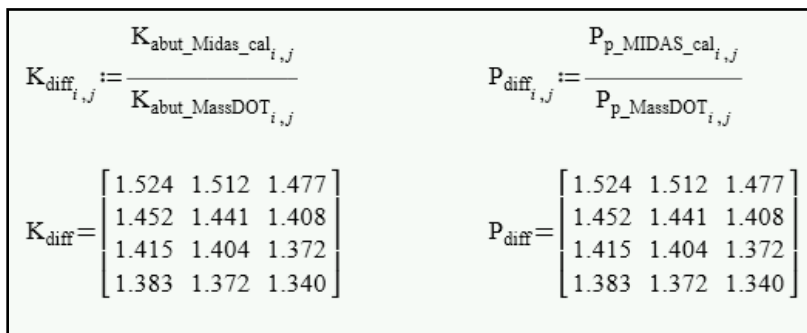


Figure 2-5: Numerical Comparison of Midas and MassDOT Spring Calculations

The modeled springs should fall within the range of values calculated by these various methods. The MIDAS inputs for soil springs include the void ratio and specific gravity of the backfill, a cycling factor, and thermal displacement. Abutment backfills are relatively consistent in the Northeast, and a void ratio of 0.26 and specific gravity of 2.423 were used to mimic typical bridge approach conditions. The thermal range is also known. The intent of the cycling factor is to capture ratcheting effects as the soil expands and contracts. The default value of 2 produces extremely high stiffnesses on the order of 3x the largest Caltrans spring stiffness. This value was adjusted to calibrate the springs to provide a minimum of 30% increased stiffness over the MassDOT approach to consider ratcheting is occurring. The ratio of the force value and the corresponding ratio of stiffness values (Midas/MassDOT) is the same for all data points, as shown in Figure 2-5.

The calibrated MIDAS full abutment spring stiffness, as shown in Figure 2-6, falls between the MassDOT and Caltrans effects. As evident in Figure 2-7, the total abutment force between the calibrated MIDAS and MassDOT approaches is similar. The differences in the spring stiffnesses between the two appear exaggerated, however this is the result of a nonlinear relationship between force and displacement in the Caltrans approaches. In each of these charts, the 3 lines for Caltrans 2.0 indicate the values for 0-, 10-, and 20-degree skews.

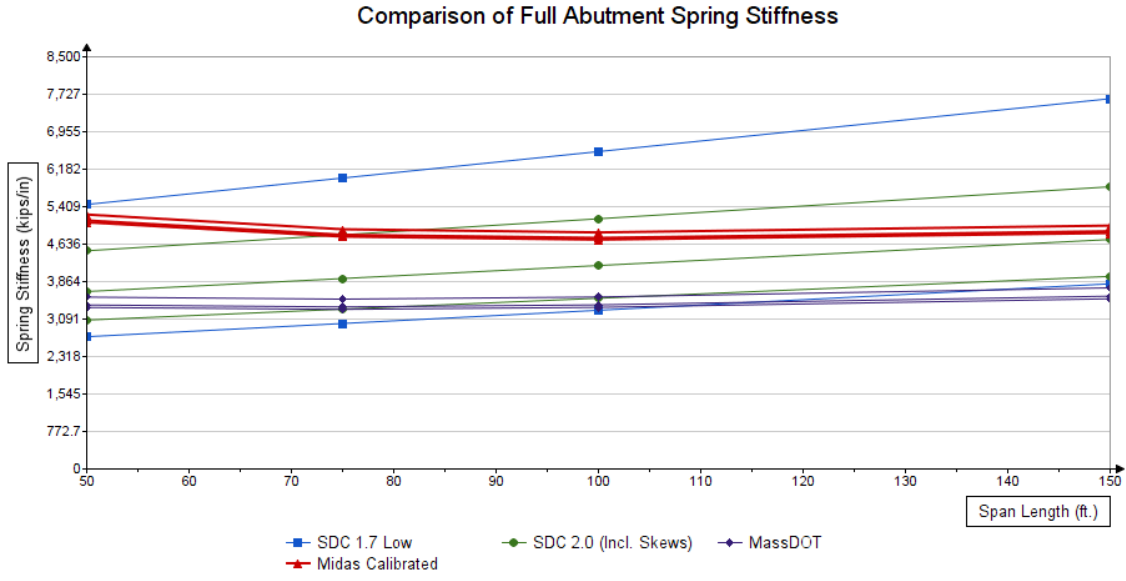


Figure 2-6: Comparison of Full Abutment Stiffness

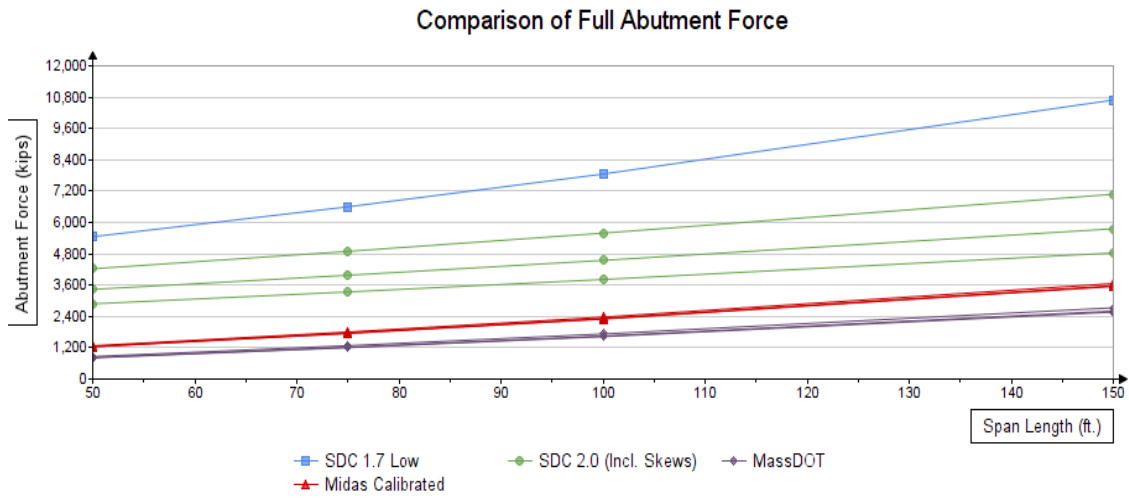


Figure 2-7: Comparison of Mobilized Soil Force on Abutment

2.4 ANALYSIS

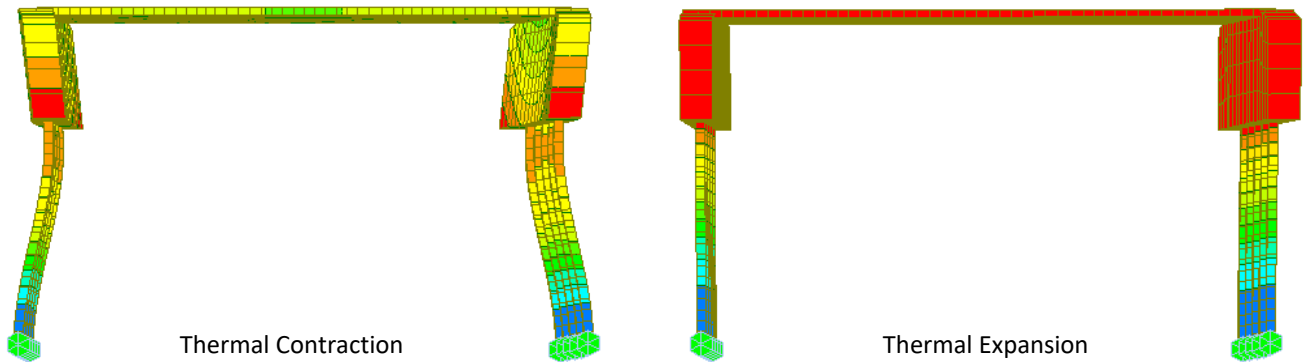


Figure 2-8: Typical Displacement Contour for 50 ft. Spans

All

analyses were completed utilizing a live load generator and construction stage manager in a cumulative static fashion. Nonlinear analysis, including P-delta effects was not incorporated. Therefore, extreme displacements that may be shown in the data results are indicative of a bridge system failure and should not be interpreted as “real” displacement. The intention is to limit the simplified parameters to bridges that are producing expected displacements and force effects in the system. Further research may be used to refine the final results of this study and may utilize nonlinear analysis approaches. In all cases, soil springs are compression only springs that do not engage for movements away from the backfill. This type of spring is considered a nonlinear spring in some finite element packages, requiring a nonlinear analysis be completed. This is not the case for MIDAS Civil and engagement of the springs for expansion cases only was observed amongst the cases, as evident in the displacement contours shown in Figure 2-8. The compression spring iterations were capped at 20 with a convergence tolerance of 0.001.

Time-dependent effects were applicable for properties in the deck but are not a critical component of this analysis considering that no concrete beams were considered applicable for simplified design in curved structures. Equivalent stresses for Von-Mises effects and maximum shear were calculated.

All results provide the maximum or minimum value of the force effect in question for a given model component. Displacement, force, and stress outputs are non-concomitant.

3 FINITE ELEMENT STUDY RESULTS

The following series of results is broken down by the various parameters under consideration for limitations of the simplified design method (Radius, Skew, Pile Length, Pile Orientation, and Wingwall Orientation). Various system responses are provided within each of these sections. The intention is to segment the data into individual sections for ease of discussion and understanding. Within each section there are multiple charts, which presents a representative sample of the data sets. The charts presented are not all inclusive of the entire set of data given space limitations and readability.


A series of shorthand has been developed to reduce the amount of text required in the legends to identify the various cases. Table 3-1: identifies the notation used in the charts that are presented in this section of the report.

Pile Unbraced Length		Skew (from Radial)		Wingwall Orientation		Pile Orientation	
Key	Description	Key	Description	Key	Description	Key	Description
P1	10 ft. Pile	S0	No skew (radial)	In	In-line Wingwall	W	Weak Axis (Pile Web perpendicular to girder)
P15	15 ft. Pile	S1	10 degrees	U	U-Wingwall	S	Strong Axis (Pile Web in line with Girder)
P2	20 ft. Pile	S2	20 degrees				
P3	30 ft. Pile						

Table 3-1: Chart Key Descriptions

Similarly, a system of color coding and symbology was utilized to maintain consistency amongst the data set. This system is identified in Table 3-2.

Table 3-2: Chart Symbology Descriptions

Span and or Radius		Pile Length and Skew		Wingwall and Pile Orientation	
Color Range	Description	Symbol	Description	Symbol	Description
	Smallest Value	•	10 ft. pile or 0 degree skew	●	Inline Wing, weak axis pile
		◆	15 ft. pile	▲	Inline Wing, Strong Axis Pile
		▲	20 ft. pile or 10 degree skew	■	U-wing, weak axis pile
	Largest Value	■	30 ft. pile or 20 degree skew		

3.1 GENERAL STRUCTURE PERFORMANCE

Prior to evaluating bridge behavior based on the various parameters, a series of sanity checks were completed to ensure that the model results were producing the expected responses. A portion of these checks are described below to provide confidence in the modeling approach.

To check the application of thermal loads, the total displacement contour (xyz) was observed to ensure the bridge moves inward (contracts) due to thermal loss, and that the bridge moves into the soil mass (expands) during thermal gain. Due to the activation of soil springs in the expansion condition, a noticeable non-axial impact on the superstructure should be observed. These trends are confirmed as shown in Figure 3-1.

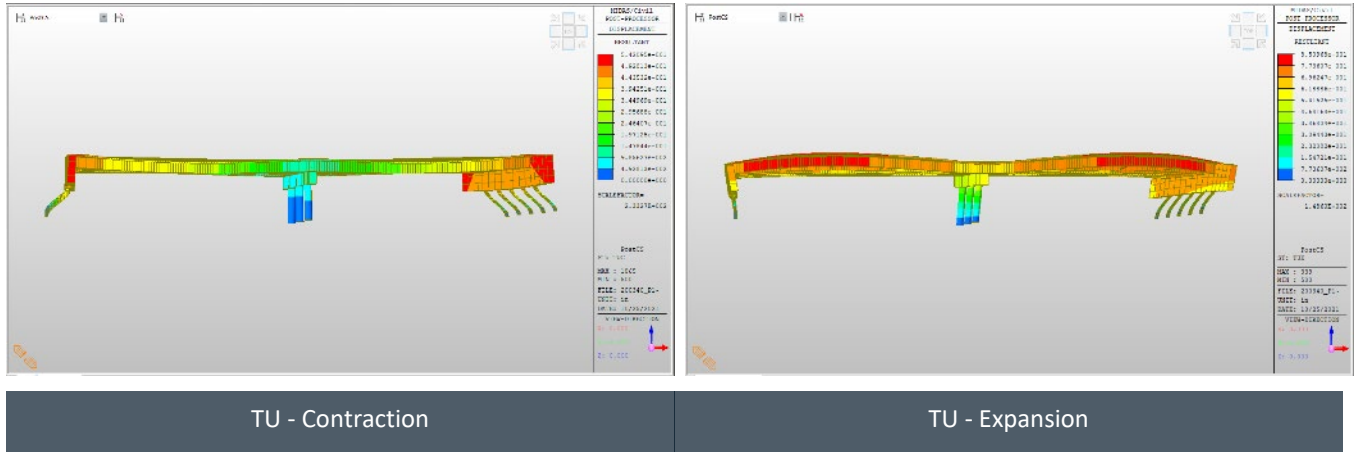


Figure 3-1: Deformation Contours for Thermal Responses

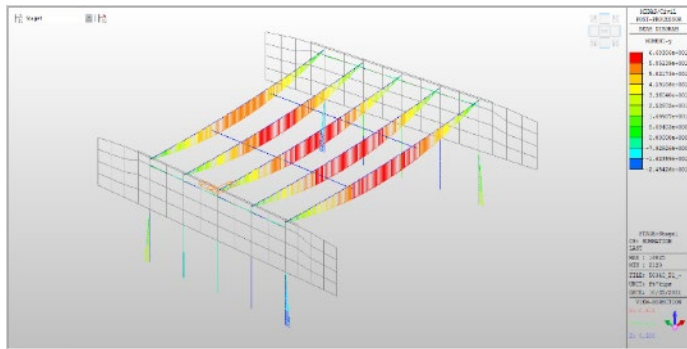


Figure 3-2: Stage 1 My Results - Bending about Transverse Bridge Axis w.r.t. Local Girder Axis

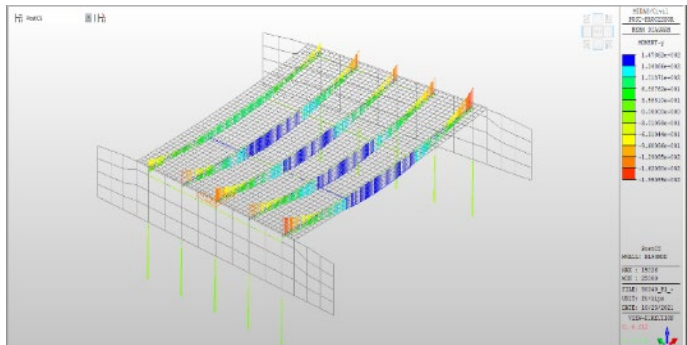


Figure 3-3: Stage 4 My Results - Bending about Transverse Bridge Axis w.r.t. Local Girder Axis

To check the construction stage manager, the bending moments in both the girders and the piles were observed in various stages of loading. Prior to deck curing, the bridge should function as a simply supported structure (Figure 3-2) with no moment transfer to the piles (Figure 3-4). After deck cure, negative moments should be seen at the girder ends (Figure 3-3) and moment transfer should be evident by bending in the piles (Figure 3-5). These trends are confirmed. Also evident in these images is the increase in moment on the exterior most girder when compared to the girder on the inside of the curve. This is a function of the increased arc span length as the radius increases toward the outside of the curve.

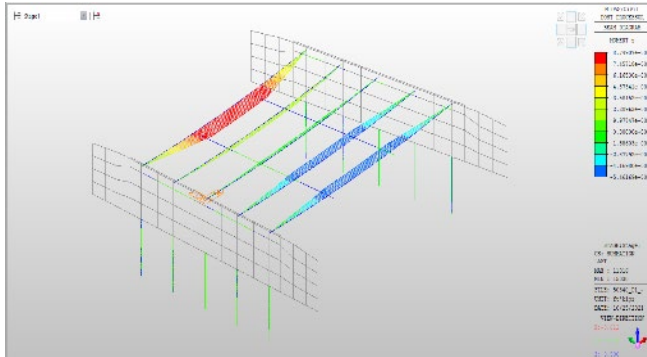


Figure 3-4: Stage 1 Mz Results - Bending about Transverse Bridge Axis w.r.t. Local Pile Axis

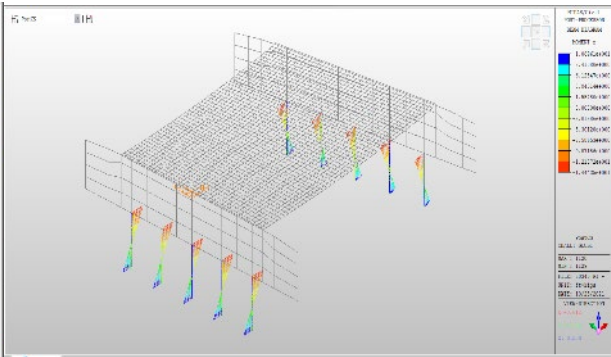


Figure 3-5: Stage 4 Mz Results - Bending about Transverse Bridge Axis w.r.t. Local Pile Axis

Two-span configurations were checked for the same parameters and showed expected trends, including negative moments over the piers, as shown in Figure 3-6, which shows the beam bending moment envelope (max positive and max negative) for the strength 1 load combination. Negative moments are observed over the piers and the girder ends, with the largest moments occurring on the exterior most (longest) girders. The extension of negative moment into the spans is also observed by plotting the envelope of the moment for various truck placements and thermal conditions.

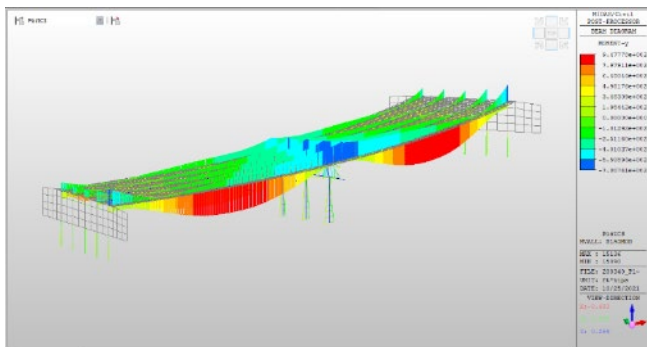


Figure 3-6: 2-Span Continuous Beam Flexure Envelope

Additionally, a stress check was performed for the central girder at stage 1 for its self-weight with simply supported boundary conditions. The stress value in the bottom flange at midspan for the 100 ft. span with a 1500 ft. radius was hand calculated at 2.61ksi, and the output from MIDAS for the same case was also 2.61ksi, indicating that simply supported behavior was occurring in stage 1.

3.2 THERMAL MOVEMENT

Thermal movement in integral structures produces force effects throughout the system, with the superstructure acting as a strut between the two abutments. The abutments and piles act as vertical legs in a frame. Thermal expansion is resisted by the backfill, resulting in smaller total movement but increasing force effects in the superstructure. Thermal contraction is only resisted by the stiffness of the vertical legs of the frame (no soil engagement) and the resistance provided by the strut (superstructure), resulting in greater total movements and increasing force effects in the piles.

For curved structures and skewed structures, lateral components of thermal movement can be substantial, and result in damage or serviceability issues in supporting components, joints, and bridge rail. Skewed bridges often experience significant diagonal movement, introducing large transverse movements. Sharp curvature may result in excessive lateral thermal forces at supports when movement is restrained.

The width of a structure also impacts thermal movements in the lateral direction. This is particularly true in skewed conditions. A typical two-lane highway with a total bridge width of 40 ft. was considered for this study. Wide structures with a curved alignment may experience complex thermal movements, which should be evaluated by refined methods. As such, a 50 ft. width limit has been placed on the simplified design guidelines until additional research can be completed in this area.

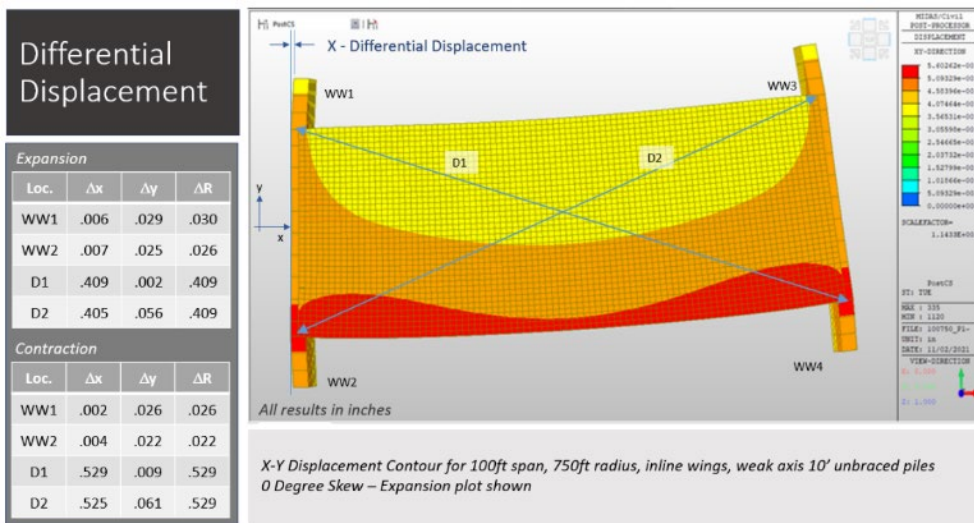


Figure 3-7: Resultant Displacements on 100 ft. Span, 0-Degree Skew

When movements occur along the diagonals between bridge corners, the effect of skew becomes amplified by one diagonal being longer than the other. For example, in Figure 3-7 the resultant displacement along the diagonals is the same for both diagonal 1 (D1) and diagonal 2 (D2), measuring 0.409 in. elongation for the expansion load case and 0.529 in. shortening for the contraction case.

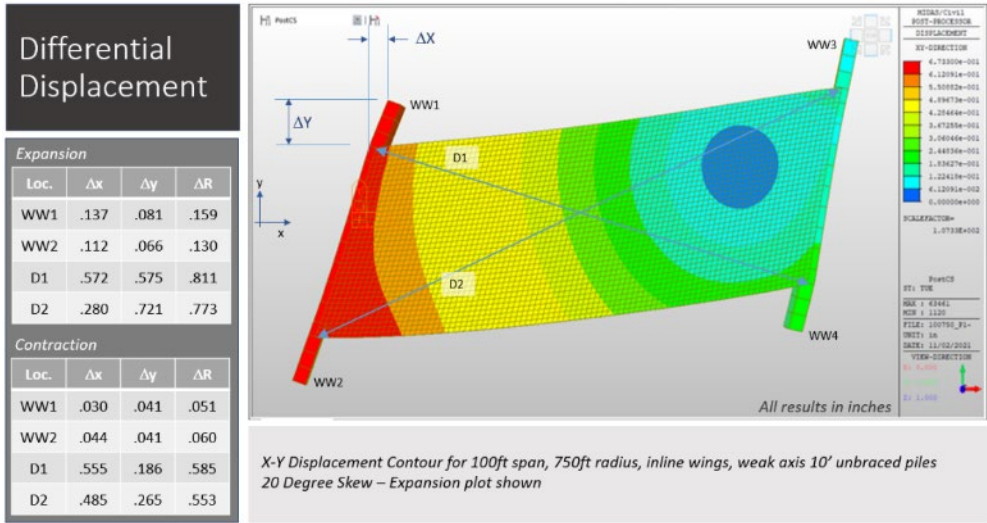


Figure 3-8: Resultant Displacements on 100 ft. Span, 20-Degree Skew

For the skewed case shown in Figure 3-8, a differential exists with larger diagonal displacements on all four measures (D1, D2, Expansion and Contraction) compared to the non-skewed condition, and nearly double the expansion movement along D1 compared to the non-skewed condition.

Note that this is the center of x and y movement, which is a planar measure, and does not align with the tangent chord of the structure. This is indicative of greater translation (y-direction movements), which is very evident in the numerical data also shown in the above referenced figures.

A similar exercise was completed for the 200 ft. multi-span structure (also 100 ft. individual span lengths with a 750 ft. radius, in-line wings, and weak axis pile orientation for 10 ft. piles) with similar results observed, as shown in Figure 3-9 and Figure 3-10. A shift in the center of movement is evident as well, with the displacement center near midspan and toward the inside of the curve for the non-skewed condition, and a shifted center on the skewed cases.

Attention to the delta y values should be given to both figures above. The lateral movement increases dramatically in the skewed case compared to the non-skewed case. Additionally, the movement in the direction of the D2 diagonal is approximately half of that for the D1 diagonal for the 20-degree skew expansion condition.

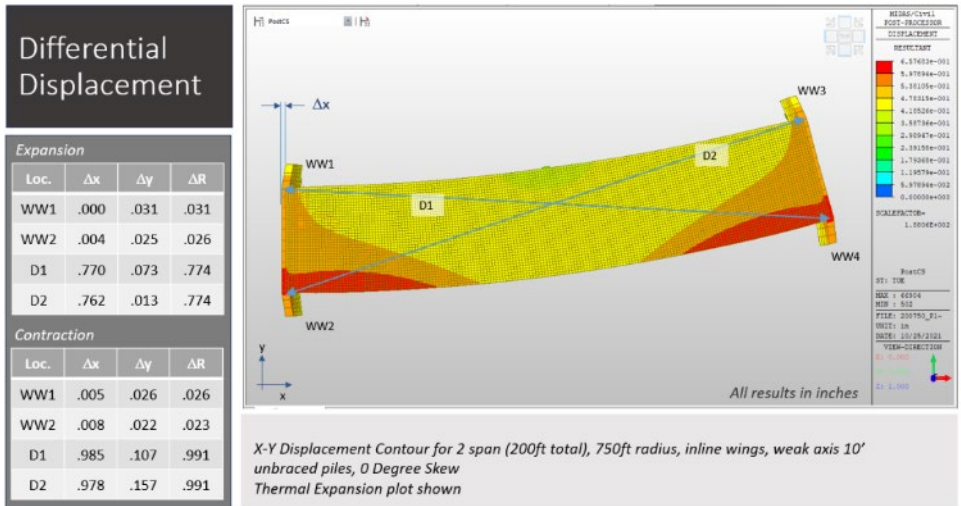


Figure 3-9: Resultant Displacements for 200 ft. Series, No Skew

The stark increase in the lateral movement is noted for the contraction case as well, but the delta X movements are very similar on the two diagonals. This occurrence is due to the lack of soil engagement. As the soil engages to resist thermal expansion, the structure will respond by warping, twisting out of plane, or kicking laterally along the path of least resistance.

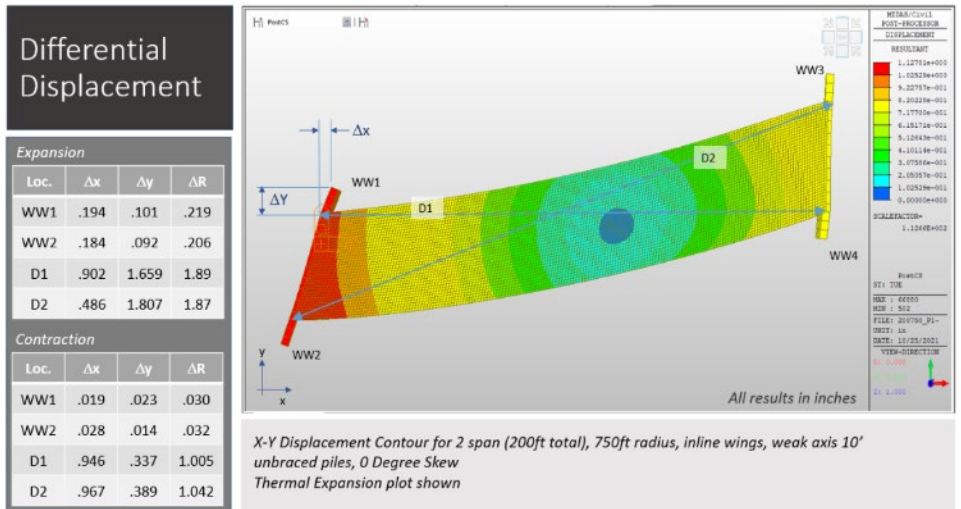


Figure 3-10: Resultant Displacements for 200 ft. Series, 20-degree Skew

This is evidenced by the fact that expansion along the D2 diagonal in this case would tend to push the abutments *across* their soil mass where movement is resisted by friction between the backfill and abutment stem, as opposed to directly into them where movement is resisted by passive pressure in the backfill, as the D1 diagonal does. Hence the large difference in values for the expansion case. For thermal contraction, there is no corresponding resistance of the soil and thus no response of the structure due to its restraint. As such, the delta x values are simply a function of the total length along the diagonal, resulting in deltas that are relatively similar, with D2 being only slightly longer than D1.

3.3 PILE HEAD DISPLACEMENTS

All displacement data shown in this section are taken with respect to the global axis system. At abutment 1 with no skew, this corresponds to global x displacements being representative of longitudinal bridge movement, and global y displacements being representative of lateral movement along the transverse bridge axis. All displacements are reported in inches and are recorded at the top of the piles. Results at Abutment 2 will be skewed with respect to the x-y plane.

3.3.1 BY RADIUS

Figure 3-11 shows scatter plots of abutment 1 pile head displacements for cases with 10 ft. long piles, 0-degree skew angles, In-line wingwalls, and weak axis pile orientation across all bridge lengths and curve radii subject to the expansion load case. For these cases, the global y direction aligns with the transverse bridge direction and is parallel to the abutment. The groupings of colors represent the five pile head results plotted together. Displacements in the negative x direction indicate movement of the abutment into the soil due to expansion. Displacements in the negative y direction indicate movement toward the outside of the curve.

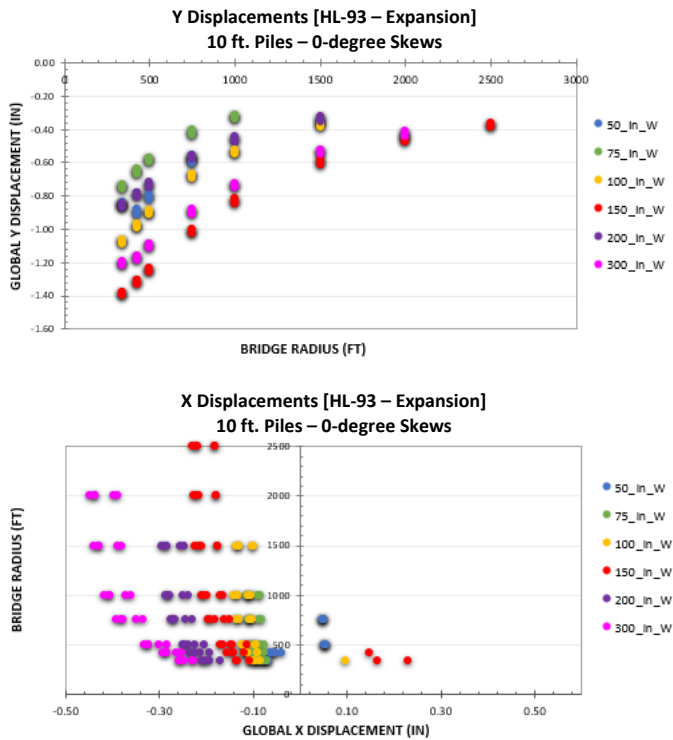


Figure 3-11: Span vs. Radius Displacements – Expansion

This plot shows how curve radius impacts the magnitude of transverse pile displacement during bridge expansion. There is a measurable increase in displacement magnitude as the radius decreases, ranging from approximately 0.4 in. to 1.4 in. for the 150 ft. bridge lengths. As the bridge tries to expand, the soil engages, and forces movement out laterally. In all conditions, the tighter radii exhibit slightly higher lateral displacements than broader radii. This trend is consistent and expected. As the radius of curvature decreases, the thermal outward kick is emphasized. The corresponding longitudinal displacements (global x) display a reduction in magnitude for shorter radii. This indicates that as the radius tightens, the primary mode of displacement for

bridges with in-line wingwalls is in the transverse direction. Note that in some cases the longitudinal displacement reverses direction. This may be attributed to abutment rotations due to extreme horizontal displacements.

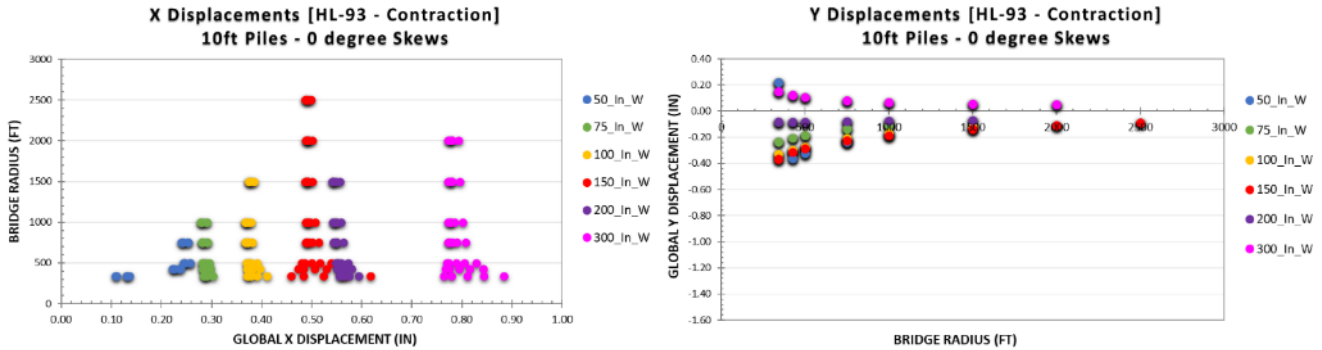


Figure 3-12: Span vs. Radius Displacements – Contraction

Figure 3-12 shows similar plots to Figure 3-11, except the models are subject to the contraction load case. The longitudinal displacements (global x) are nearly independent of curve radius and have a slightly larger magnitude as compared to the expansion case. This is attributed to the soil resistance to expansion resulting in smaller magnitudes in that direction. The spread of data points at the smaller radii for contraction can be attributed to the greater difference in girder arc length between Girder 1 (interior) and Girder 5 (exterior). The transverse displacements (global y) show a considerably smaller magnitude as compared to the expansion case. This is an expected result because the design process assumes no active pressure from the abutment backfill during contraction.

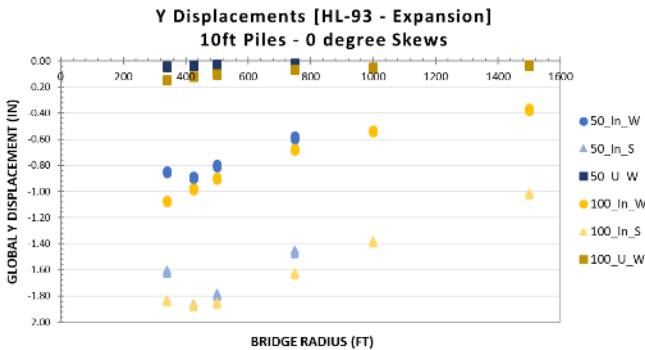
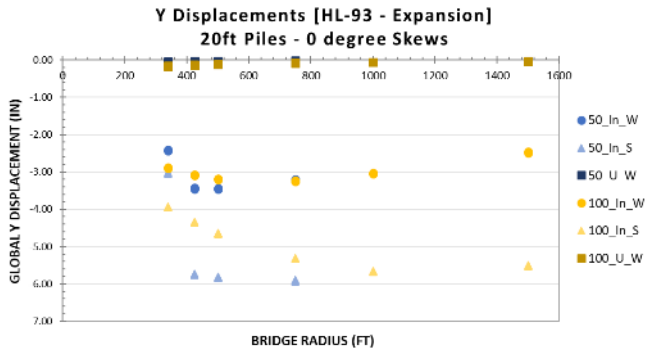


Figure 3-13: Span vs. Radius Displacement Comparison of Wingwall and Pile Orientation

3.3.2 BY PILE ORIENTATION AND WINGWALL ORIENTATION

Figure 3-13 shows scatter plots of transverse pile head displacements from 50 ft. and 100 ft. bridges with combinations of in-line wingwalls with weak axis piles, U-wingwalls with weak axis piles, and in-line wingwalls with strong axis piles. The y-axis shows the transverse displacement due to the expansion load case, and the x-axis shows the corresponding bridge radius. Each plot displays a different pile cantilevered length ranging from 10 ft. minimum to 30 ft. maximum for 0-degree skew angles.



In all cases, U-wingwall orientations display minimal transverse movement when compared to in-line wingwall cases. This may be attributed to the integral U-wingwalls engaging the backfill soil springs to restrain movement in the transverse bridge direction.

The strong axis pile orientation consistently results in the largest magnitude lateral displacements when compared to the weak axis pile cases. This is expected behavior because the weak axis piles provide more stiffness in the transverse direction. The difference in magnitude decreases as pile cantilever length increases, which is expected because the length variable is cubed in the cantilever deflection equation, and therefore will have a greater effect on the structure response. See Section 3.3.4 for more discussion on effects of pile length.

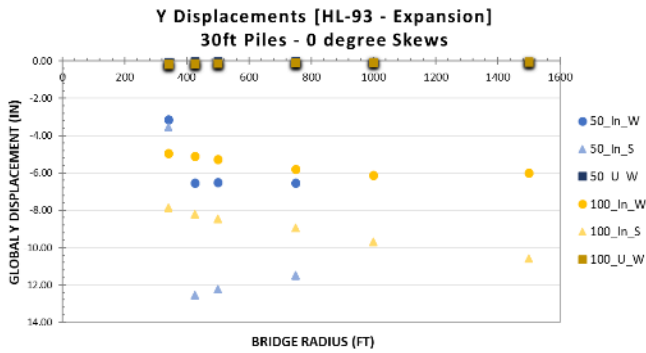


Figure 3-14: Longitudinal and Transverse Displacement Comparison of Wingwall and Pile Orientations

The expected unrestrained longitudinal thermal displacements of the 50 ft. and 100 ft. bridge lengths are approximately 0.25 in. and 0.5 in. respectively based on a 125-degree thermal range for steel. In all cases, the U-wingwalls result in transverse displacements less than the free longitudinal expansion, indicating that the primary direction of movement remains in the longitudinal direction for expansion load cases. The in-line cases with piles oriented in the weak axis direction result in displacements up to and exceeding the expected unrestrained thermal displacements, and all in-line cases with strong axis piles result in transverse displacements beyond the expected longitudinal. This indicates that the primary direction of movement of the abutment is in the transverse direction.

Figure 3-14 displays a series of plots showing the abutment 1 pile head displacements from expansion and contraction loads. Each axis on the charts has been scaled for direct comparison between the two load cases and the expected unrestrained longitudinal displacement has been plotted on the x displacement charts.

The U-wingwall cases exhibit the greatest magnitude of longitudinal displacement during the expansion load case with lesser magnitudes exhibited from the in-line wing cases. All cases show a significantly smaller magnitude of longitudinal thermal expansion compared to the expected unrestrained displacement which is a result of the backfill passive pressure resistance. During the contraction case, the longitudinal displacements approach the magnitude of the expected unrestrained displacement which is expected behavior since the backfill does not restrain movement in this direction. U-wingwalls and in-line wingwalls with weak axis piles exhibit similar displacements, with significantly smaller magnitudes resulting from the in-line wingwall with strong axis pile cases. This is due to the strong axis piles providing more restraint in this direction.

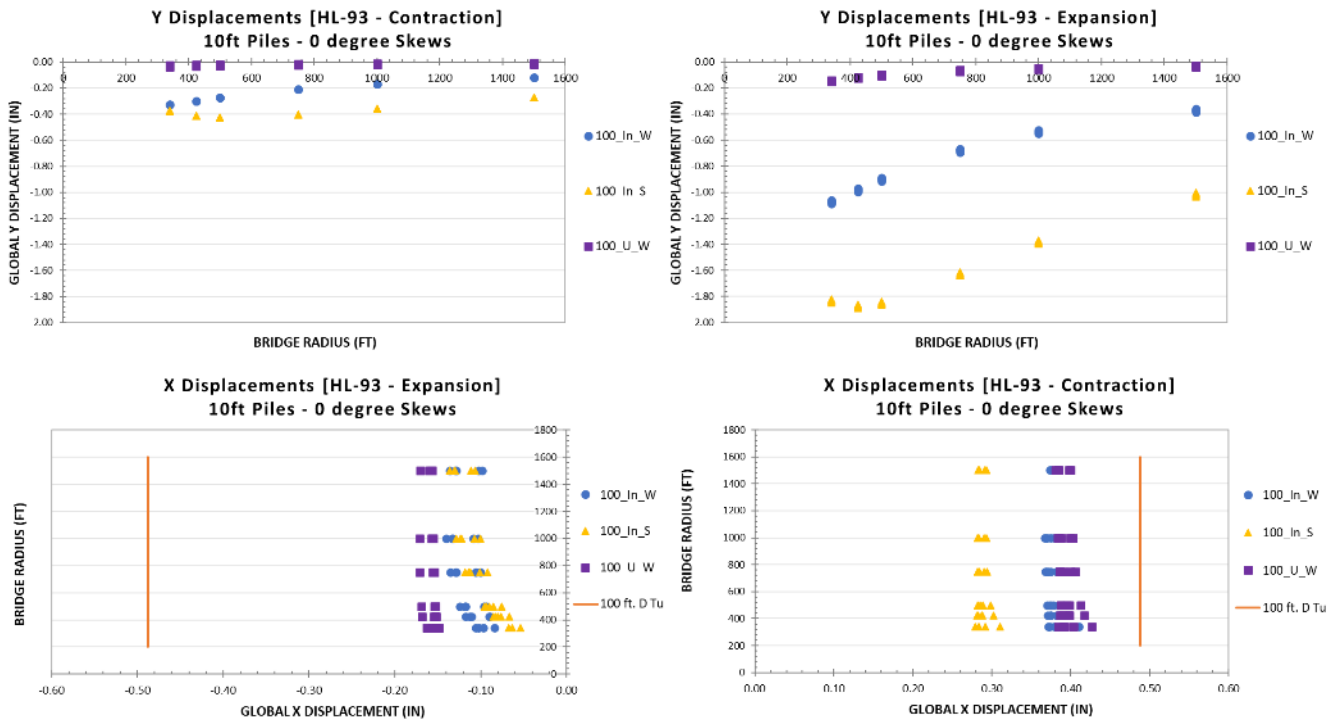


Figure 3-15: Longitudinal and Transverse Displacement Comparison by Skew

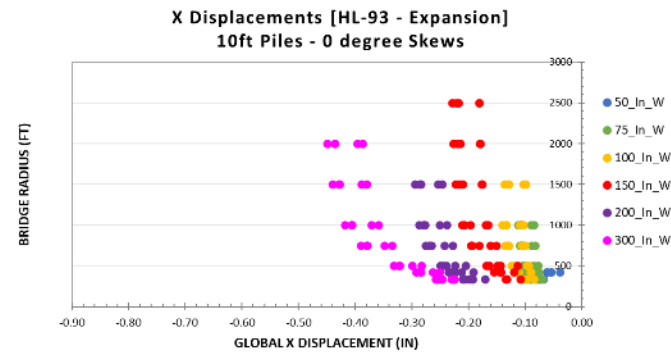
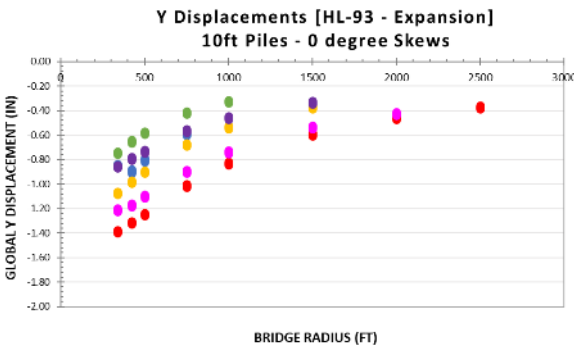
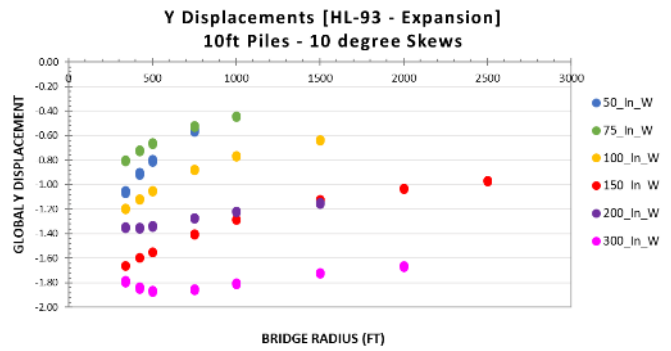
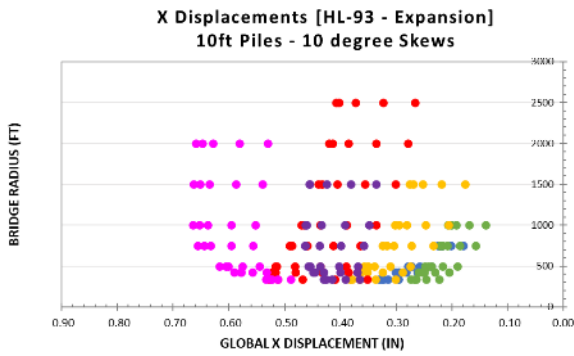
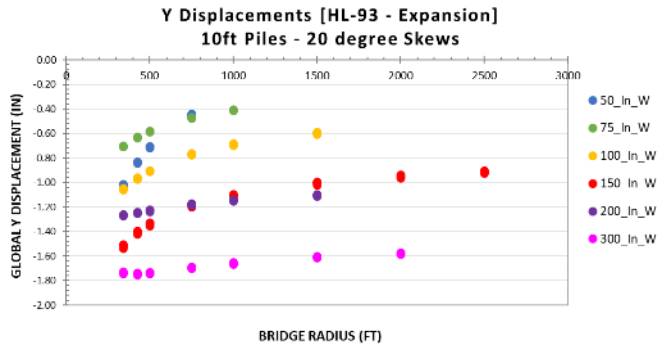
The transverse displacements (global y) resulting from expansion are greatly affected by the wingwall and pile orientation as discussed previously. In the contraction case, the magnitudes of transverse displacements are much smaller than those resulting from expansion. This difference is a result of the backfill passive pressure restraining longitudinal expansion and forcing the bridge to displace toward the outside of the curve. The contraction case does not experience this soil interaction and therefore results in significantly smaller displacements. In all cases, the U-wingwall orientation exhibits the smallest magnitude of transverse displacement and the strong axis piles result in the largest magnitude of transverse displacements for the 10 ft. pile cases.

3.3.3 BY SKEW

As discussed in Section 3.2, thermal movements in skewed structures happen along the diagonals between the acute corners (long diagonal) and obtuse corners (short diagonal). In curved integral abutment bridges with skew, the transverse displacements are compounded between the curve effects discussed in Section 3.3.1 and the skew effects. In this study, the acute corner on the outside of the curve is placed at abutment 1 and the acute corner on the inside of the curve is placed at abutment 2. During the expansion case, it is observed that the bridge moves toward the outside of the curve. It can be expected that during the expansion load case, the acute corner at abutment 1 will result in the largest magnitude of transverse displacement. At abutment 2, the skew and curve effects on expansion counteract each other and result in a smaller net transverse displacement.

Figure 3-15 displays a series of charts plotting longitudinal displacements (left column) and transverse displacements (right column) of abutment 1 piles for bridges with in-line wingwalls. The bridge skew angle increases from 0-degrees to 10-degrees to 20-degrees in each row with corresponding cases plotted in each chart. The axis scales have been set to be equal in all charts for a direct magnitude comparison between each chart. The clusters of same-colored data points for each radius represent each of the five pile heads. Note that these are global displacements and therefore do not align with the centerline of the abutment in the skewed cases.

APPENDIX D – TECHNOLOGY TOOLBOX



The primary observation from these charts is that the longitudinal displacements (global x) increase with increasing skew angle. The transverse displacements (global y) increase slightly from the 0-degree skew case to the 10-degree skew case, but remain fairly constant between the 10- and 20-degree skew angles. When these two displacements are combined, the result indicates an increasing net displacement along the abutment centerline, with the 20-degree skew cases exhibiting the greatest combined

APPENDIX D – TECHNOLOGY TOOLBOX

longitudinal and transverse displacement. This is expected behavior for curved integral abutment structures with skew since the curved and skew effects are additive.

This effect is also visible in the spread of the data points. In the 0-degree skew case, the longitudinal displacement data points are relatively clustered, indicating similar magnitudes across the piles. In the 10- and 20-degree skew cases, the data points are more spread, indicating that the piles are experiencing variable longitudinal displacements.

As discussed in Section 3.3.2, the wingwall and pile orientations have a significant effect on the pile head displacements. Figure 3-16 shows a similar layout of results to Figure 3-15, with a comparison of the U-wingwall and in-line wingwall cases and weak axis and strong axis pile cases for the 100 ft. bridge lengths only.

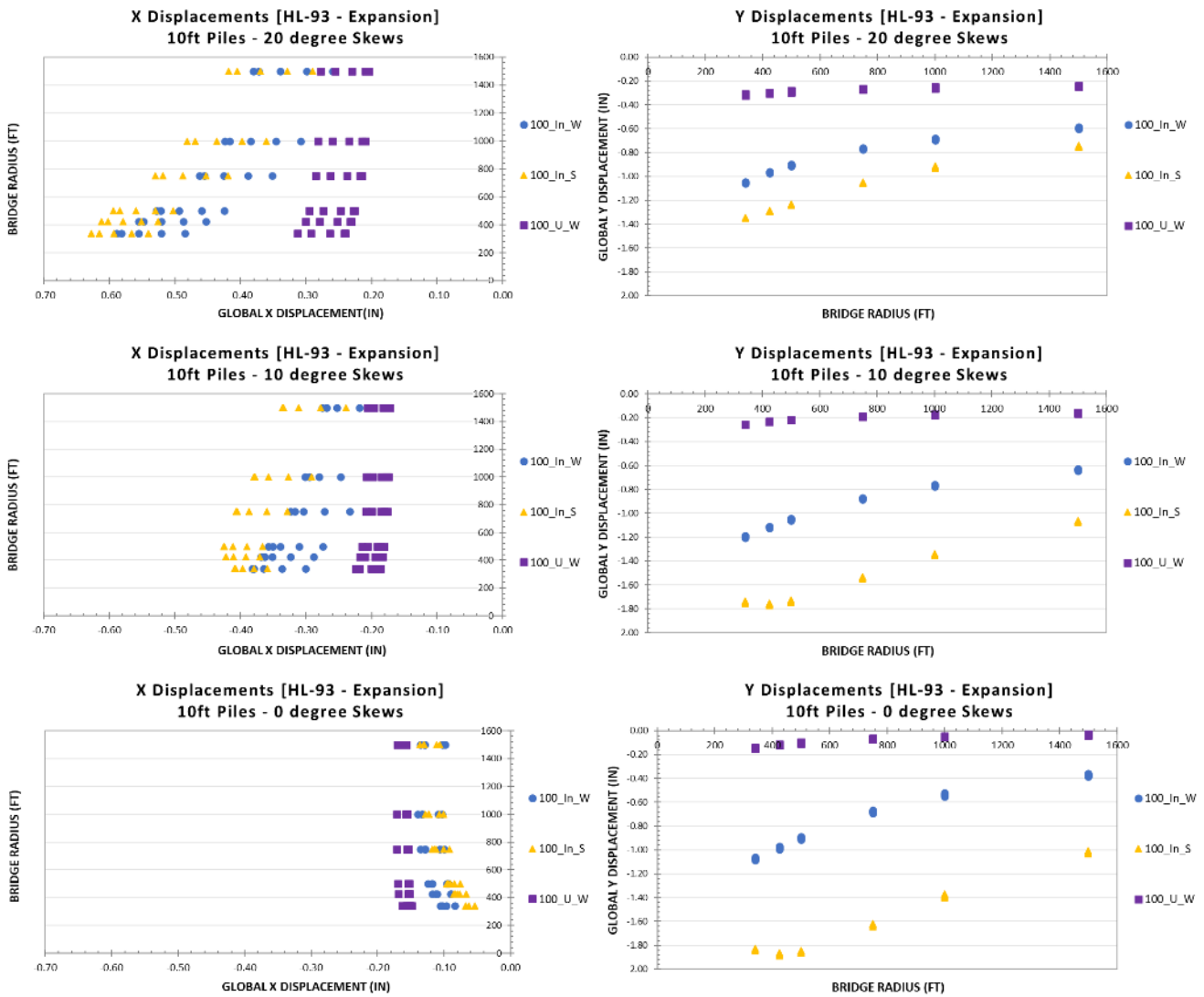


Figure 3-16: Displacement Comparison of Wingwall and Pile Orientation by Skew

Building off the previous discussion on the effect of skew angle on pile head displacements, the U-wingwall cases and strong axis pile cases exhibit the same trends in behavior as the in-line wingwall with weak axis pile cases. The same trends discussed in Section 3.3.2 are displayed here, with the U-wingwalls presenting the smallest magnitude of displacement of all orientations. The data points in the longitudinal displacement charts (global x) show a consistent trend of spreading as the skew angle

APPENDIX D – TECHNOLOGY TOOLBOX

increases, indicating that the primary mode of displacement is no longer in the global coordinates and shifts to align with the skew angle.

The expected unrestrained thermal expansion for a 100 ft. bridge is approximately 0.5 in. With an increase in skew angle, the net displacements for the in-line wing cases steadily exceed this magnitude, particularly with increasing curvature. The U-wing cases maintain a much more consistent longitudinal and transverse displacement, which increase with skew angle as expected.

Figure 3-17 provides charts plotting the global x-y movement of the pile heads at both abutments for 100 ft. bridge length cases. In all cases, the clusters of data on the left of the plot areas correspond to abutment 1, and the right clusters correspond to abutment 2. The left column of charts displays results for in-line wingwalls and the right column displays results for U-wingwalls. Skews increase from 0-degrees to 20-degrees in each row of charts, and colors represent changing radii.

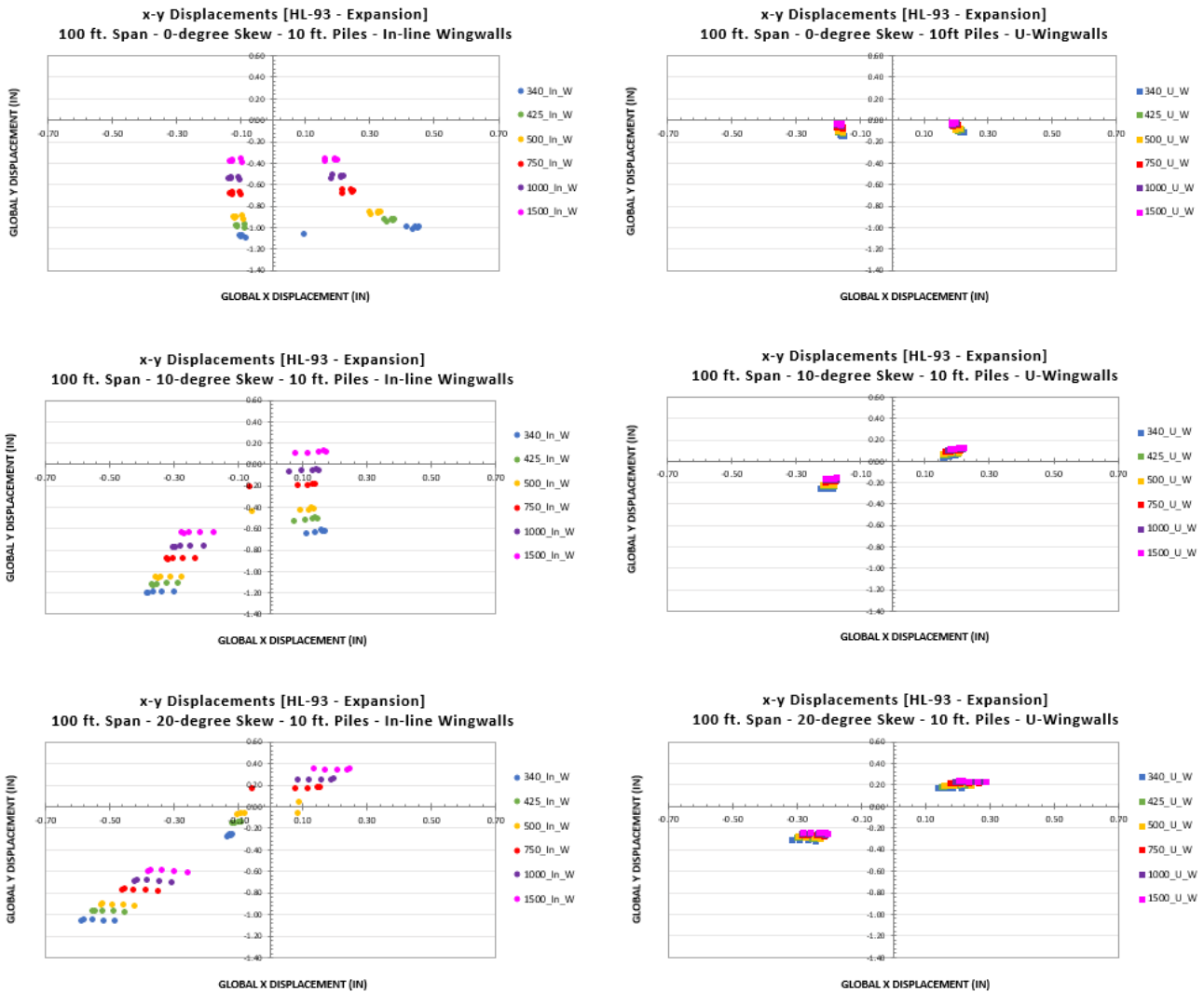


Figure 3-17: Displacement Comparison of Abutment 1 & 2 by Skew and Wingwall Orientation

As previously discussed, increasing skew angle results in an increase in net displacement at abutment 1, which is further compounded by decrease in curve radius. This is evident in the charts above. At abutment 2, however, the effects of curve radius and skew are opposing, with the radial effect moving the bridge toward the outside of the curve and the skew effect moving the bridge toward the inside of the curve. As skew increases for the in-line wingwall cases (left column), the abutment 2

APPENDIX D – TECHNOLOGY TOOLBOX

displacements shift toward the positive global y direction, indicating that in these cases abutment 2 is shifting toward the interior of the curve. This trend is significantly more apparent in U-wing cases, where the inward movement of abutment 2 is nearly the same magnitude as the outward movement of abutment 2 in the skewed cases.

In both in-line and U-wingwall cases, the transverse displacements at abutment 1 are more severe in the expansion case than abutment 2. In-line wingwall displacements are more heavily impacted by changing curve radius than the U-wingwall displacements as shown by comparing the tight spacing of curve radius data points in the U-wingwall case to the wide spacing of the in-line wingwall data points. This indicates that skew angle is a primary driver for pile head displacements for U-wingwalls, with curve radius presenting a secondary impact.

3.3.4 BY PILE LENGTH

It is expected that increasing the pile length will increase the flexibility of the frame in the longitudinal and transverse directions. Greater displacements are expected in the transverse directions for increasing pile length. However, for expansion cases, the longitudinal displacement is not expected to significantly increase due to the backfill soil resistance.

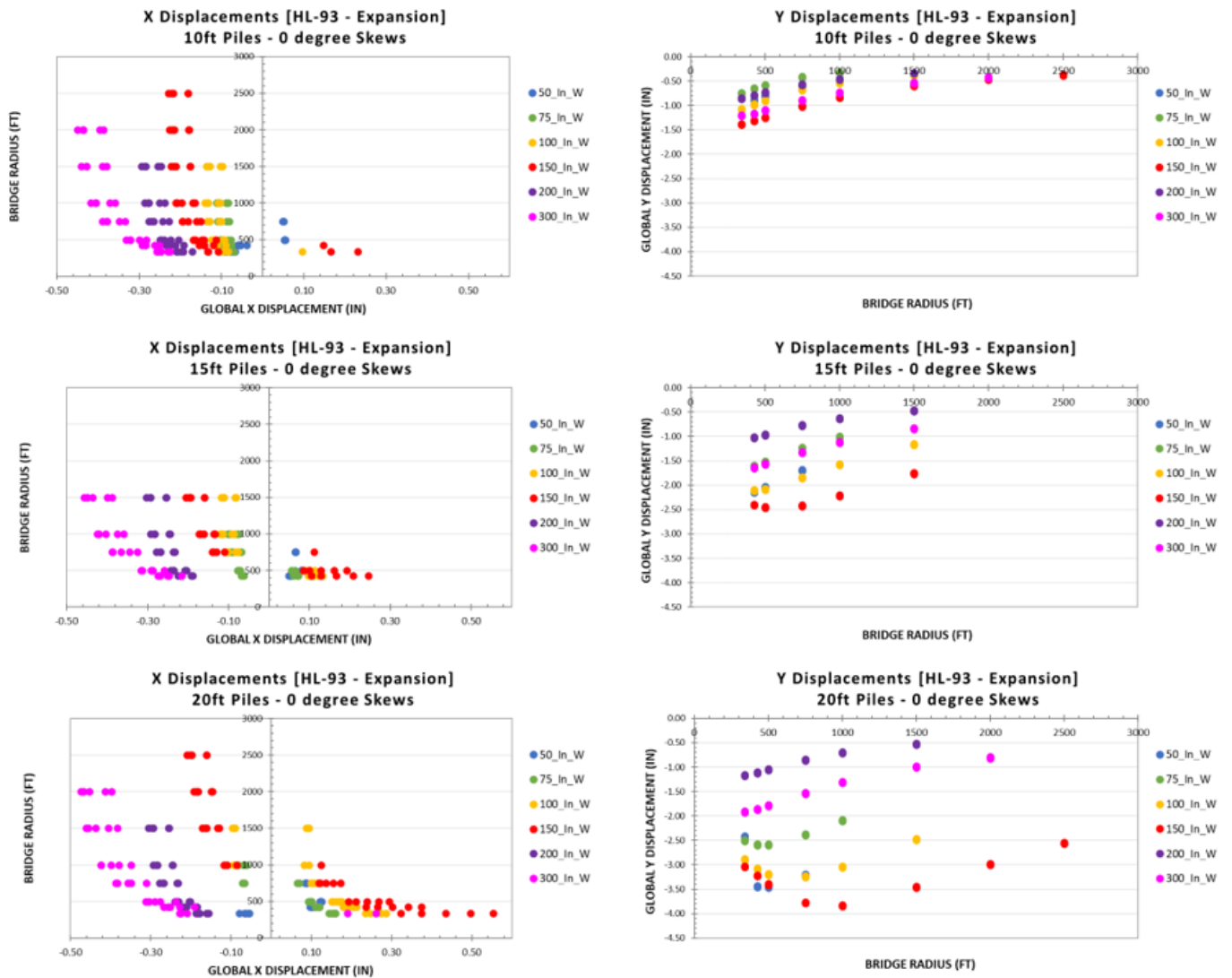


Figure 3-18 Displacement Comparison w.r.t Pile Length



APPENDIX D – TECHNOLOGY TOOLBOX

displays a series of charts which plot longitudinal (global x) and transverse (global y) displacements with respect to changing pile cantilever length. The longitudinal displacement charts show a consistent magnitude indicating that the soil pressure during expansion has the most significant effect. The transverse displacements are heavily influenced by the changing pile length for the in-line wingwall cases as they are the only component of the bridge which provides resistance in this direction. The 15 ft. and 20 ft. pile length cases result in up to 4 in. of transverse displacement, and are indicative of system failure for longer pile lengths and tighter radii. Given that a static analysis was performed, the analysis was not terminated or adjusted for geometric or material nonlinearity.

The effect of pile length on transverse displacement of the pile is significantly affected by the wingwall and pile orientations. This effect is shown in Figure 3-19 where the change in pile length from 10 ft. to 20 ft. results in a considerable increase in transverse displacement for the in-line wingwall cases compared to the U-wingwall cases. This trend is consistent across all parameter combinations and pile cantilever lengths.

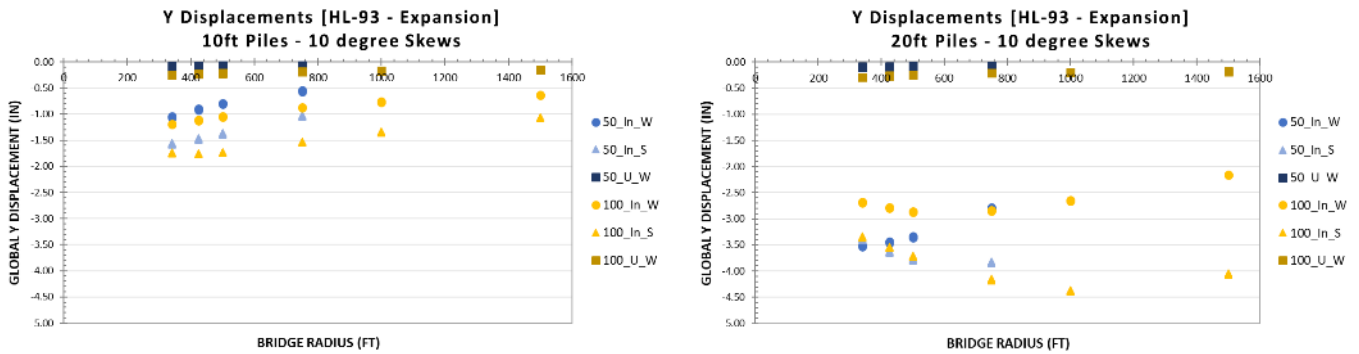


Figure 3-18: Transverse Displacement Comparison w.r.t. Pile Length and Wingwall and Pile Orientation

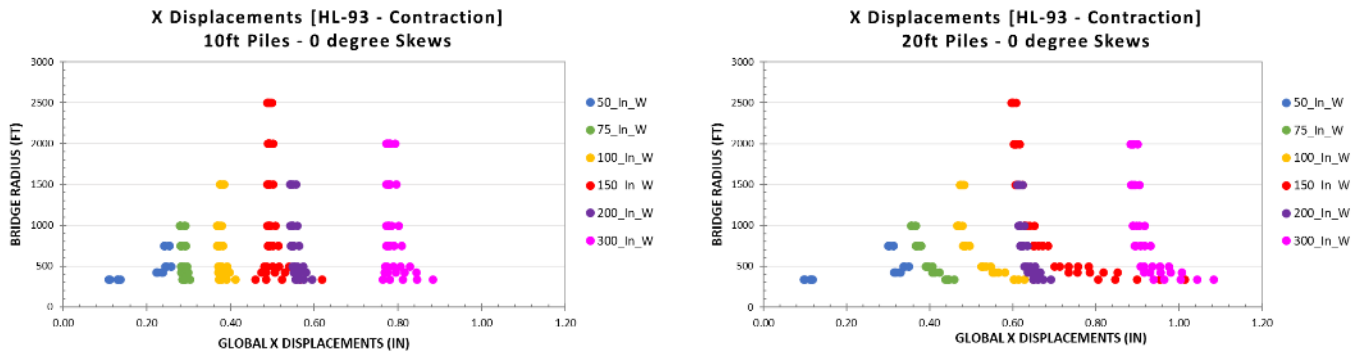


Figure 3-19: Longitudinal Displacement due to Contraction w.r.t. Pile Length

Changing pile cantilever length does affect the structure longitudinal displacements during the contraction load cases. This is expected behavior since the piles (and pier for two span cases) are the only components resisting this movement. Figure 3-20 displays this trend where small increases in longitudinal displacement magnitude are observed between the 10 ft. and 20 ft. pile cantilever lengths.

3.3.5 BY SPAN

Increasing bridge length naturally increases the overall demand on the bridge system. Longer bridge lengths result in greater magnitude unrestrained thermal displacements as well as greater loads on the piles. The two longest bridge lengths in this study are 200 ft. and 300 ft. cases, both of which are two-span structures. As the pier connection is fixed for translation, it can be expected that the pier would help reduce the bridge lateral movement.

When considering the two-span configurations it is helpful to remove unapplicable spans from the data set. For instance, the two-span 200 ft. cases should be compared to the 100 ft. single span cases, and the 300 ft. two-span cases should be compared to the 150 ft. cases. The 50 ft. and 75 ft. spans are not applicable to the study of the two-span behavior since they do not have a two-span equivalent. Figure 3-21 displays two plots with varying pile length of the above mentioned bridge lengths for comparison. Cases with 100 ft. span lengths have been colored blue and cases with 150 ft. span lengths have been colored red.

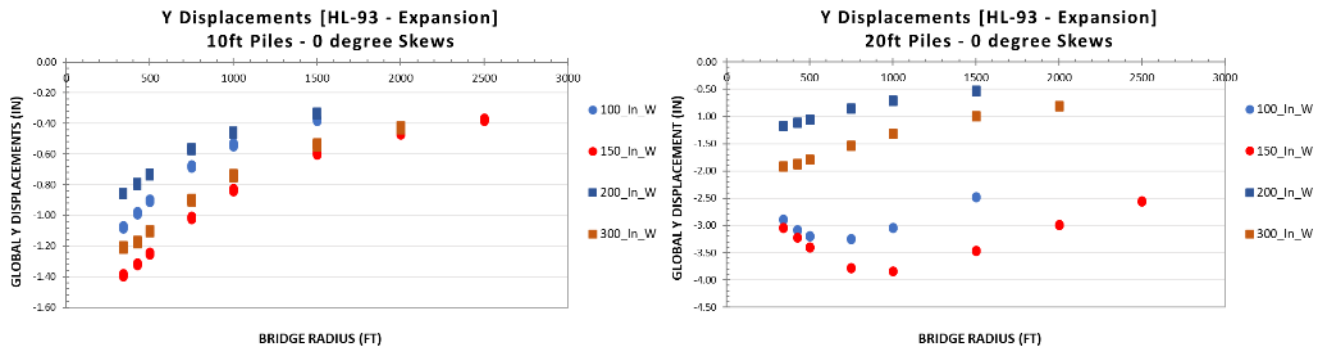


Figure 3-20: Transverse Displacement Comparison w.r.t. Span Configuration – Expansion

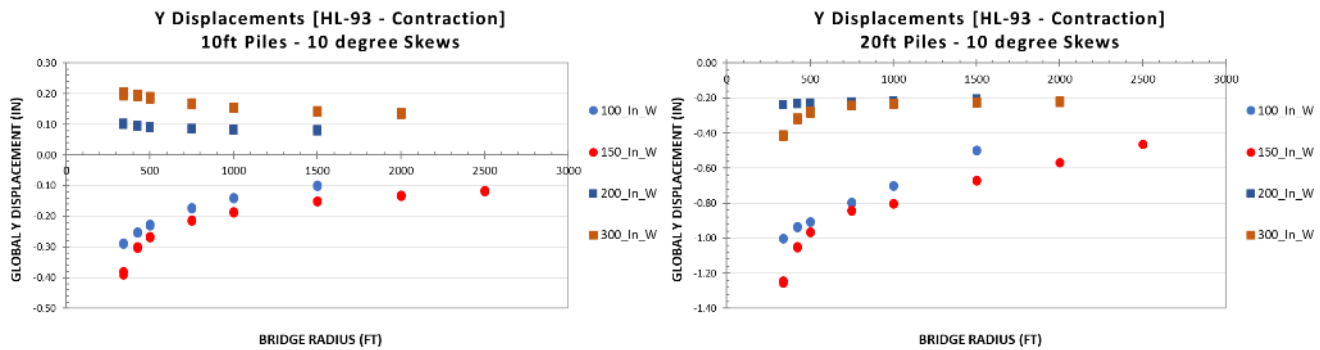


Figure 3-21: Transverse Displacement Comparison w.r.t. Span Configuration – Contraction

In both pile length cases, the two span structure results in smaller magnitude pile head displacements. Note that the scales of these two charts have not been held constant between the two. This trend is consistent across all study parameters. This behavior may be attributed to the stiffness of the pier restraining movement of the bridge in this direction.

Figure 3-22 displays a similar set of charts except the displacements are resulting from the contraction load case on models with 10-degree skew angles. The results shown in these plots again highlight the effect of the pier on pile head displacements. During the contraction case, the expected displacement would occur in the positive y direction as the bridge shrinks. In the 10 ft. pile length, two-span cases there is a shift in direction of the displacement. In the 20 ft. pile length cases, the pier solely results in a reduction. Though the pier seems to provide some reduction in pile head transverse displacements, the interaction is complex and ultimately is dependent on pile stiffness, bridge length, and skew angle.

3.4 PILE HEAD ROTATIONS

All rotation data shown in this section are about the global axis system. At abutment 1 with no skew, this corresponds to Global x rotations being representative of lateral rotation about the bridge longitudinal axis, and Global y rotations being representative of normal rotation about the transverse bridge axis. All rotations are reported in degrees and are recorded at the top of the piles unless noted otherwise.

3.4.1 BY RADIUS

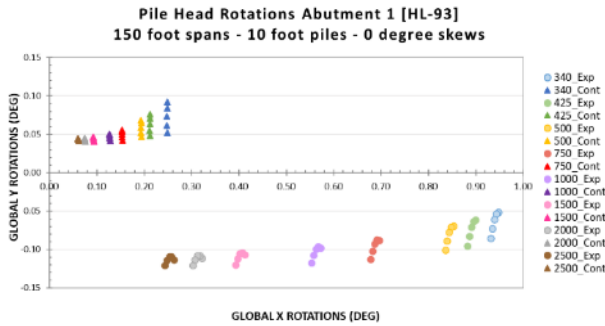
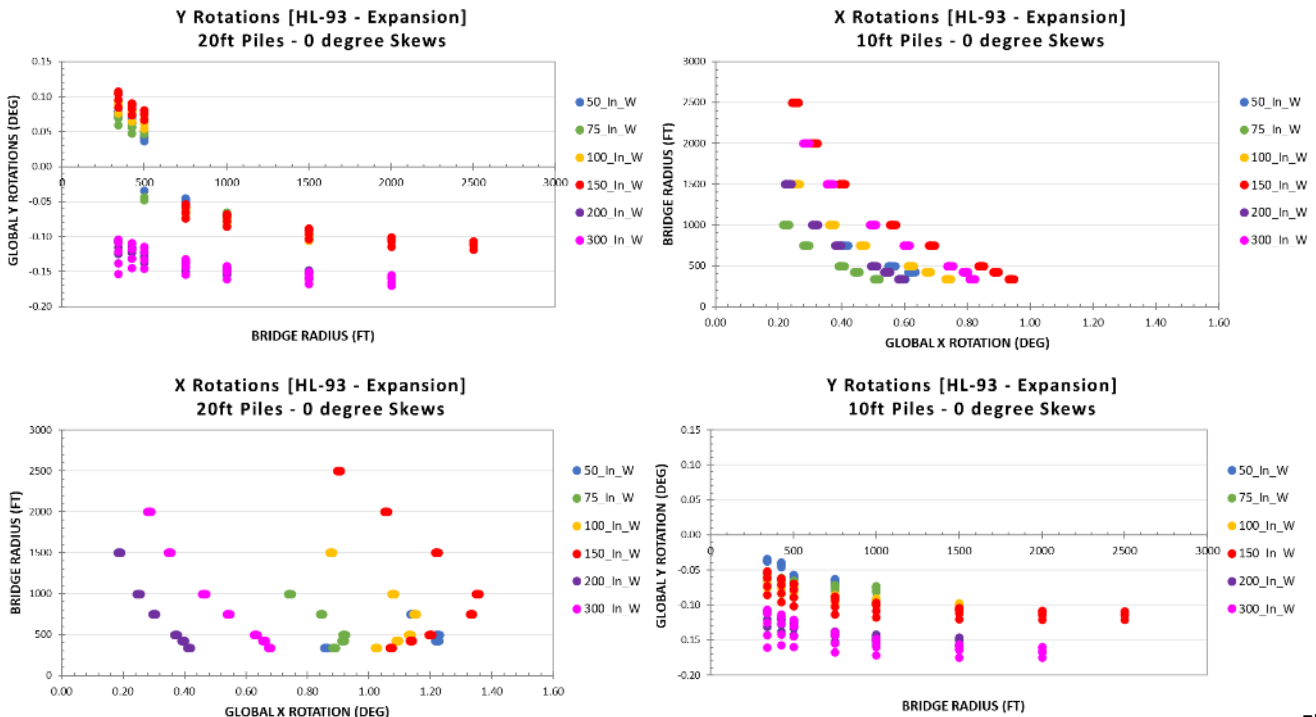


Figure 3-22: Pile Head Rotations for 150 ft. Case

Pile head rotation data shows a consistent trend of larger rotations occurring on the tighter radii, primarily about the bridge longitudinal axis (global x rotation). Abutment 2 data must consider the orientation of the abutment with respect to the global axis system, and thus the data shown here is shown for Abutment 1 only. This trend is observed across all span lengths. Results for the 150 ft. span case are provided in Figure 3-23. The stark increase in pile head rotations about the longitudinal bridge axis can be attributed to the increase in transverse displacements for the tighter radii during the expansion case. In the contraction load case, the global y rotation switches to the positive direction and displays smaller magnitude rotations about the longitudinal bridge axis (global x rotation).

3.4.2 BY PILE LENGTH



Flexible

systems will see greater rotations at the frame corners than shorter, stiffer systems. It is expected that shorter piles will have the smallest rotation about the bridge transverse axis (global y direction). This trend is confirmed in Figure 3-24 which plots global x and y rotations for 10 ft. and 20 ft. piles length cases subject to expansion. The 10 ft. pile lengths result in smaller rotations about the longitudinal bridge axis (global x rotation) when compared to the 20 ft. pile lengths. The trend of increasing rotations about the longitudinal bridge axis with decreasing radius no longer holds at the 20 ft. pile length for the single span cases. This is likely due to the extreme transverse displacement occurring for the in-line wingwall cases at these pile lengths and

curve radii. A similar trend is visible in the y rotations plot, where the single span cases with small radii result in a rotation reversal.

Figure 3-23: X and Y Rotations based on Pile Length

3.4.3 BY SKEW

Similar to displacement data, the largest lateral rotations should be seen on the largest skews as the bridge twists and warps in response to loading and thermal movement. This trend is visible in the charts presented in Figure 3-25 which present global x and y rotations for each span and radius combination of In-line wingwall cases. Increasing skew angle from 0- to 10-degrees results in an increase in rotation about the longitudinal bridge axis (global x rotation). There is minimal change in this direction from 10- to 20-degree skews, which corresponds to the skew effect on transverse displacements. There is a steady increase in rotation about the transverse bridge axis (global y rotation) with increase in skew angle, with an increased spread of the pile head data points. This behavior also corresponds to the observed skew effect on longitudinal displacement.

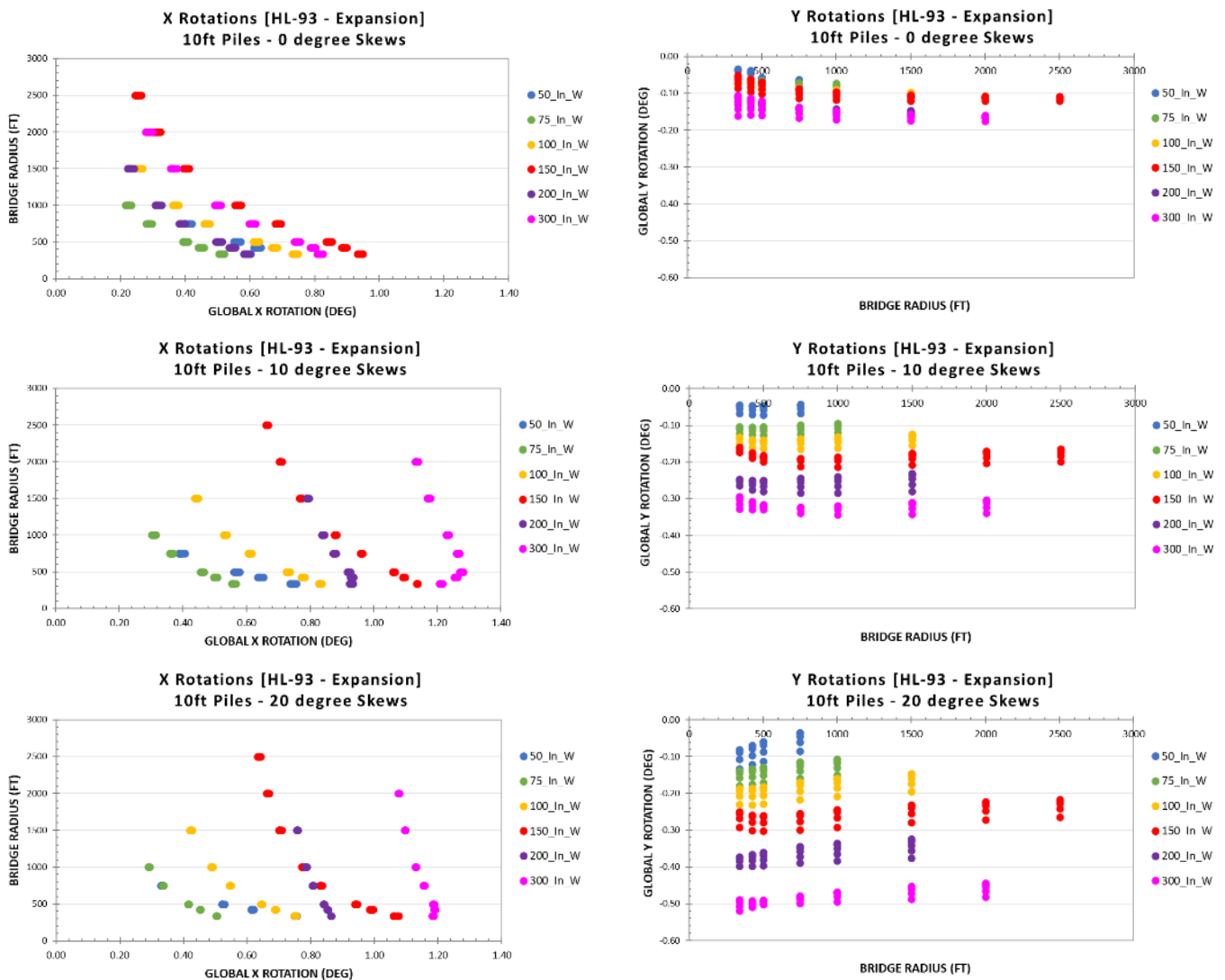


Figure 3-24: X and Y Rotations by Skew Angle

3.4.4 BY PILE ORIENTATION AND WINGWALL ORIENTATION

The x-y rotations for the 100 ft. span series are shown in the set of plots in Figure 3-26, which includes expansion and contraction load results for the 100 ft. bridge length, 10 ft. pile length, 20-degree skew cases. The results for the U-wingwall cases and both in-line wingwall cases are presented.

The results of this comparison are similar to the displacement results. This is unsurprising, given that pile head rotations are related to the displacement. In all cases, the U-wingwalls result in the smallest rotations indicating that they provide the greatest restraint to movement. The in-line wingwall with strong-axis pile configuration results in consistently large rotations, similar to the displacement results. The rotations about the transverse bridge axis (global y rotation) during the contraction load case are similar between the two weak axis pile cases (in-line and U-wingwalls). This is because they provide similar resistance to movement in this direction due to the pile orientation and lack of backfill passive pressure effects during this load case.

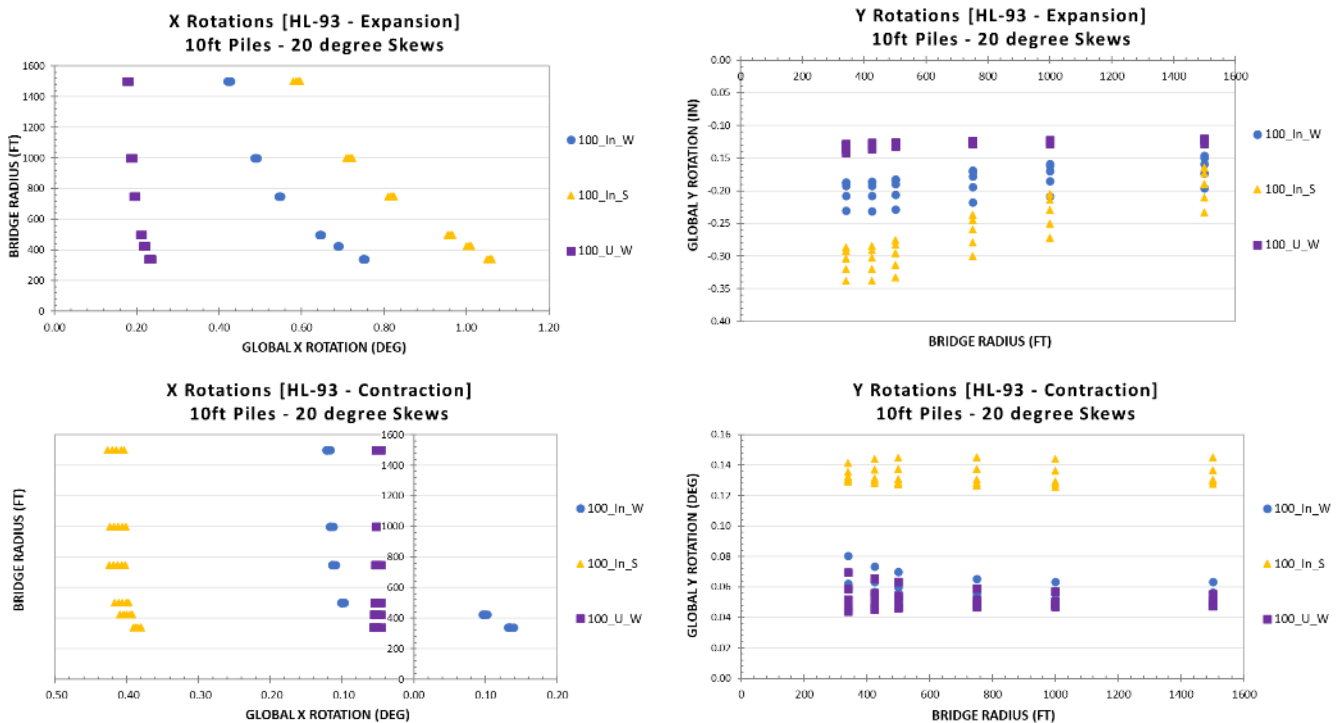


Figure 3-25: X and Y Rotation Comparison w.r.t. Wingwall and Pile Orientation

3.4.5 BY SPAN

As span length increases the horizontal leg of the frame increases in length accordingly. This lengthening of the strut of the frame creates a tendency for longer span lengths to see increased rotations in both orthogonal directions as the frame legs lose stiffness (Consider the stiffness parameter EI/L . Given that length is in the denominator, a lower stiffness is realized, similar to longer pile lengths providing increased flexibility.) More influential, however, is that longer span lengths produce larger thermal deformations, which will in turn cause the pile heads to rotate more than shorter spans.

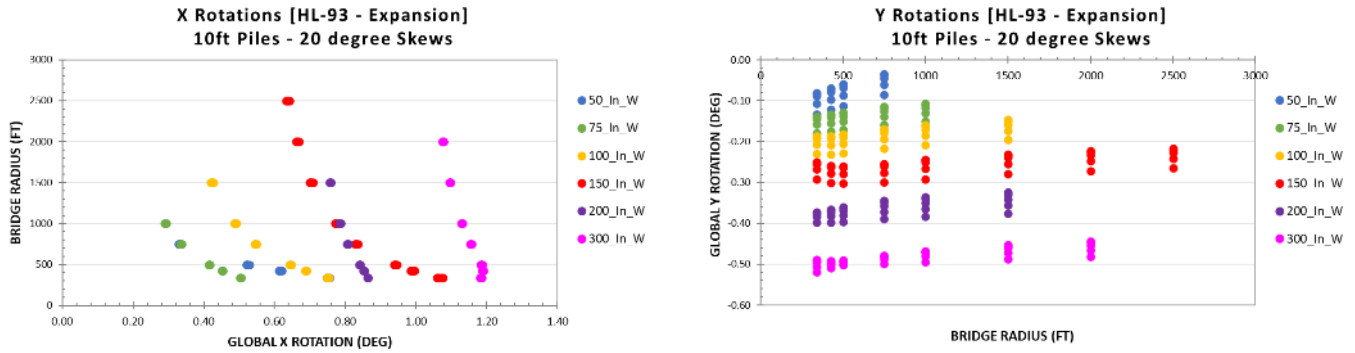


Figure 3-26: X and Y Rotations w.r.t. Bridge Length and Curve Radius

Figure 3-27 displays plots of rotations about the longitudinal bridge axis (global x rotation) and transverse bridge axis (global y rotation) for 10 ft. pile length and 20-degree skew cases. There is a clear trend that the y rotations increase consistently with increasing span length, which is expected behavior. The x rotations also exhibit this behavior when considering the one- and two-span cases separately. The two-span cases are slightly shifted towards smaller magnitude rotations about the longitudinal bridge axis. This is expected behavior since the pier provides additional transverse stiffness, and matches the trend discussed in Section 3.3.5.

3.5 PILE FORCES / REACTIONS

All pile forces are presented in kips and kip-ft unless otherwise specified. Strong and weak axis moments and shears along the piles have been adjusted to coordinate with the bridge axes rather than local pile axes in order to observe the bridge performance for strong and weak axis pile rotations. This adjustment is applicable only to the 50 ft. and 100 ft. span series since they are the only bridge lengths studied with strong axis pile orientation.

Given the assumed equivalent cantilever approach, the point of maximum force effects tends to occur at the base of the column rather than at or near the pile head.

3.5.1 BY RADIUS

Figure 3-28 displays scatter plots of the axial utilization ratio of the piles for the 150 ft. spans, including responses at both abutments for both thermal cases and all skews. Cases with tighter curve radii result in a significant shift in axial load toward the outermost piles (node 1500 for abutment 1, node 2500 for abutment 2). As the bridge straightens with larger radii, the axial distribution begins to normalize towards what could be expected for a straight bridge. Structures with smaller radii (tighter curves) result in an offset of the load from the major chord of the structure. The vertical loads then result in a global torsion of the entire structure about the major chord and are resisted by axial load in the piles. Since these plots consider the axial yielding utilization, the trend is independent of pile length, and produces similar results across all skew angles. This trend is consistent across all bridge lengths and other study parameters.

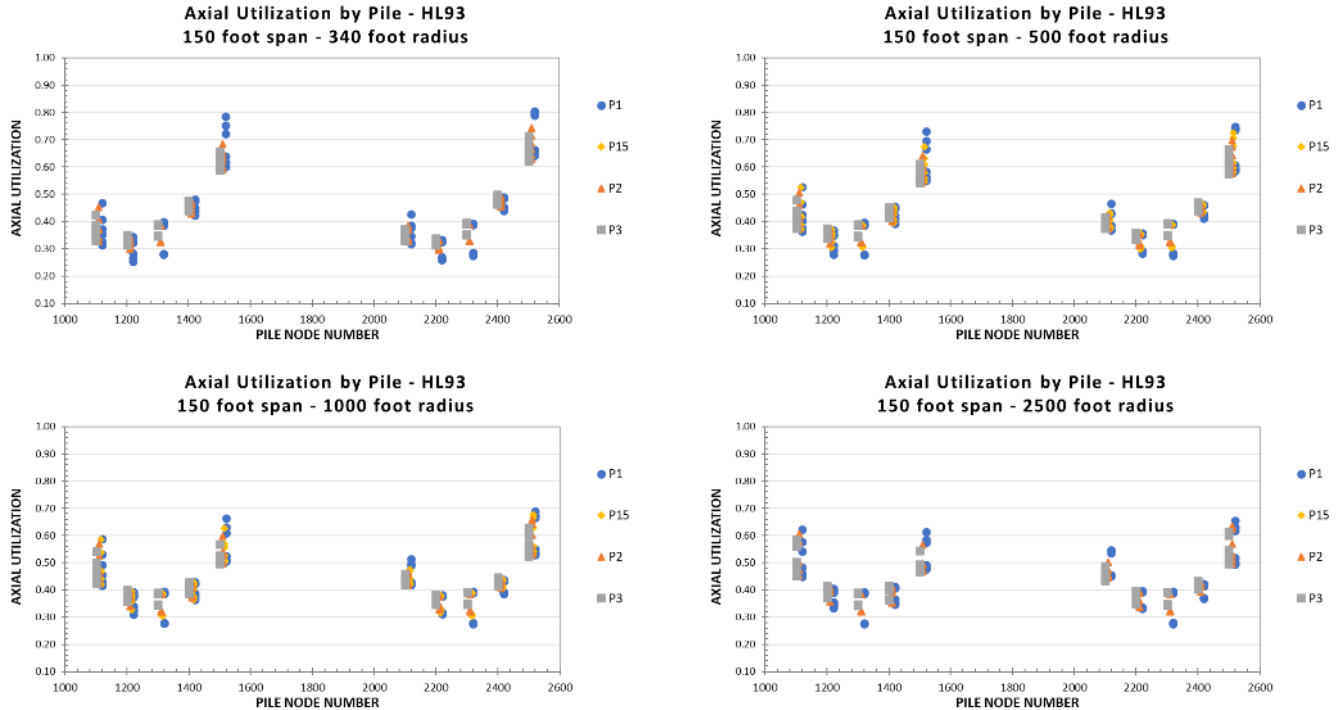


Figure 3-27: Axial Utilization of Piles for 150 ft. Cases

Pile moments and shears are directly related to the displacements and rotations of the pile head, so it is expected that they will respond similarly to changing radius. Figure 3-29 displays a series of charts plotting the moment utilization ratio and shear about the transverse and longitudinal bridge axis from the expansion load case.

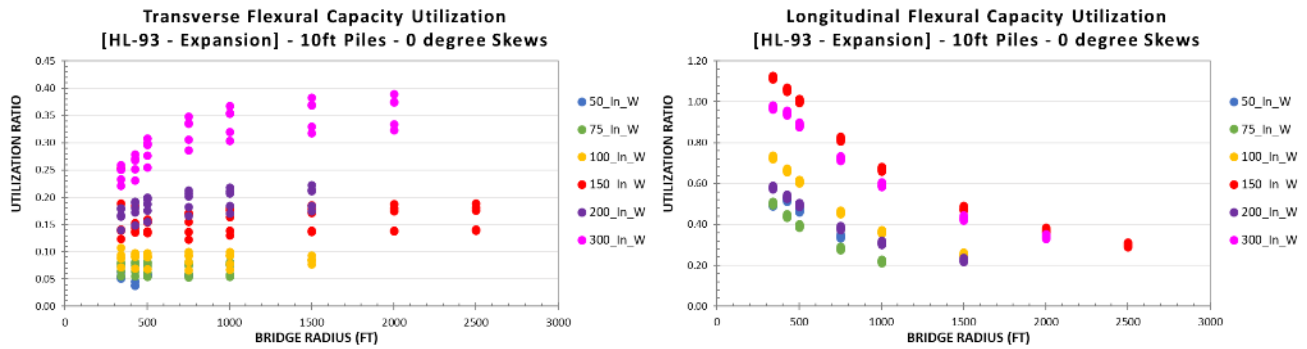
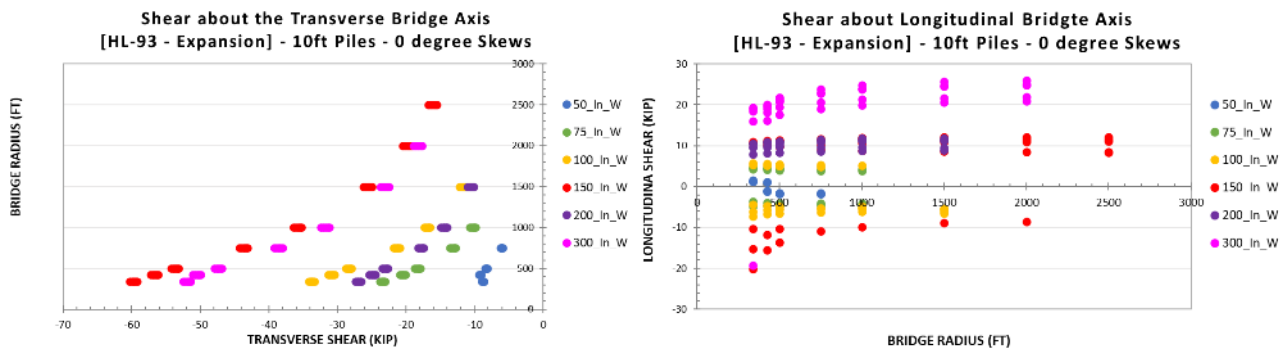


Figure 3-28: Radius Comparison of Shear and Moment in Longitudinal and Transverse Directions - Expansion



The effects of curvature are most noticeable in the moment utilization about the longitudinal bridge axis and the shear in the transverse bridge axis plots. This is an expected result as these force effects are both resultant from transverse bridge

displacements. The relationship between curve radius and transverse bridge displacements is discussed in Section 3.3.1. Moments and shears in the transverse bridge direction are expected to increase with decreasing bridge radius since the force effects and pile head displacements are directly related. The longitudinal force effects are not as significantly impacted as those in the transverse direction, though the single span bridges do show some reversal of moment at the tighter radii which is likely a result of extreme displacements and rotations for these cases.

The results for the same plots subject to the contraction case are presented in Figure 3-30. Note that the force effects in the longitudinal direction (longitudinal shear and moment about the transverse axis) are relatively unimpacted by curve radius. This is expected since these force effects are resulting from the free contraction of the bridge in the longitudinal direction. The flexural utilization ratio in this direction is significantly higher than in the expansion case, which is expected due to the greater net displacement in the longitudinal direction.

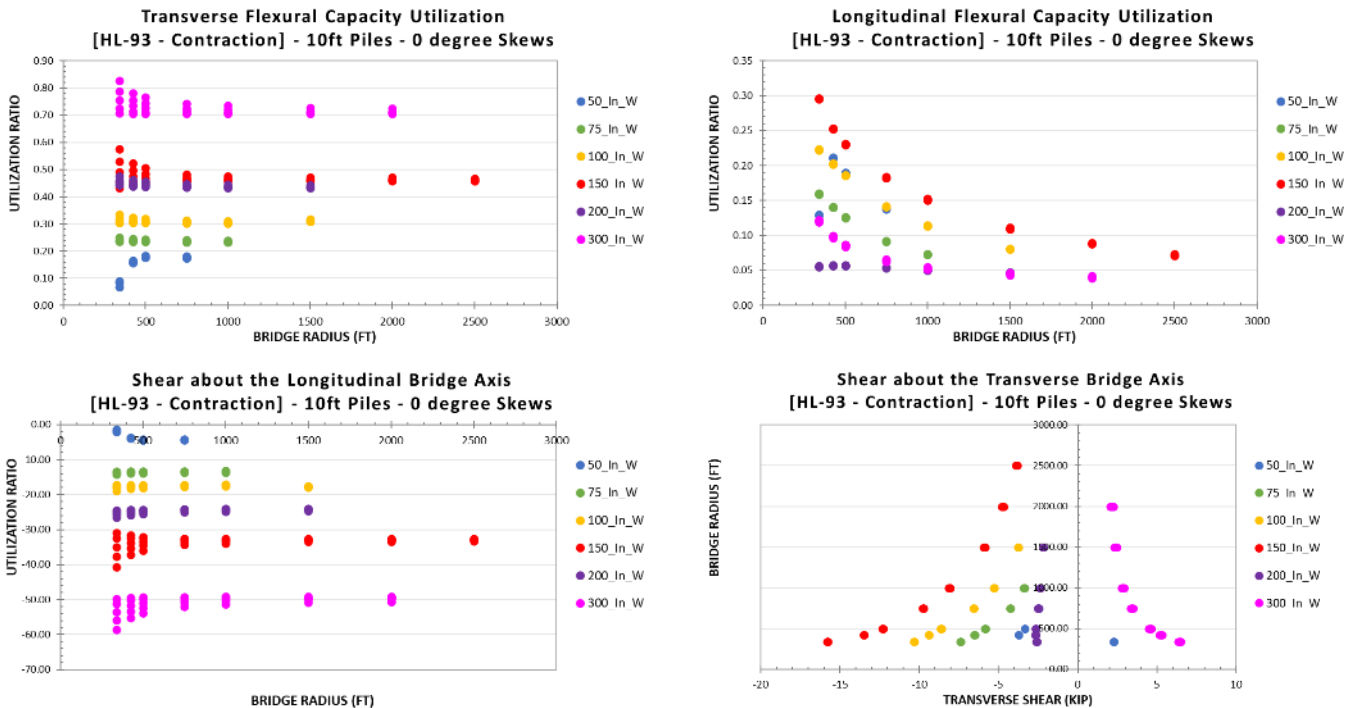


Figure 3-29: Radius Comparison of Shear and Moment in Longitudinal and Transverse Directions - Contraction

The force effects in the transverse bridge direction due to the contraction case are similarly impacted by radius as compared to the expansion case. However, the magnitudes of these force effects are significantly smaller. This is expected behavior since the transverse displacements in the contraction case are significantly smaller than the expansion case.

3.5.2 BY SKEW

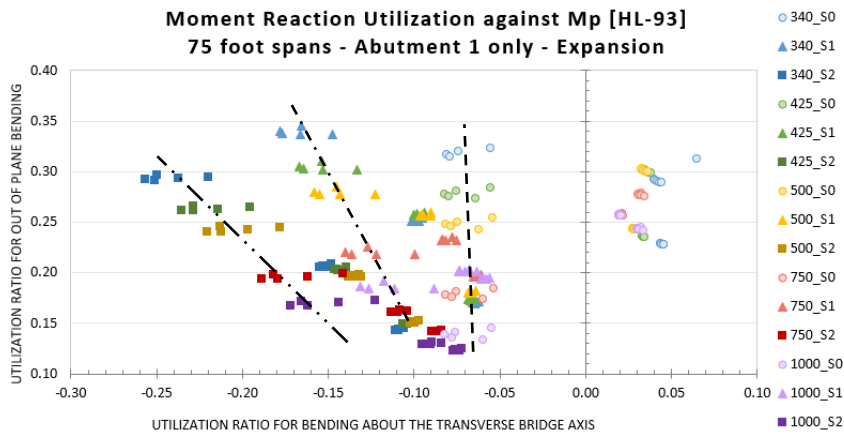


Figure 3-30: Moment Responses in Piles at Abutment 1 (75 ft. Spans)

When a bridge is skewed but pile orientation remains along the tangent of the girders, any force effects or movements will tend to contribute to the bridge warping or twisting along its length, and piles will be loaded in both planes. This effect increases as the radius of the curve gets tighter. Both of these increases in lateral moment are evident in Figure 3-31. A relatively linear increase in biaxial bending along each skew is seen as the radius decreases for the maximum force response cases, as portrayed by the dashed lines in Figure 3-31. Additionally, values increase substantially for lateral bending as the radius decreases.

3.5.3 BY PILE LENGTH

Figure 3-32 shows the utilization ratios for the 100 ft. span, 425 ft. radius series and the 50 ft. span, 750 ft. radius series. The left grouping of 5 columns of datapoints (1000 range on x axis) in each of these plots represents output at the 5 piles at abutment 1, and the rightmost grouping (2000 range) are the piles at abutment 2. Left to right, each grouping represents the innermost pile to exterior pile, as labeled on the first plot. The series of plots considers axial utilization only, axial + bending in the primary bridge bending direction (about bridge transverse axis) and finally axial with biaxial bending. These charts show the higher axial demand on the exterior columns, but that all cases are adequate for axial carrying capacity, indicating an appropriate approximate pile selection for the analysis. The axial + primary bending utilization shows the significant difference seen in the 20 ft. and 30 ft. piles as compared to the 10 ft. and 20 ft. piles, similar to the trends discussed in the deflections section. The axial plus bi-axial bending plots show the jump in magnitude when considering lateral bending effects, and their importance for consideration during design. Note that the 50 ft. and 100 ft. cases use different pile sizes and therefore may result in utilization ratios that are not scaled to the pile head deformations.

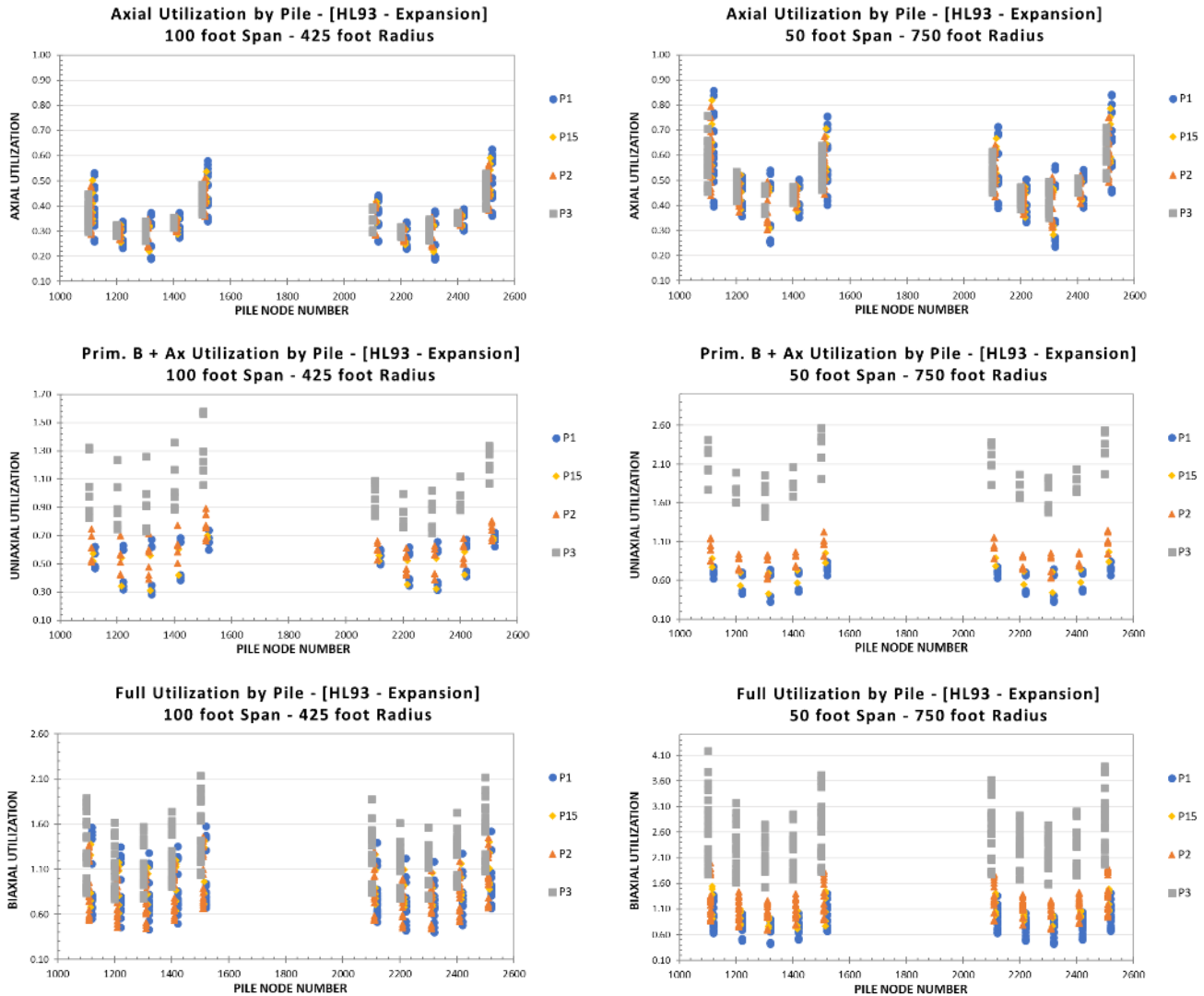


Figure 3-31: Pile Utilization Ratios for the 50/750 Series and 100/425 Series

The charts displayed in Figure 3-32 are representative of the utilization ratio of the piles. This accounts for the combined axial and bending forces applied to the pile. As length changes, the biaxial capacity of the pile decreases significantly, which is why an increase in utilization is observed for the longer pile lengths. If the forces alone are considered, not the utilization ratio, longer piles may be expected to result in smaller force effects. The structural principle of “stiffness attracts load” is based on the fundamental principle that flexible structures move, and restrained structures develop force effects as a result of that restraint. In the case of an integral abutment, the stiffness of the vertical legs of the frame is the direct indicator of the lateral flexibility of the entire structure. As such, it is expected that long, flexible piles will deform more than short stiff piles, and that short stiff piles will see higher maximum force effects than their flexible counterparts. This effect is visible in Figure 3-33 which plots the pile moment about the transverse bridge axis (weak axis moment) for varying pile lengths subject to the contraction load case.

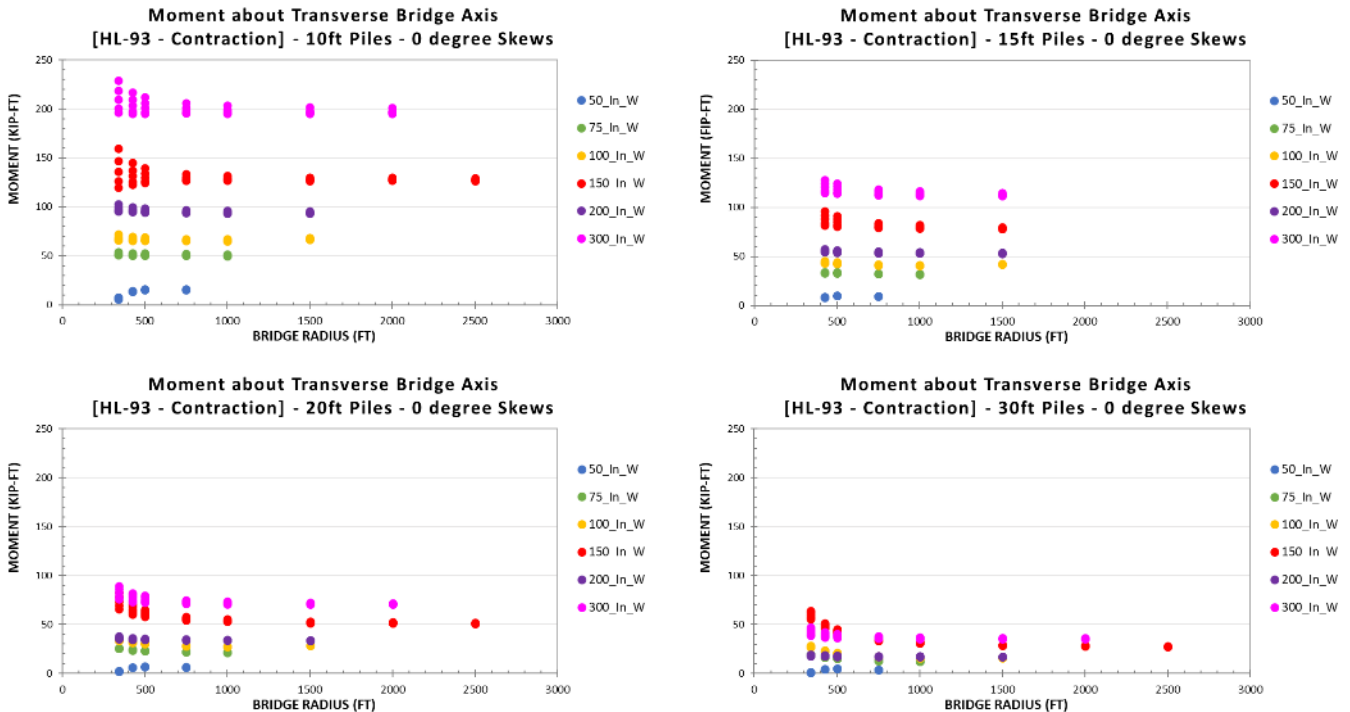


Figure 3-32: Pile Moments about the Transverse Bridge Axis due to Contraction w.r.t Pile Length

These charts clearly display how the pile force effects decrease with increasing pile length, supporting the expectations of this behavior. Note that different span lengths use differing pile sizes, so that primary comparison in these charts should be between the same color in varying charts. This trend occurs across all study parameters for changing pile length.

3.5.4 BY PILE ORIENTATION AND WINGWALL ORIENTATION

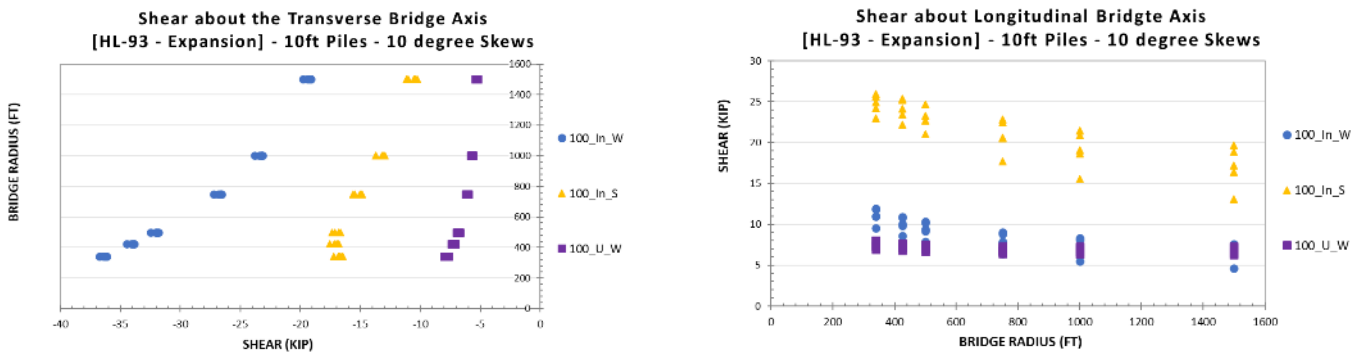


Figure 3-33: Comparison of Pile Shear w.r.t. Pile and Wingwall Orientation

When piles are orientated for weak axis bending, they give the bridge flexibility to move along the longitudinal bridge axis. An added benefit of this orientation is the larger lateral stiffness, as lateral loads are resisted by the strong axis stiffness of the pile. The reverse of this is true for strong axis pile orientations, where the strong axis resists longitudinal bridge movement, and the weak axis provides flexibility for lateral movements. Wingwall configuration is expected to have a similar effect on pile forces compared to displacements and rotations since all effects are related. These effects are visible in Figure 3-34 which plots the 100 ft. span length longitudinal and transverse pile shears for each wingwall and pile orientation. As expected, The U-wingwall orientation produced the smallest transverse shear with the in-line wingwall with weak axis piles producing the highest transverse shear. The results align with the expectations based on pile axis orientation.

3.5.5 BY SPAN

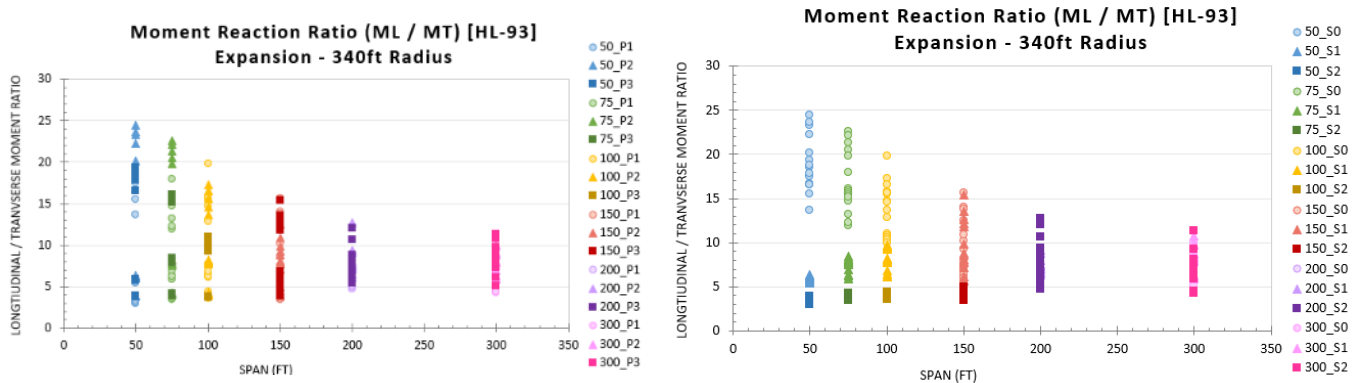


Figure 3-34: Moment Reaction Ratio for 340 ft. Radius

Increasing span length will naturally increase the demand on support structures. This is an obvious and expected outcome of lengthening a span and can be addressed in design. What is of greater interest is whether or not span length reduces the effects of the increased lateral loading due to a tight radius. Or, stated alternatively, is it radius only, or does arc span also impact lateral structure behavior? Figure 3-35 is a plot of the longitudinal bridge moment to transverse bridge moment in the piles for the 340 ft. radius only. The left image is sorted by pile length and the right image by skew.

Strong axis and U-wing cases for the 50 ft. and 100 ft. spans are *not* included in this data set in order to compare uniformly across all spans. This ratio is highest when lateral bending responses have the highest overall impact. It can be observed from this figure that for the 340 ft. radius, the impact of the lateral response *decreases* as the span length increases. In other words, increasing the arcspan assists in decreasing the effects of a tight radius. Skew data is highly segregated for span lengths of 100 ft. or less, where the soil mass comes into play to decrease lateral force effects at higher skews. The data begins to normalize for the 150 ft. radius and is fully blended by the 200 ft. spans. The 200 ft. and 300 ft. span cases are also braced by the midspan pier.

3.6 BEAM END FORCES

The design of the steel superstructure is not in the scope of this research effort, however, considering the behavior at the beam ends may inform decisions on logical limitations and guidance. All force effects are presented in kips and kip-ft unless otherwise noted and are taken at the beam end connection at the superstructure. These force effects are cumulative throughout the construction staging and take into account the applicable changing boundary conditions. As beam length increases, vertical shear and strong axis bending in the beams will naturally increase. Therefore, the focus of this data set will be lateral effects, torsion, and induced axial loads in the beams.

3.6.1 BY CONSTRUCTION STAGING

Torsion at the beam ends is cumulative throughout construction staging and loading. The construction staging that occurs prior to curing of the concrete deck, such as steel girder placement and application of wet concrete, results in torsion that is localized to the individual girders. Torsion observed after the deck is cured, such as the application of wearing surface in Stage 3 and the live load in Stage 4, results in global torsion resulting from the offset of the applied load centroid to the central chord of the superstructure. Refer to Section 3.5.1 where the effect of global torsion is evident in the pile reactions.

APPENDIX D – TECHNOLOGY TOOLBOX

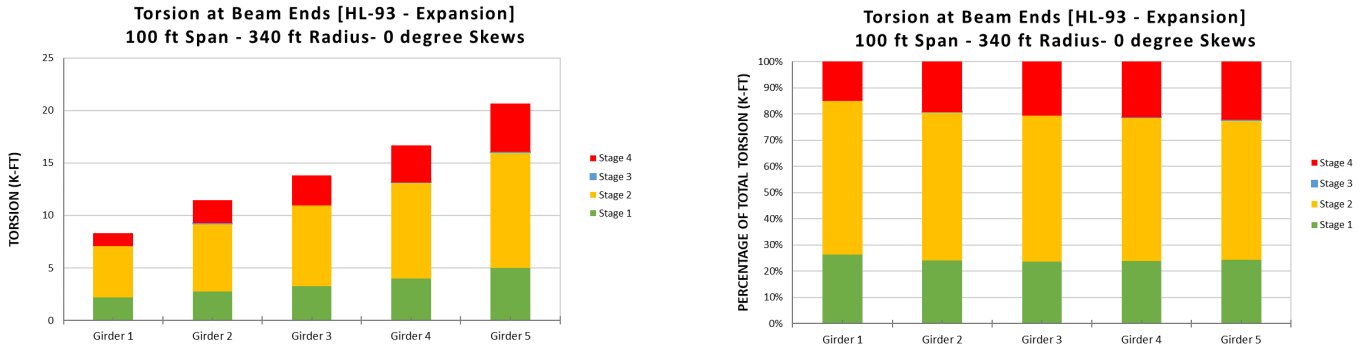


Figure 3-35: Torsion in Beam Ends Sorted by Construction Stages for 100 ft Span - 340 ft Radius – 0 degrees Skew

Figure 3-36 shows the torsion in each of the girders. The data is sorted by the stages of load application in the models. Looking at the torsion resulting from each stage of load application, approximately 80% of total torsion at the beam ends results from the placement of the steel girders and the wet concrete. The application of live load and other Stage 4 loads contributes approximately 20% of the total torsion of the girders.

3.6.2 BY RADIUS

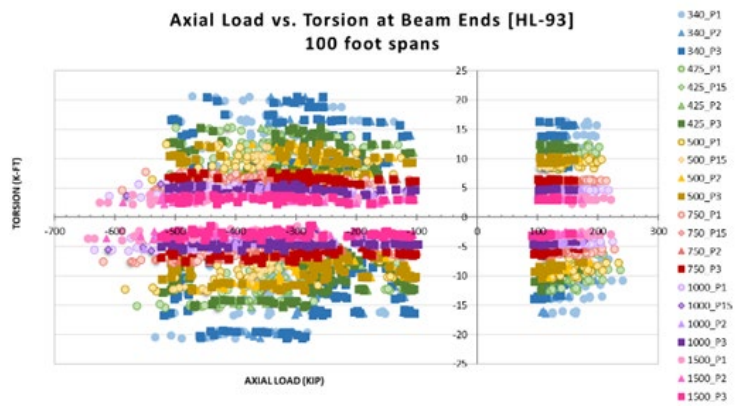


Figure 3-36: End of Beam Force Effects – 100 ft. Spans

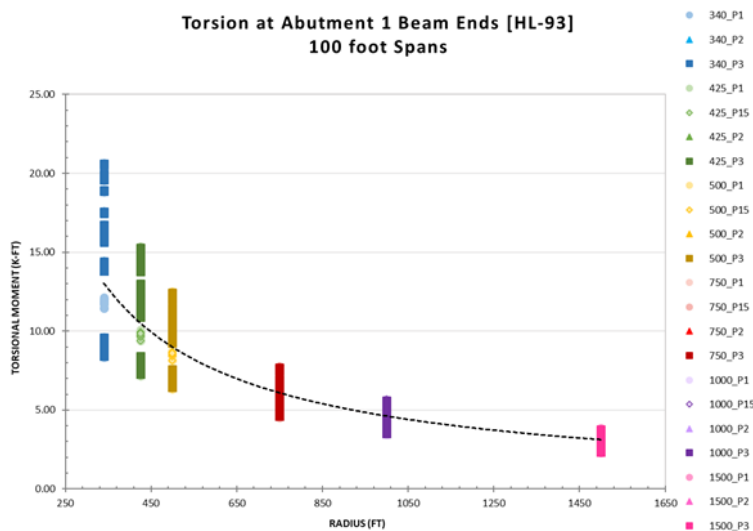


Figure 3-37: Torsion in Beam Ends – 100 ft. Spans

Figure 3-37 is a scatter plot of the axial load and torsion responses at the beam ends for all data points in the 100 ft. long span series of cases. From this figure a clear trend of increasing torsion with tightening radius is observed. This is expected behavior.

APPENDIX D – TECHNOLOGY TOOLBOX

The axial force effects for expansion (negative values on x axis) are noticeably higher than contraction (positive values on x axis), which is also expected as the movement is restrained by the soil mass in the expansion condition. For the 100 ft. long span girder utilized, which was approximately sized to provide adequate moment capacity at midspan, an axial load of 200 kips represents 4% of yield stress, and an axial load of 500 kips represents 10% of the yield stress. These results are not insignificant, particularly for curved girders. Generally, girder design guidelines provide direction on boundary conditions and moment requirements (such as designing positive moment assuming all construction stages are a simply supported condition), but direction on inclusion of additional axial stresses is generally not provided. Given that the bottom flange is in tension for positive flexure, this omission is not unreasonable for force build up due to axial expansion. At the beam ends, however, when negative moments are present, this level of axial response should not be ignored.

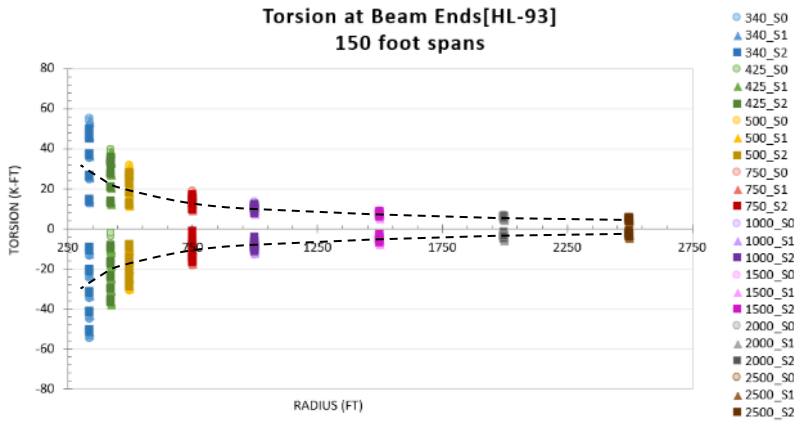


Figure 3-38: Torsion in Beam Ends – 150 ft. Spans

Plotting the torsional response only with respect to radius, as shown in Figure 3-38 and Figure 3-39, it becomes evident that the relationship between end of beam torsion and radius is not linear. The highest torsional responses occur in the tightest radius (340 ft.), which on average produces torsion values of approximately 3 times higher than those for a 1000 ft. radius. Differences between the 750 ft. radius and the largest radius for a given span are nearly linear, with a noticeable increase by the 500 ft. radius. Torsion in the beam ends will increase shear stresses in the girder and warping stresses in the flanges, and will transmit these stresses into the concrete end diaphragm. Though beams can be designed for torsion, limiting the magnitude of torsional stress transmission to the diaphragm is an important factor from a serviceability standpoint to reduce cracking and distress in this region. This trend is observed across all span series.

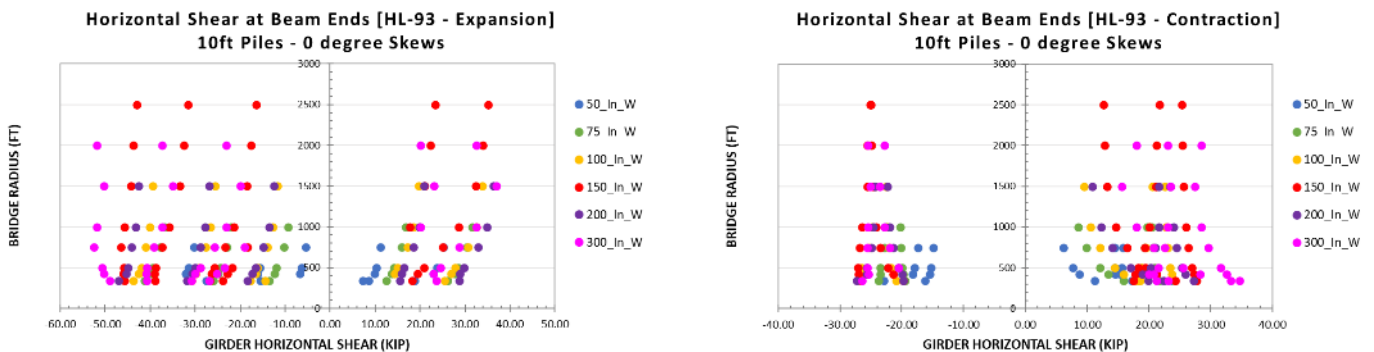


Figure 3-39: Girder End Horizontal Shear in Expansion and Contraction Load Cases

Figure 3-40 displays two charts plotting the girder end horizontal (weak axis) shear under the expansion and contraction load cases. These charts show that curvature has a relatively minor effect on the horizontal shear developed in the girders. There are differential shear magnitudes and directions between each girder. For the expansion case, there are three data points per bridge length in negative shear (girders 1-3) and two in positive shear (girders 4 & 5). These directions reverse for the contraction case, however in all cases the magnitude of shear is relatively small.

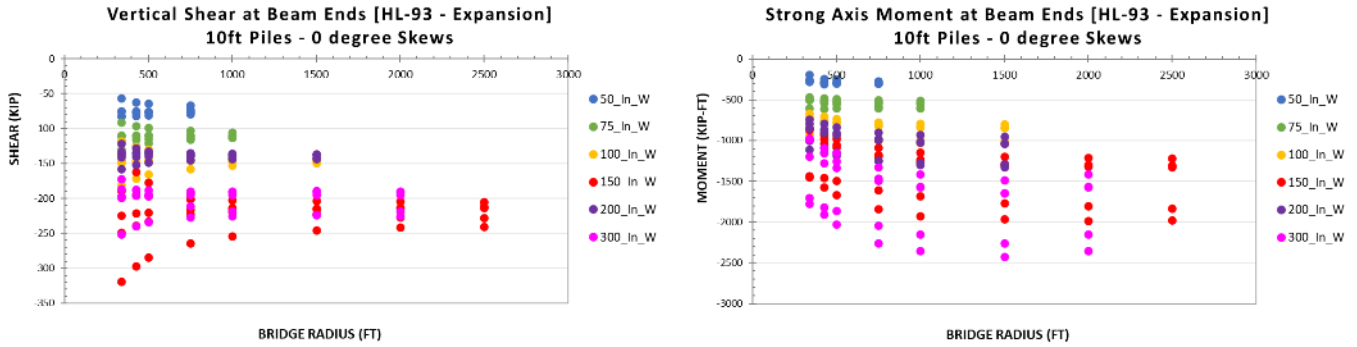


Figure 3-40: Girder End Vertical Shear and Strong Axis Moment

Figure 3-41 displays two charts plotting girder end vertical shear and strong axis moment across all bridge radii and bridge lengths. Similar to horizontal shear, the vertical shear is minorly impacted by bridge radius. There is an apparent spreading of data points at the smaller radii which can be attributed to the varying arc lengths of the girders. The strong axis moment does appear affected by bridge radius, however, the largest magnitudes are present at the middle radii values.

3.6.3 BY SKEW

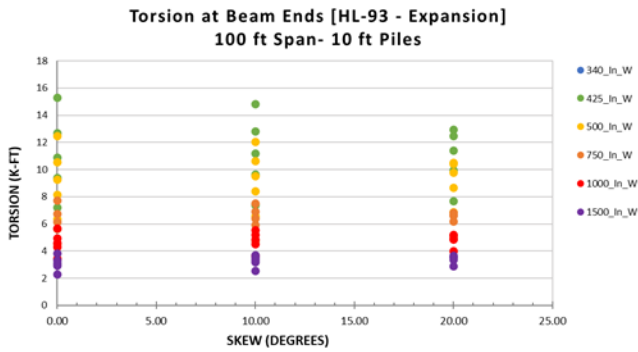


Figure 3-41: Torsion and Axial Force at Girder Ends vs Skew for 100 ft. Spans with 10 ft. Piles

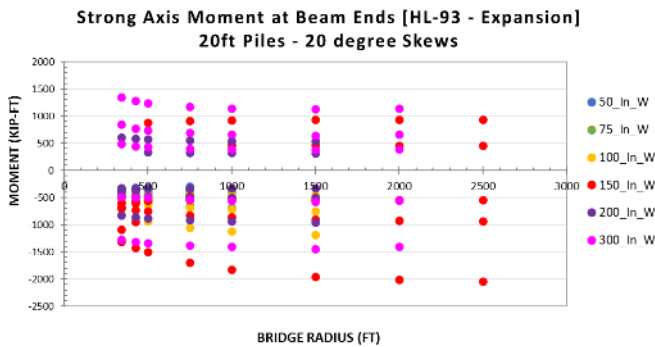


Figure 3-42: Strong Axis Moments for 20-degree Skew Cases

Figure 3-42 shows the girder end force results for the 10 ft. long piles for the 100 ft. span series. The data is sorted by radius. From this plot it is evident that skew does not have a major impact on axial or torsional results, and that radius is still the primary driver for torsional response.

In skewed bridges, there is a concern of uplift at the acute corners. Figure 3-43 displays the 20-degree skew cases with 20 ft. piles. For the longer span cases, there is positive strong axis moment occurring in the girders at the exterior of the curve, indicating uplift in this location. Note that this effect appears independent of the curve radius, indicating that the response is dictated by a combination of the span length and skew angle. The loads displayed in the chart are absolute maximum force effects, not coincident loads, which means there are likely positive moment effects in most skewed bridge cases.

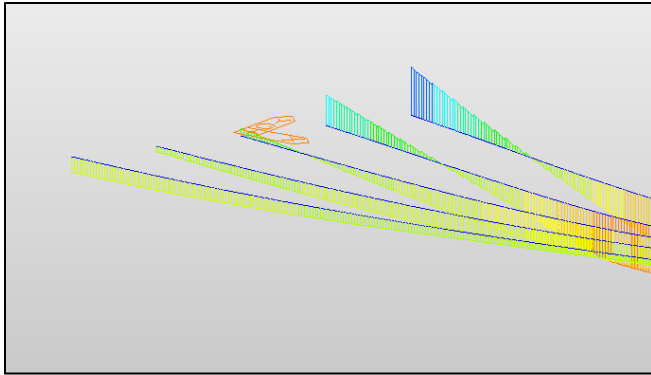


Figure 3-43: Maximum Positive End Moment Beam Diagram for 100-500 S2 Case

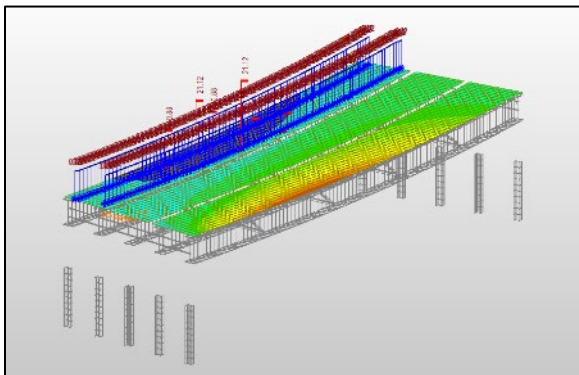


Figure 3-44: Live Load Placement for Maximum Positive End Moments in 100-500 S2 Case

Figure 3-44 displays the coincident strong axis beam diagrams and Figure 3-45 displays the live load placement for the maximum positive moment in girder 5 (outermost girder) of the 100 ft. long, 500 ft. radius, 20-degree skew case.

3.6.4 BY PILE LENGTH

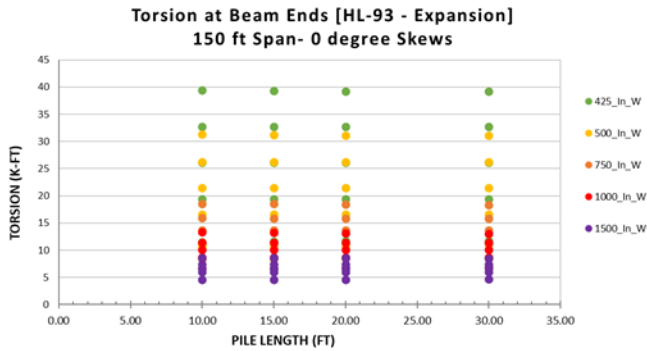


Figure 3-45: 150 ft. Span Girder End Torsion

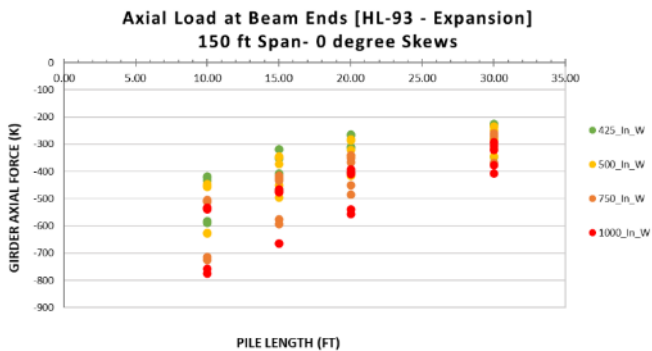


Figure 3-46: 150 ft. Span Girder End Axial Load

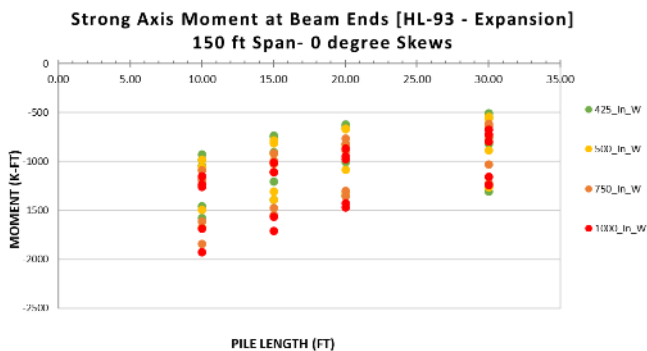


Figure 3-47: 150 ft. Span Girder End Strong Axis Moment

Figure 3-46 through Figure 3-48 show the torsional, axial load and strong axis moment responses in the beam ends for the expansion load case for the 150 ft. spans with 0-degree skew at the Abutment 1 end over the various pile lengths. These charts are broken down by radius. Pile length is found to have negligible effect on torsion at the girder ends. Pile length does however result in substantially larger axial forces and strong axis moments in the superstructure for the stiff leg frames (10 ft. long piles). Introducing flexibility to the system with longer piles tends to normalize this response.

3.6.5 BY PILE ORIENTATION AND WINGWALL ORIENTATION

The effects of pile and wingwall orientation on superstructure force effects is primarily a concern in the transverse direction (weak axis moment) and with a potential increase in axial loads. The change in transverse restraint by the wingwall orientation and pile orientation may cause load to shed into the superstructure. Figure 3-49 plots the weak axis girder end moments and the axial forces during the expansion load case for each of the different wingwall and pile orientation cases at 10-foot pile

APPENDIX D – TECHNOLOGY TOOLBOX

lengths and 0-degree skews. The results shown in these charts indicate that there is a minimal change in these responses based on the pile and wingwall orientation.

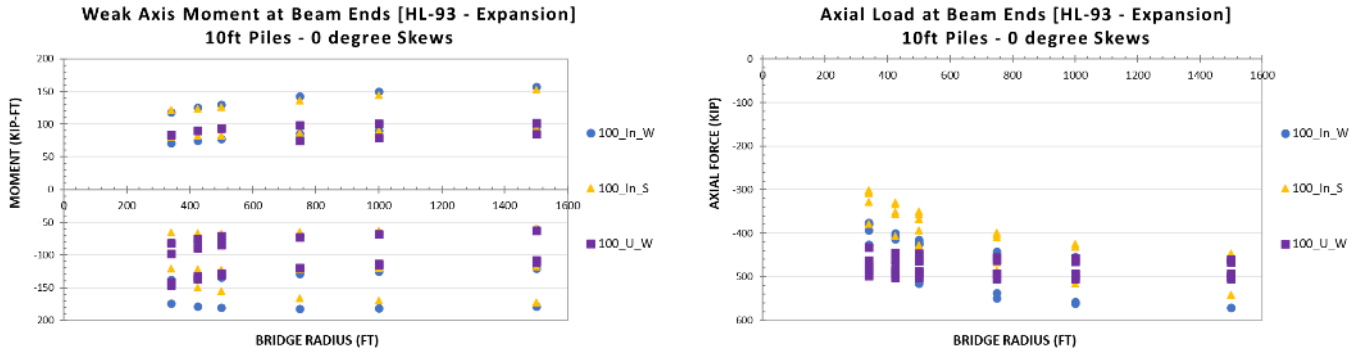


Figure 3-48: Girder End Weak Axis Moment and Axial Load w.r.t. Pile and Wingwall Orientation

3.7 DECK STRESSES

Tension in the top of the deck resulting from negative end moments due to frame behavior must be resisted by supplemental reinforcing steel if the tension exceeds ϕ_f , or 0.9 times the modulus of rupture of concrete. This limit is depicted by the solid line in each of the following images, which assumes 4ksi deck concrete. All stresses in the following graphs are plotted in ksi unless otherwise noted, and all stresses were taken at the top surface of the deck, approximately 6” from the face of the abutment diaphragm.

3.7.1 BY RADIUS

Top of deck stresses are minimally impacted by radius. A slight reduction in maximum tensile stress as radius increases is observed which can be attributed to the longer arc span length of the outermost girders in bridges with smaller radii. Stresses in the top of the deck for the 75 ft. span cases are shown in Figure 3-50, where most of the expansion tensile data points exceed the modulus of rupture limit and indicate the need for continuity reinforcement.

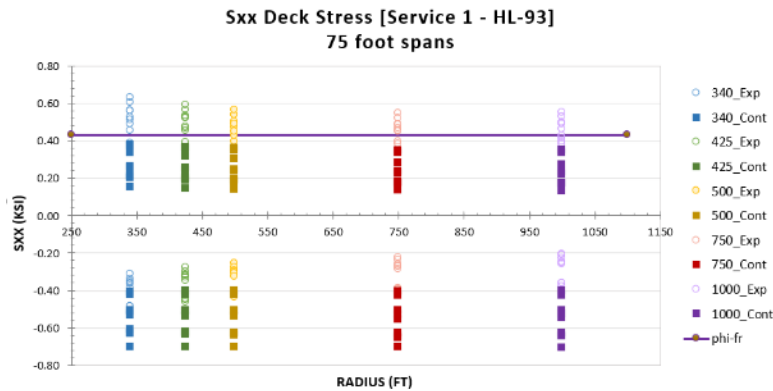


Figure 3-49: 75 ft. Span Deck Stresses

3.7.2 BY SKEW

The series of plots in Figure 3-51 show the various stresses in the 300 ft. multi-span series sorted by skew. In these cases, Sxx indicates longitudinal stress at abutment 1, Syy indicates lateral stress at abutment 1, and Smax/Smin indicate the principal stresses. No strong correlations are observed that would require a limitation on skew with respect to deck stress.

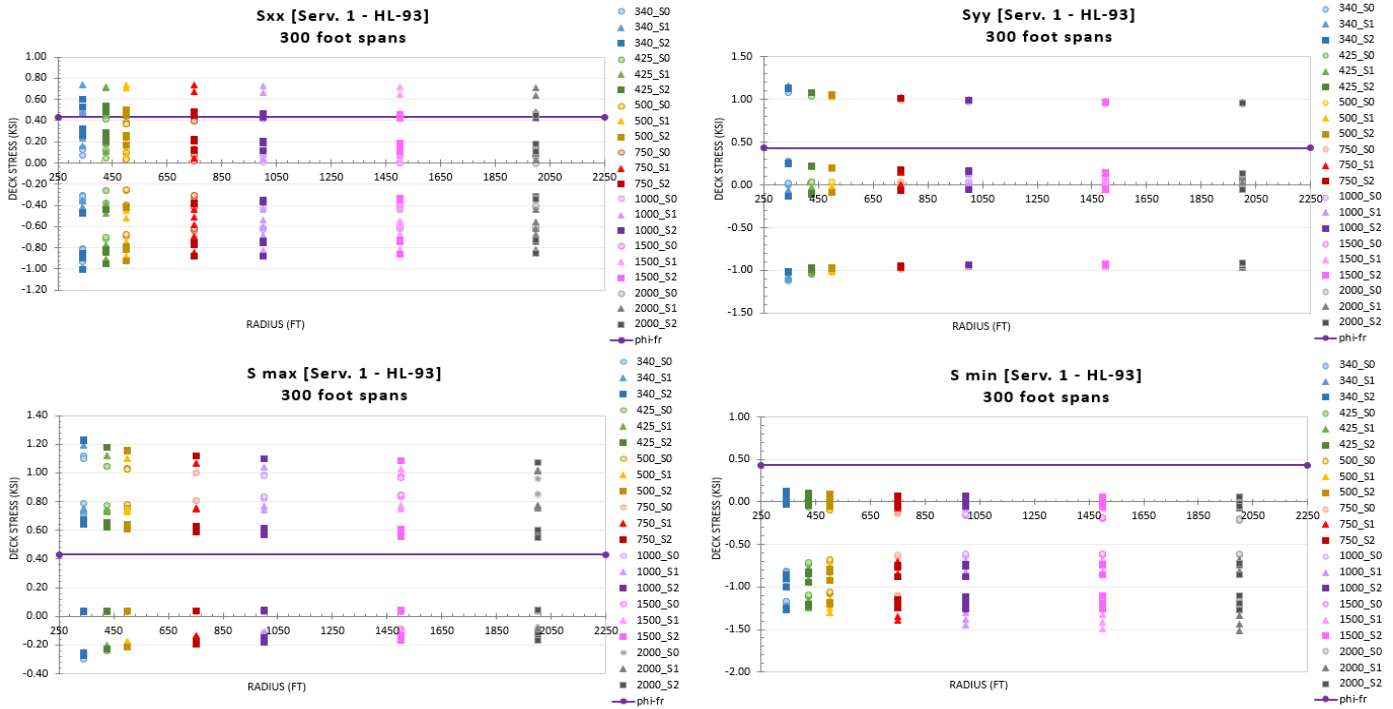


Figure 3-50: 300 ft. Series Deck Stresses

3.7.3 OTHER PARAMETERS

Deck stresses are relatively unimpacted by pile length as indicated in Figure 3-52, which shows the global x direction stress in the top surface of the deck for the 150 ft. spans. While the pile moments are higher for short, stiff piles, resulting in higher expected deck stresses for these cases, the large stiffness of the superstructure causes the deck stresses to remain low even in the most severe cases. Only slight increases are observed in the tensile deck stresses at longer span lengths. Similar observations are noted for various spans, wings, and pile orientations.

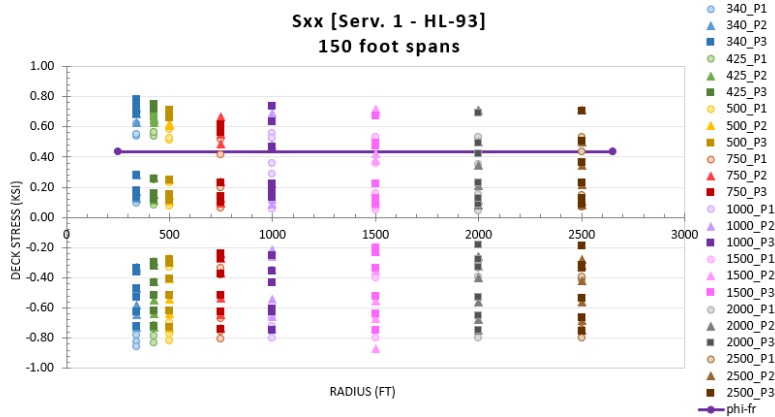


Figure 3-51: Deck Stresses in 150 ft. Spans by Pile Length

3.8 SUMMARY OF FINDINGS

Pile head displacements were the most sensitive response to the changing parameters in this study. The effects of curve radius, pile length, skew, bridge length, pile and wingwall orientation, and span configuration were significant. The pile and wingwall parameter seemed to be the most impactful on the results, where U-wingwall cases with weak axis pile orientation showed less sensitivity to changes in the other parameters compared to in-line wingwall cases. This is attributed to the additional restraint to transverse displacement provided by the passive pressure acting on the U-wingwalls. When comparing the weak axis and strong

APPENDIX D – TECHNOLOGY TOOLBOX

axis pile cases with in-line wingwalls, the strong axis piles showed more severe responses in all cases. This is attributed to the strong axis orientation providing greater stiffness in the longitudinal bridge direction and increased flexibility in the transverse bridge direction. Pile head rotations and pile forces are related to the pile head displacements and therefore exhibited similar trends.

Girder end forces exhibited strong responses to curve radius, span length, and skew angle. It was expected that these parameters would result in varying responses at the girder ends since they are all parameters relating to superstructure geometry. Pile length and wingwall and pile orientation did not appear to have a significant effect on the girder end moments.

Deck stresses were not meaningfully impacted by the varying parameters included in this study. In all cases, the magnitude of stress at the ends of the deck was within an acceptable design range of stress, and in some cases below the modulus of rupture. This result can be attributed to an appropriate girder size selection for the model and flexibility provided by the piles resulting in a low tensile stress in the deck ends.

4 APPLICATION OF RESULTS TO DESIGN GUIDELINES

This section is intended to provide an overview of the results of the finite element studies with respect to the design guidance. The reader is directed to the Curved Integral Abutment Bridge Design Guidelines developed for this project for additional information and full guidelines, which includes definitions, instructions, and guidance for both the simplified design method and refined analysis.

4.1 WINGWALL AND PILE ORIENTATION

Wingwall and pile orientation was investigated as part of this research to determine if they have significant impacts on structural response of curved integral abutment bridges. It was observed that both wingwall and pile orientation do result in significantly different structural responses. In order to make recommendations for a simplified design method, pile responses due to wingwall and pile orientation were investigated.

The research models investigated in-line wingwalls, where the wingwalls are a parallel extension of the abutment stem, and U-wingwalls, where the wingwalls were oriented perpendicular to the abutment stem. The effects of wingwall orientation are most apparent when observing pile head displacements under the thermal expansion load case. In Section 3.3.2, it was observed that for all cases the U-wingwall orientation resulted in significantly lower transverse movement of the pile heads when compared to the in-line orientation. This is attributed to the U-wingwalls engaging the backfill soil springs to restrain movement in the transverse bridge direction. The large soil mass contained between the U-wingwalls helps to restrain the abutment movement and provide favorable displacements for maintenance and serviceability, independent of pile length, skew, and radius. The structural response for the in-line wingwalls cases resulted in a wide range of lateral displacements that were highly sensitive to pile length. Therefore, it is recommended that U-wingwall orientation be utilized for the simplified design method. However, to account for curvature effects, a lateral displacement needs to be considered for design.

The sensitivity of skew on lateral pile displacement was investigated for the U-wingwall orientation to determine if a recommendation could be made for a prescribed lateral displacement for the simplified design method based on the geometric parameters. Because the displacements were relatively low and did not vary greatly with respect to the bridge radius, 150 ft. span models with 340 ft. radius and U-wingwalls at the 0-, 10- and 20-degree skews were developed to further define the maximum limitations on transverse lateral displacements. Results for lateral displacement vs radius with the data sorted by skew are presented in Figure 4-1. It was observed that as skew increased the bridge response resulted in increased rotation about the vertical axis, and therefore higher transverse displacements were observed in the piles. Traditionally, for integral abutment bridges the piles are conservatively designed for free longitudinal expansion and contraction displacements. A correlation between lateral displacement and free longitudinal displacement was made to provide a prescribed upper and lower limit for recommended lateral displacements for the simplified design method (refer to Table 4-1 **Error! Reference source not found.**). Bridges with tight radii near 340 ft. shall consider the upper limit and bridges with radii that approach the upper bound for near straight condition, per AASHTO Article 4.6.1.2.4b, shall consider the lower limit in Table 4-1 **Error! Reference source not found.** to provide a conservative lateral displacement for design of the piles. Bridges with skews and radii between those provided in Table 4-1 **Error! Reference source not found.** may be interpolated.

Table 4-1: Recommended Lateral Displacement for Simplified Design Method

	Percent of Free Longitudinal Displacement to Determine Recommended Lateral Displacement	Percent of Free Longitudinal Displacement to Determine Recommended Lateral Displacement
Skew	Upper Limit (Radii approaching 340 ft.)	Lower Limit (Radii approaching $L_{as} / R = 0.06$ Radians)
0 degrees	40%	10%
10 degrees	65%	35%
20 degrees	80%	50%

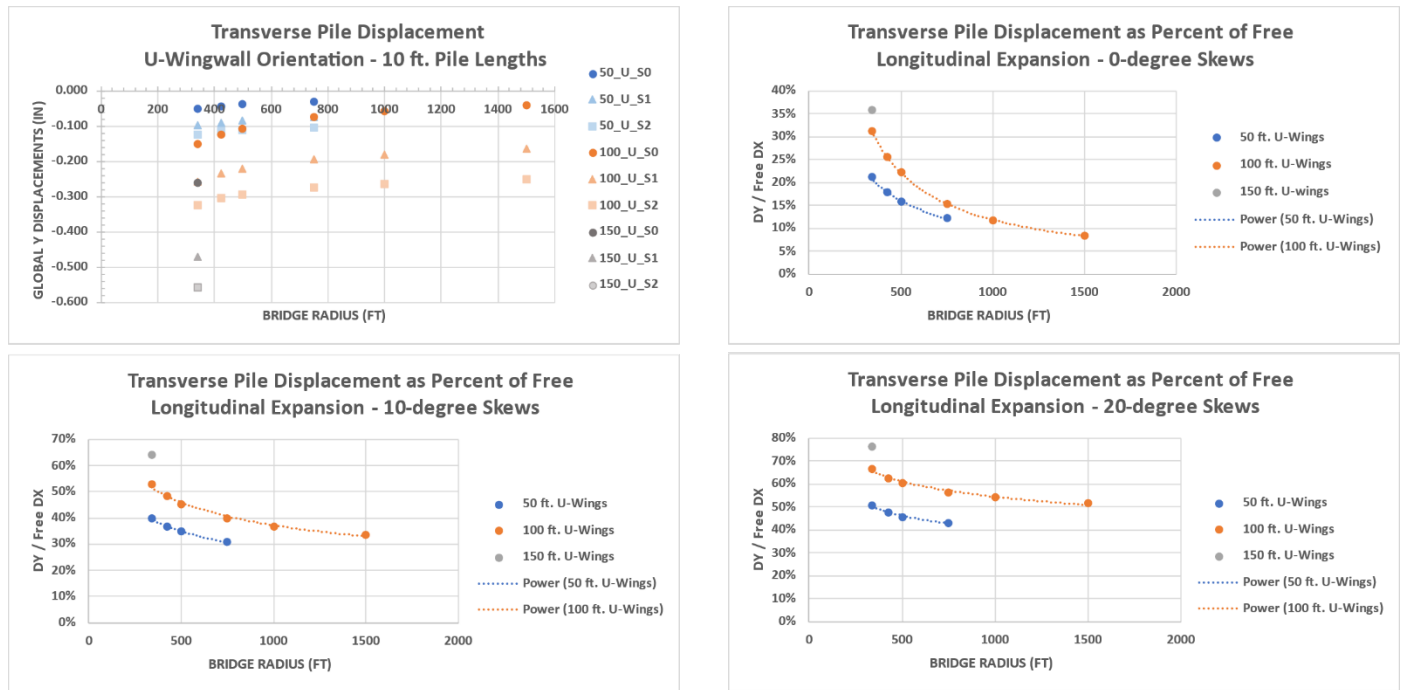


Figure 4-1: U-wingwall pile displacements (top left) and transverse displacements as a percentage of free longitudinal expansion

The recommendation for U-wingwall orientation is supported by the performance of existing in-service bridges. Particularly, Bridge No. 9 over the Mill Brook in Danby, VT has demonstrated favorable performance¹. This curved integral abutment bridge is an 86 ft. single span with 240 ft. radius and 8 ft. U-wingwalls. After several years of service, there is no cracking in the integral wingwalls at the abutment details. This bridge pushes the limits on curved integral abutment bridge design with an extremely tight radius, a superelevation around 5% and a vertical elevation difference of approximately 4 ft. between the start and end of the bridge. The good performance of this bridge, particularly the wingwall to abutment detail and joints in the pavement, demonstrates the success of the U-wingwalls laterally restraining the bridge movements.

The other bridge parameters (skew, span length, and radius) were investigated for any trends that might arise in establishing limitations on the use of a simplified design method. Based on the results presented in Section 3, there were not such limitations identified. The skew, span length and radius are rather accounted for by providing a prescribed transverse displacement based on these parameters. Additionally, the designer of the wingwalls shall consider passive earth pressure when designing the horizontal reinforcement in the back of the wingwalls and abutment stem.

This study primarily considered U-wingwalls with lengths of 10 ft. from the back-face of the abutment stem. Additional analysis was performed to assess the effects of wingwalls shorter than 10 ft. on the transverse displacement of the bridge. Five additional models with U-wingwall lengths of 5 ft. were completed representing bridges with 100 ft. span lengths, 340 ft. radii, and 0-, 10-, and 20-degree skew angles, a bridge with a 100 ft. span length, 750 ft. radius, and 0-degree skew angle, and a bridge with a 50 ft. span length, 340 ft. radius, and 0-degree skew angle. The transverse displacement results of these models are summarized in Table 4-2.

¹ (Civjan, Lacroix, Takeuchi, & Higgins, 2021)

Table 4-2: Transverse Displacements for 5 ft. and 10 ft. U-Wingwall Lengths

Span (ft)	Radius (ft)	Skew (deg)	Transverse Displacement (in)			
			10 ft. U-Wingwall	5 ft. U-Wingwall	Difference	% Increase
50	340	0	0.052	0.069	0.017	33%
100	340	0	0.152	0.202	0.05	33%
100	340	10	0.257	0.332	0.075	29%
100	340	20	0.324	0.385	0.061	19%
100	750	0	0.074	0.079	0.005	7%

The maximum additional increase in transverse displacement from a 5 ft. U-wingwall compared to a 10 ft. U-wingwall is 33% at the 340 ft. curve radius. As the radius increases, the difference becomes less significant as seen when comparing the 340 ft. radius and 750 ft. radius bridges with 100 ft. spans and 0-degree skews. There is also a reduced difference between the wingwall lengths as skew increases. Bridge length does not appear to influence the effect of wingwall lengths. Note that the observed difference between the 5 ft. and 10 ft. displacements is a relatively small value of approximately 1/16 in. in the most severe case studied. This magnitude is important to include in the design but suggests that a range of wingwall lengths is allowable for the simplified design method. It is recommended that bridges with 5 ft. long U-wingwalls be designed using the same process as described for those with 10 ft. U-wingwalls with an additional 33% magnitude of transverse displacement. For bridges with U-wingwalls between 5 ft. and 10 ft., this value may be linearly interpolated. Wingwalls of shorter length may be considered when utilizing a refined analysis to confirm that pile head displacements are favorable.

Pile orientation was investigated as part of this research to determine the effects of weak-axis and strong-axis orientation of the pile on the structure response. Due to the nature of the horizontally curved abutment bridges, lateral displacement occurs at the abutments and needs to be adequately restrained to prevent maintenance and serviceability issues. It was observed that weak-axis orientation resulted in much more favorable responses, with significantly lower lateral displacements when compared to strong-axis orientation. This is the expected behavior since the piles in this orientation allow for flexibility due to thermal expansion and contraction of the bridge while also providing transverse lateral restraint. The strong-axis orientation models resulted in higher displacements that can be seen in Figure 3-13. It is recommended that the piles be in weak-axis orientation for all curved integral abutment bridges.

4.2 PILE LENGTHS

Changing pile length proved to be one of the most impactful parameters regarding the pile head displacements, rotations, and force effects. For the in-line wingwall cases, increasing pile length resulted in an increase in transverse displacement, which is magnified by tightening curve radius and increasing skew angles. As discussed in Section 4.1, the orientation of the piles for strong and weak axis affected these responses. U-wingwalls effectively restrained the abutment from translating, resulting in an insensitivity to pile length in those cases.

This study used an equivalent cantilever pile length method to model the combined stiffness of the pile section as well as the surrounding soil. This is modeled as a beam section that is rigidly connected to the abutment node at the pile head, a fully fixed support at the pile base, and no springs representing the soil stiffness along the length. This differs from a depth-to-fixity model, which would provide a pile with similar end conditions, but a much longer beam length as well as springs along the full depth of the pile. An equivalent cantilever pile provides the same pile head stiffness as would be found in the depth to fixity model, and ultimately should result in the same maximum force effects and deflections.

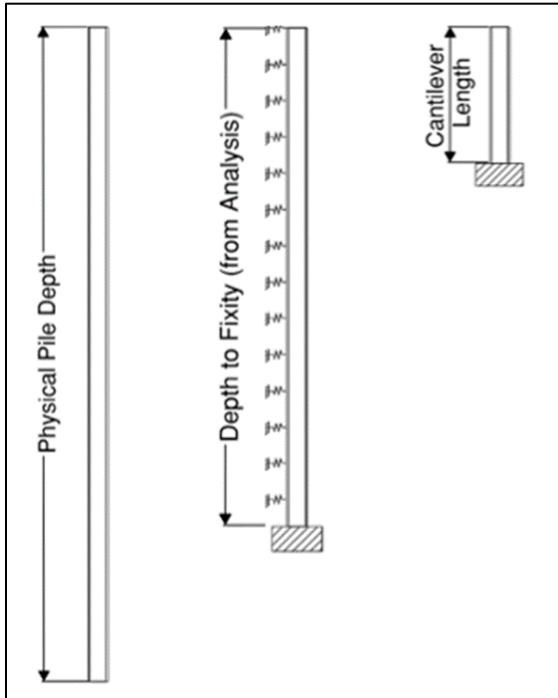


Figure 4-1: Pile Model Diagram

Figure 4-2 shows an example of this difference related to the model. The equivalent cantilever model will have a significantly shorter length as compared to the depth to fixity model, which is discussed in Section 2.1.2. For a given load applied to the pile head of each pile example, there will be an equal pile head displacement.

Changing the pile equivalent cantilever length for a given section size models changing soil parameters. For a stiffer soil, there is more support given to the pile and therefore would result in a shorter pile cantilever length. For a softer soil, less restraint is given to the pile and therefore results in a longer equivalent cantilever length. This effect was included in this study by changing the pile lengths between 10, 15, 20, and 30 ft.

The exact pile head stiffness value for any of the equivalent cantilever models included in this study can be calculated using Equation 4-1, which is based on the beam deflection equation for a beam fixed at one end and free to translate at the other end, where the variable “L” is the cantilever pile length shown in Figure 4-2. These boundaries are analogous to those used in the model.

The most impactful response from changing pile cantilever lengths was the bridge transverse displacement, with longer pile lengths resulting in high, and in many cases unacceptable, displacement magnitudes. By defining an acceptable transverse displacement for design and serviceability, the corresponding pile length from the models can be targeted. This length is specific to the pile size of the model. Based on these known and calculated values, a target stiffness for the piles may be calculated which would result in acceptable performance.

The acceptable limit for transverse displacement was set to be equal to the same magnitude of the unrestrained longitudinal thermal displacement for the given span length. This was chosen such that translation would not be the primary mode of displacement for design and serviceability and would limit the magnitude of displacement along the abutment line for detailing concerns. In the skewed cases, the values have been reduced to the radial component for comparison with the global displacement results. These values are provided in Table 4-3, which are based on a full 125-degree rise and fall in temperature applied to an unrestrained steel girder with the total steel movement divided by two based on equal abutment distribution.

Equation 4-1: Stiffness of Equivalent Cantilever Pile

$$K\left(\frac{\text{kip}}{\text{in}}\right) = \frac{12 * E * I}{L^3}$$

Table 4-3: Allowable Transverse Displacements for Acceptable Response

Bridge Length (FT)	50	75	100	150	200	300
0-degree Skew (in)	0.244	0.366	0.488	0.731	0.975	1.463
10-degree Skew (in)	0.240	0.360	0.481	0.720	0.960	1.441
20-degree Skew (in)	0.229	0.344	0.459	0.687	0.916	1.375

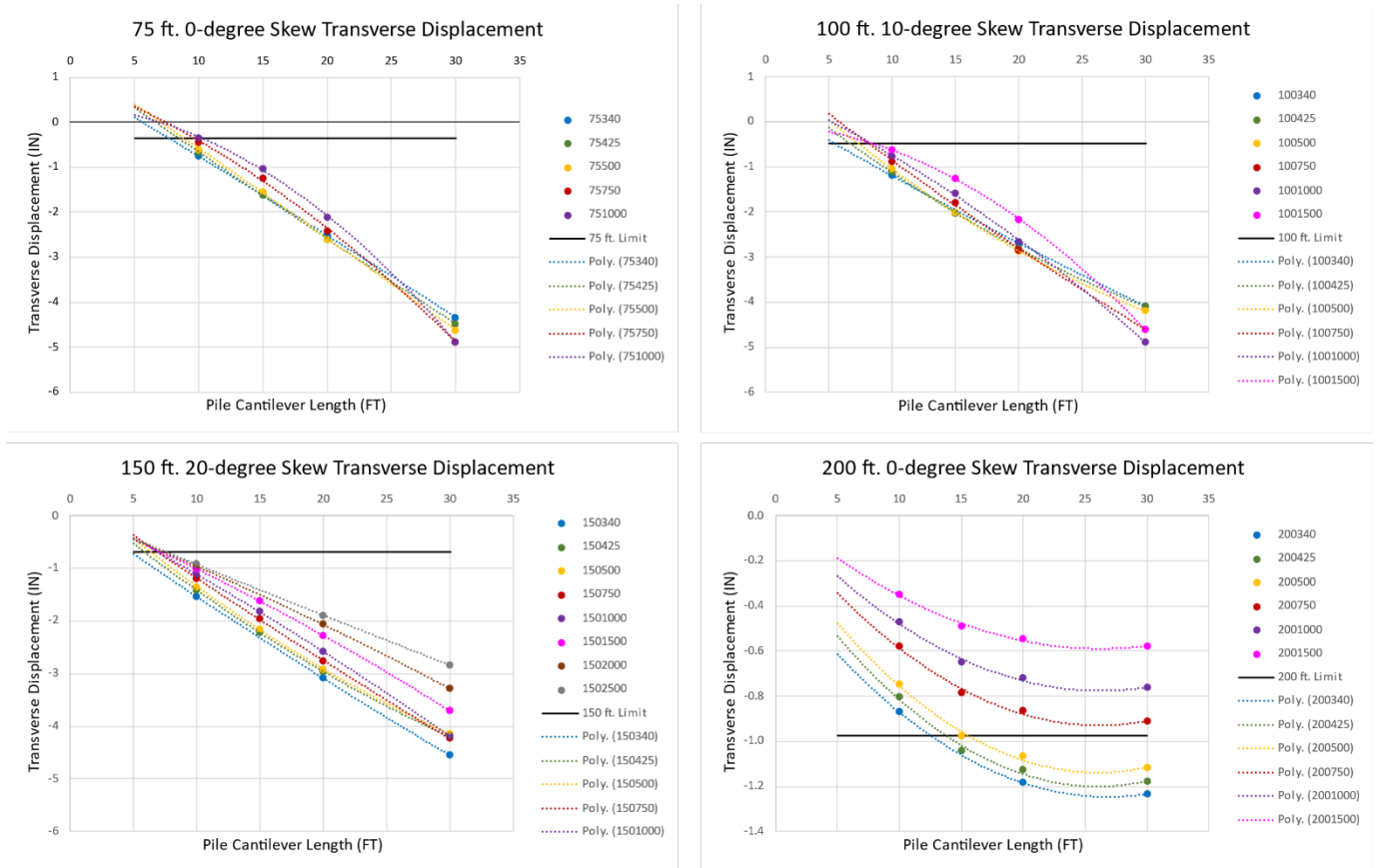


Figure 4-3: Subset of Transverse Displacement Trendlines for Pile Stiffness Analysis

Trendlines were developed based on the transverse displacement results from each model for the varying lengths of piles in the weak axis orientation. A subset of these trendlines is displayed in Figure 4-3, which displays the transverse displacement results and trendlines for specific bridge lengths and skews, broken down by curve radius. The acceptable displacement value for that bridge length has been displayed with a black line. The projected pile length that corresponds to the intersection of the trendlines and the allowable displacement line represents the stiffness that would result in acceptable bridge performance. The addition of the 15 ft. pile length allowed for much more accurate trendlines as they approach the acceptable displacement limit.

A target stiffness value that would result in acceptable bridge performance can be calculated based on Equation 4-1, where the pile properties modulus of elasticity (E), moment of inertia (I), and calculated pile length (L) are known. This value is then multiplied by the number of piles to provide a transverse abutment stiffness value that results in acceptable displacement values. Table 4-4, Table 4-5 *Error! Reference source not found.*, and Table 4-6 *Error! Reference source not found.* provide these values, broken out by skew angle and tabulated by bridge length and curve radius. The values in these table logically increase as the bridge length increases, curve radius decreases, and skew increases, which aligns with the trends observed in Section 3.3. Note that in some cases the two-span cases reach a constant stiffness value at larger radii. This is because the models do not approach the transverse displacement limit, so a pile length of 20 ft. was chosen as the limit. See Section 4.3 for more information on the effect of multi-span structures on bridge performance.

Table 4-4: Target Transverse Stiffness Values for Bridges with 0-degree Skew Angles

Radius (ft.)	Structure Length (ft)					
	50	75	100	150	200	300
340	597	1414	2527	4949	333	495
425	568	1108	1313	2013	282	450
500	515	1004	1157	1712	199	372
750	449	770	898	1263	82	179
1000	-	604	738	1047	82	114
1500	-	-	510	752	82	114
2000	-	-	-	618	-	114
2500	-	-	-	483	-	-

Table 4-5: Target Transverse Stiffness Values for Bridges with 10-degree Skew Angles

Radius (ft)	Structure Length (ft)					
	50	75	100	150	200	300
340	727	1789	2587	5701	2713	2053
425	665	1536	2011	4286	2238	1900
500	628	1356	1779	3499	2058	1805
750	606	1158	1540	2554	1616	1690
1000	-	981	1484	2390	1378	1554
1500	-	-	1299	2251	1132	1364
2000	-	-	-	2065	-	1332
2500	-	-	-	1900	-	-

Table 4-6: Target Transverse Stiffness Values for Bridges with 20-degree Skew Angles

Radius (ft)	Structure Length (ft)					
	50	75	100	150	200	300
340	836	1897	3267	6762	3306	2716
425	751	1829	2667	5134	3195	2668
500	688	1754	2552	4160	2772	2527
750	646	1511	2418	3425	1986	2408
1000	-	1179	2221	3050	1671	2141
1500	-	-	2010	2657	1382	1813
2000	-	-	-	2315	-	1653
2500	-	-	-	2108	-	-

A designer can use these stiffness values to develop a baseline pile stiffness for their bridge geometry. The requirements for usage of these tables should be limited to structures within the scope of this study and as defined in the resulting design guide. The primary limitations are based on the abutment geometry and soil characteristics. Soil characteristics differing from a

standard compacted granular backfill, typical of New England states, would result in a different stiffness value and therefore result in different transverse stiffness targets for acceptable structure performance. Additionally, the tables are not applicable to bridges with abutment geometry differing greatly from those included in the study for similar reasons, with an upper limit of 50 ft. wide suggested. These tables were only developed for use with in-line wingwalls, with U-wingwall configurations being covered by separate guidance discussed in Section 4.1. Values for extreme curve radii and skew angle may be difficult to achieve in design, but are provided here for reference to the designer and for use as a basis for design.

To verify the assumptions made in the development of Table 4-4, Table 4-5 **Error! Reference source not found.**, and Table 4-6 **Error! Reference source not found.**, a geotechnical soil-structure interaction analysis was performed. In this analysis, a pile extending significantly past the expected depth-to-fixity was modeled with assumed soil properties. The resulting pile head displacements and axial load from the 100 ft. long, 750 ft. radius bridge with in-line wingwalls, 0-degree skew, and 10 ft. long piles were applied to the pile, which resulted in a depth-to-fixity of 36 ft. This depth aligns with the expected values provided by the straight integral abutment bridge guidance from MassDOT, summarized in Table 2-2. The resulting forces in the pile were used to calculate the equivalent cantilever length which was slightly longer than the 10 ft. provided in the model, but within acceptable range. This process indicates the need for an iterative design process for curved integral bridges with in-line wingwalls since the responses are dependent on the soil and pile stiffness.

The pile design for the bridges studied here requires consideration for transverse displacements, and therefore requires that the designer calculate the expected transverse displacement of the piles. In the U-wingwall cases, evaluation of these displacements is independent of the pile length and surrounding soil conditions. For in-line wingwalls, the response is highly dependent on the pile length and soil conditions and requires these conditions be accounted for in the design process. To do so, a model including the superstructure, abutment, piles, and soil conditions must be completed. To verify what amount of detail is required to capture the transverse displacements, a stick model was created based on the refined model guidance provided by the MassDOT bridge design manual. This model is based on the 100 ft. long, 750 ft. radius bridge with in-line wingwalls, 0-degree skew, and 10 ft. long piles. A thermal range of 125-degree expansion and contraction was applied to this stick model for comparison with the 3D models completed in the finite element study. Figure 4-4 displays the characteristics of this model.

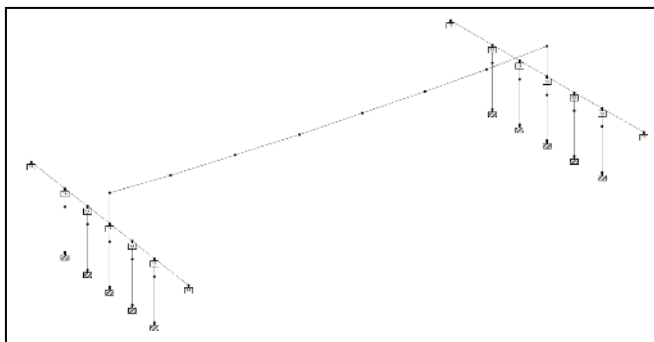


Figure 4-2: Stick Model for Verification

The transverse displacements of the pile heads at abutment 1 resulting from thermal expansion are compared in Table 4-7. The stick model calculated significantly smaller transverse displacements compared to the refined analysis model. This indicates that the stick model approach is not able to accurately calculate the expected transverse displacements and is unconservative. A model with the superstructure modeled using a grillage method at a minimum is recommended for accurately calculating transverse pile head displacements.

Table 4-7: Stick and Refined Model Comparison

Transverse Pile Head Displacement (in) - Tue

Model Type	Pile 1	Pile 2	Pile 3	Pile 4	Pile 5
Refined	0.451	0.448	0.444	0.440	0.437
Stick	0.113	0.113	0.113	0.113	0.113

A refined analysis approach is recommended for all curved integral abutment bridges with in-line wingwall orientations. This conclusion is based on the sensitivity of this orientation to varying soil conditions. This sensitivity requires a model accounting

for soil-structure interaction with abutment backwall springs and piles modeled with a minimum refinement of the equivalent cantilever method, as well as the superstructure modeled using the grillage method. All geometric parameters must be included in the model including curve radius and skew angle.

The stiffness tables developed in this section provide the designer with a logical starting point for the iterative design process. A model can be developed using equivalent cantilever pile lengths based on the designer’s chosen pile section and the stiffness provided in the tables. The resulting loads and displacements from the model are then input to a pile analysis program to provide design values based on the site soil conditions. The equivalent cantilever lengths used in the model may then be revised based on those developed from the pile analysis for continued refinement of the design model.

4.3 MULTI-SPAN BRIDGES

The parametric study included the investigation of multi-span bridges to determine their influence on structure response. The research models only considered two span bridges of equal individual span lengths. The pier was modeled as a 3-column bent with an assumed typical column and pier cap arrangement. The bearings supporting the superstructure were modeled as fixed for translation and free for rotation. Refer to Figure 4-5 for the pier configuration used for all models. The models also only considered the in-line wingwall case. The results from the multi-span bridge models produced favorable responses at the abutments with lower lateral displacements of the pile heads compared to their single-span counterparts, refer to Figure 3-21.

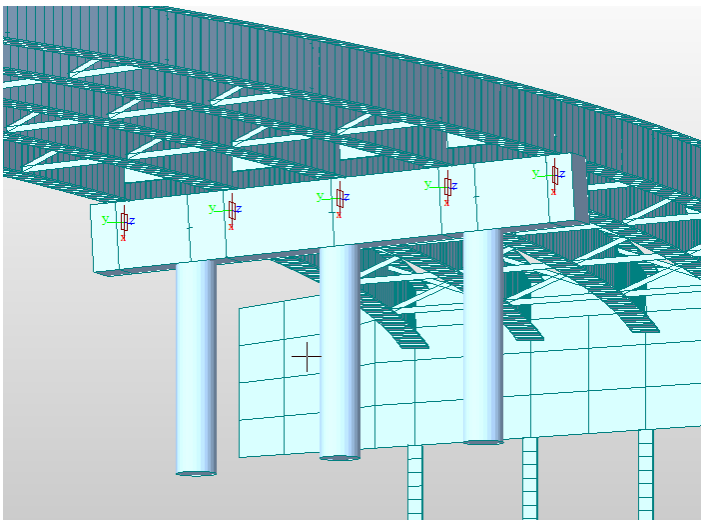


Figure 4-3: Pier Configuration in Midas Models

Displacement of the pile heads alone cannot be the only consideration for the favorability of the multi-span bridges. The lower displacements of the pile heads are a result of the pier providing lateral restraint to the movement of the curved bridge. The pier is subjected to significant shear and torsional forces while restraining the lateral displacement of the bridge. The bearings, additionally, need to provide adequate restraint to transfer the superstructure forces down into the pier. These forces in the bearings and pier are not insignificant and shall be considered for design of the bearings, pier, and pier foundation.

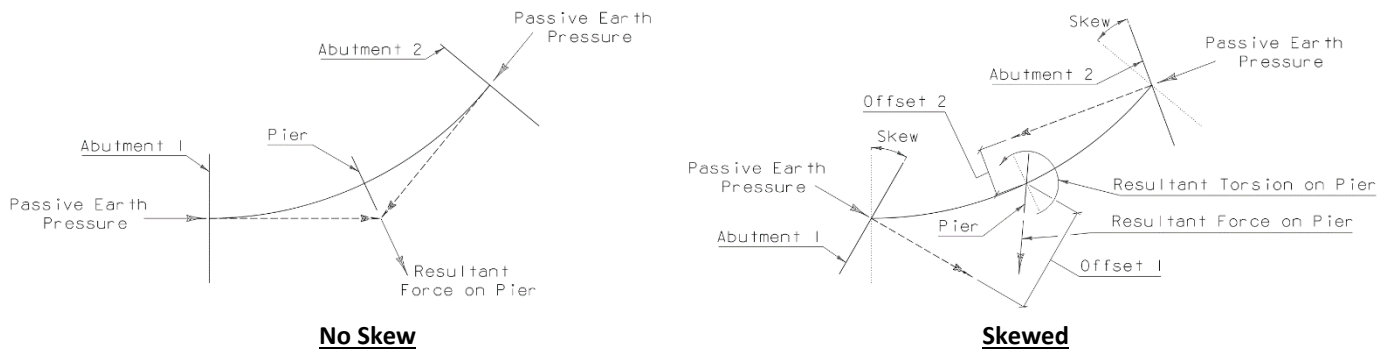


Figure 4-4: Resultant Forces on the Pier for No Skew (left) and Skewed (right) Substructure Components.

As the curved bridge is subjected to thermal loading, the expansion of the superstructure pushes the abutments into the soil. The largest force the soil can impart on the abutment due to displacement into the soil is passive earth pressure. Figure 4-6 shows the resultant forces on the pier for no skew and skewed substructure components resulting from passive earth pressure applied at the abutments. For the no skew case, where the abutments and pier are all in radial orientation, the passive earth pressure at the abutments results in a shear force at the pier in the radial direction. When the substructure components are skewed in the same direction, the whole bridge will want to rotate about the vertical axis of the pier.

The shear in the pier was investigated to determine if there was a predictable maximum resultant shear force at the pier based on a percentage of passive earth pressure at the abutments. Refer to Table 4-8 for the calculated passive earth pressure at the abutments, the resultant shear force at the pier and the actual resultant shear force on the pier from the research models. It was observed that as the radius decreases the resultant shear force from passive earth pressure in the pier increases, which is the expected behavior. The same trend was observed in the models with an increase in shear in the pier as radius decreases. The difference between resultant passive earth pressure and the shear observed in the models varies with radius of curvature. By inspection, the stiffness of the pier influences the response of the structure. If the pier is very stiff, such as a pier wall, it would restrain the bridge movement more and be subjected to higher forces to consider for its pier. A very flexible pier, such as a pile bent, would allow for more displacements of the pier and subsequently at the abutments as well. Similar to the pile lengths affecting the stiffness of the integral abutment bridge, the stiffness of the pier would have similar effect. The research did not investigate the sensitivity of the pier stiffness on the abutment response. The type of pier used for any given bridge in New England is dependent on the site conditions and bridge geometry. Piers may consist of a wall pier, hammerhead, multi-column, or pile bent and should consider the preference of local or state guidelines. Considering this, a reduction to the resultant force on the pier due to passive earth pressure at the abutments cannot be recommended at this time, however an upper limit is recommended for design.

Table 4-8: Comparison of Resultant Shear from Passive Earth Pressure to Modeled Shear on Pier

Span	Radius	Passive Earth Pressure at the Abutment Back Face	Resultant Shear Force on Pier from Passive Earth Pressure	Actual Shear on Pier from the Models	Proportion of Actual Shear to Resultant Passive Earth Pressure
(ft)	(ft)	(Kips)	(Kips)	(Kips)	
200	340	3252	1912.94	430.29	22%
200	500	3252	1300.8	364.75	28%
200	1000	3252	650.4	216.52	33%
300	340	5018	4427.65	764.81	17%
300	500	5018	3010.8	730.36	24%
300	1000	5018	1505.4	491.22	33%

Without a refined analysis that fully models the stiffness of the pier and abutments accurately, it is difficult to quantify what the force response at the pier and bearings would be. A conservative upper limit for the response can be achieved when considering the full passive earth pressure at the abutments, which can be utilized under the simplified design method.

The recommendation for the pier design is for the designer to consider 100% of the resultant force due to passive earth pressure at the abutments. This results in the upper limit of possible forces on the pier. The resulting forces from this

recommendation are highly conservative and in cases where the bridge has tight curvature, this design load for shear at the pier may be economically cost prohibitive. For cases with tight curvature, a refined analysis may be considered to determine a more accurate response at the pier.

The designer shall first calculate the full passive earth pressure at each abutment and then determine the radial force vector at the pier based on the chord length of the bridge span and radius of curvature. For skewed cases, the shear is calculated in the same manner and the torsion at the pier shall be calculated based on the offset of the passive earth pressure vector from each abutment to the pier centroid of rotation. Note that the skew of the substructure component shall be the same at each component, and not to exceed 20 degrees from radial orientation.

All two-span models under this research were run with in-line wingwalls. By inspection, the behavior of U-wingwalls consistently provides favorable responses in the structure, regardless of pile length, and it is therefore recommended that U-wingwalls be used for all multi-span integral abutment bridges for the simplified design method. The pile response under the in-line wingwall cases is too sensitive to determine a conservative pile head displacement without a refined analysis.

4.4 DESIGN OF SUPERSTRUCTURE

The superstructure design was not the focus of this research; however, several observations were made that can lead to recommendations for the superstructure design.

The largest effect the bridge curvature has on the superstructure design is torsion at the beam ends. The effect of this torsion on the abutment closure and pile response was investigated under this research. Figure 3-36 illustrates that approximately 80% of the torsion in the beam ends is developed during the construction stages prior to the curing of the deck and beam end closures. This indicates that the primary torsional force applied to the girders can be designed for through a superstructure only analysis considering construction staging and appropriate diaphragm conditions. Torsion in the girder ends developed after integral behavior has been achieved (deck and closure pour curing) is minimal. The effect of live load eccentricity along the length of the bridge is primarily resolved through global torsion of the superstructure, and is resolved through differential pile loading. It is recommended that the superstructure be designed for torsion following the recommendations of AASHTO and state and local requirements.

The effect of skew on the superstructure response is primarily in differential strong-axis moments between adjacent girders and uplifting of the girder ends at the acute corners. The superstructure response due to changes in skew was investigated to identify any limitations for use of the simplified design method.

Figure 3-43 and Figure 3-44 show that positive and negative moments occur at the beam ends, indicating torsion occurring in the end diaphragm/abutments between adjacent beams. This effect was observed for the longer span bridges with higher skews. This torsion in the end diaphragm/abutment should be accounted for by the designer with additional consideration for utilizing stirrups with closed ends. The magnitude of the positive moments at the beam ends does not exceed those that occur at the midspan. Therefore, the superstructure is recommended to be conservatively designed for positive moments under simple support conditions and following the recommendations of AASHTO and state and local requirements.

The deck stresses were investigated to identify any parameters that would impact the design of the supplemental reinforcing steel at the deck ends. Section 3.7 discusses how the various geometric parameters have no appreciable impact on the deck stresses. The magnitude of the deck stresses for some cases was observed to exceed the anticipated modulus of rupture, however they were not so high that they couldn't be accounted for in the design of the continuity supplemental reinforcing steel at the ends of the bridge. Skew was not observed to have any limiting effects on the design for deck stresses. Additionally, shorter pile lengths were observed to have no significant impact on the deck stresses. Therefore, it is recommended that for the simplified design method, the continuity reinforcement at the ends of the bridge be designed for a fixed-fixed boundary condition to provide a conservative negative end moment at the ends of the girders.

The designer shall also consider that, based on the results of the national survey and literature review, tighter than standard bar spacing with smaller bars provides better performance to prevent cracking of deck concrete when compared to larger bars at larger spacing. It is recommended that the designer start with #6@6" for the continuity reinforcement to mitigate cracking at the ends of the deck.

4.5 REQUIREMENTS FOR THE APPLICATION OF THE SIMPLIFIED DESIGN METHOD

The simplified design method will require the following criteria as a result of the parametric study:

- Superstructure must consist of curved concentric steel I girders.
- Shall use Grade 50 steel H piles with a minimum flange width of 10 inches.
- Multi-span bridges shall have equal span lengths +/- 10% for each individual span.
- The maximum total bridge length, as measured along the curve at the bridge centerline and between the centerlines of bearing at the abutments, shall be of 150 ft. in a single span 300 ft. for multi-span bridges.
- Shall have a maximum bridge width of 50 ft.²
- The horizontal curve radius must be 340 ft. or greater, measured at the centerline of the bridge.³
- The substructure components shall have a maximum skew of 20 degrees from the radial orientation. Substructure components are permitted to have different skew angles, but must be skewed in the same direction.⁴
- Piles shall be orientated for weak axis bending with the pile webs perpendicular to the tangent line of the girders at the mid-width of the bridge at each abutment.
- Wingwalls shall be monolithic cantilevered U-wingwalls with a length of 10 ft., as measured from the back face of the abutment.⁵
- The abutments at each end of the bridge should have similar configuration and geometry.
- Lengths of piles shall be sufficient to allow for the piles to be embedded to meet the assumed depth of fixity based on a soil-structure interaction model.

Additionally, the following criteria will be required based on the best practices for straight integral abutment guidelines:

- Both abutments shall be integral connections.
- Approach slabs shall be included to reduce impacts of approach settlement and live load surcharge on the abutment.⁶
- Shall not be subjected to extreme event loading (other than Seismic Design Category A / Seismic Zone 1 general criteria).
- Shall have a minimum pile embedment length beyond the bottom of the abutment stem of 10 ft.
- Piles must achieve fixity.⁷
- Scour shall be considered when the abutments are located near a stream or river.⁸

² Larger width curved structures may produce complex thermal movements.

³ Bridge radii less than 340 ft. fall outside the parametric study that was performed. A refined analysis is recommended for bridges less than 340 ft. to accurately account for pile head displacements.

⁴ Skews greater than 20 degrees from radial orientation fall outside the parametric study that was performed. Bridges with unequal skews at the different substructure components were not investigated in the parametric study, but can be adequately designed for using the simplified design method.

⁵ Flared wingwalls fall outside the parametric study that was performed. Wingwall lengths less than 10 ft. fall outside the parametric study that was performed. Any wingwall length beyond 10 ft. shall be designed as a freestanding retaining wall with an expansion joint between the freestanding wall and the cantilevered wing capable of accommodating the full abutment movement in the longitudinal and lateral directions, or as directed in state standards for straight integral abutment bridges.

⁶ Approach slabs should be designed and detailed according to typical state standards but should be designed to accommodate the anticipated movement of the abutment.

⁷ Where high bedrock conditions are encountered the designer shall coordinate with the applicable state bridge engineer to determine whether pre-boring, blasting, or alternative bridge solutions should be considered. Piles with pinned ends, such as in cases with shallow bedrock, shall be designed using refined analysis.

⁸ Generally, abutment foundations near streams and rivers are protected by riprap or other means. Unprotected abutment foundations near stream or river channels, or based on state and local design requirements, that result in scour conditions should be evaluated in the soil-structure interaction analysis. Larger pile sizes may be required for the unbraced length under the scour condition.

- Maximum abutment heights shall be as indicated in state standards for straight integral abutments. If no standard exists, abutment height shall be limited to 12 ft. from finished roadway grade to bottom of cap to reduce passive earth pressure effects. The difference in abutment heights at each end of the structure shall not exceed a difference of 1 ft.

Bridges falling outside the above parameters have characteristics that were either not studied in the research or produced unacceptable results, deflections, or stresses. A structure that falls outside the criteria stated above may require more detailed analysis, such as a refined analysis.

4.6 IMPLEMENTATION PLAN

This Curved Integral Abutment Bridge Design Guideline is intended to aid in the design of curved integral abutment structures that would be encountered under typical conditions in New England, including cold climate thermal ranges and low seismic hazards. These guidelines should be considered a supplement to existing state structures design manuals and not a standalone guidance. The document will direct designers to state design guidelines for all load magnitudes and applications, state specific detailing requirements, and deck pour sequencing. Designers will also be directed to state guidelines for straight integral abutment bridges for the method of designing reinforcement in the abutment diaphragm and stem. Pile selection should follow state typical pile sizes where applicable. The intention with this approach is to allow the states flexibility in using the guidance to supplement their existing systems.

Individual states may elect to incorporate these guidelines in the following manners:

- Incorporate directly into existing structures manuals or integral abutment bridge design guidance as an appendix.
- Incorporate directly into existing structures manuals or integral abutment bridge design guidance by modifying the section numbers as appropriate to fit into the desired chapter of existing guidance.
- Refer to this guidance as a supplement to existing straight integral abutment design guidance when curved alignments are encountered on projects.
- Choose to not incorporate / not allow simplified procedures for curved integral structures.

This document should be supplemented by updates from further research. The scope of this study limited the number of parameters that could be feasibly included in the study. Further studies could refine or expand the guidance provided.

5 CONCLUSIONS

The parametric study yielded applicable and implementable results for development of simplified design criteria. Further research can be conducted to further refine guidance, specifically with respect to pile lengths and soil-structure interactions. Table 5-1 relists the intentions noted at the beginning of this research effort and notes the outcomes.

Table 5-1: Outcomes of Proposal Intentions

<i>Intention</i>	<i>Outcome</i>
1. For each span to radius ratio, when does the required pile properties vary from that which would be required had the straight girder simplified method have been used?	Approaching the span to radius limit set by AASHTO shows a normalization of data for lateral effects. This is expected, as the effects of curvature should become minimal as the structure straightens.
2. For all combinations of skew and degree of curvature, is there a consistent pattern of structural response to indicate how skew is impacting pile size and frame behavior? Does the passive pressure response on skew cause a measurable difference in the response of the frame?	As the skew increases, the differential movement of the bridge corners increases as the structure is restrained in a non-uniform manner. This leads to additional structure rotations and movements, which may lead to serviceability issues such as deck cracking. U-wingwalls provide predictable restraint to excess displacements.
3. How does the behavior of the structure differ between single-span and multi-span structures across all other parameters?	Two span structures can provide additional restraint to transverse bridge movement due to the stiffness of the pier. The additional load on the pier must be considered in the design process.
4. Is there a pattern in the set of results showing a span, radius, or skew combination where the sensitivity of the superstructure design may be impacted? Considering torsion in the girder ends, continuity reinforcement in the deck, and general superstructure response?	<p>The superstructure design is most directly influenced by the radius. Tight radii result in substantially higher torsion development in the girders at the beam ends but can be accounted for in a superstructure-only analysis.</p> <p>Deck stresses are not largely impacted by the parameters with the #6 at 6" bar standard being adequate for cases noted in this study.</p>
5. Is there a pattern in the set of results that shows sensitivity in any area where a known boundary can be established? Do the corresponding boundaries on all parameters allow for a defined range of conditions where simplified methods will produce acceptable designs?	U-Wingwalls lead to the best bridge performance and can be acceptably designed using simplified methods. In-line wingwalls are highly sensitive to soil conditions and therefore are recommended for refined analysis in all cases studied.

The reader is directed to the Curved Integral Abutment Design Guidelines for further information. The technology toolbox will be included with the final draft of the report.